# Multi-Channel Constant Current ($MC^3$) LED Driver for Indoor LED Luminaries

Haoran Wu

Thesis submitted to the Faculty of the Virginia Polytechnic Institute and State University in partial fulfillment of the requirements for the degree of

Master of Science

in

Electrical Engineering

Fred C. Lee, Chairman

Paolo Mattavelli

Daniel Stilwell

Nov 14th, 2011

Blacksburg, Virginia

Keywords: Light-emitting diode (LED), Multi-channel constant current ($MC^3$) LED driver, LLC resonant converter, Current sharing, Dimming

# Multi-Channel Constant Current ($MC^3$) LED Driver for Indoor LED Luminaries

Haoran Wu

Abstract

Recently, as a promising lighting source, light-emitting diodes (LEDs) have become more and more attractive and have great opportunity to replace traditional lighting sources - incandescent, fluorescent and HID because of the advantages such as high luminous efficacy, long lifetime, quick on/off time, wide color gamut, eco-friendly etc.

Based on the research from U.S. Department of Energy, over 30% of total electric consumption in U.S. each year is for lighting, 75% of which are for indoor lighting (including both residential and commercial buildings). In the indoor LED lighting application, to provide multiple current source outputs for multiple LED strings, traditional solutions usually adopt a two-stage structure, which is complicated and cost-ineffective. How to design a simple, low-cost and efficient LED driver with multiple current source outputs is in great demand and really challenging.

In this thesis, a single-stage multi-channel constant current ($MC^3$) LED driver structure has been proposed. Multiple transformer structure is utilized to provide multiple current source outputs. The current control scheme is also simple - only one LED string current is sensed and controlled; other strings' currents are cross regulated.

Firstly, a PWM half bridge topology is chosen to implement the proposed single-stage $MC^3$ LED driver concept. In order to analyze the current cross regulation, a general

model is derived. The circuit has been simulated under various LED load conditions to verify its good current sharing capability.

In order to further improve efficiency, simplify the driver's complexity and reduce cost, a LLC resonant topology is also investigated. LLC current gain characteristic has been derived by considering LED's i-v character and a design procedure is developed. A 100 kHz, 200 W, 4-string $MC^3$ LLC LED driver is designed and tested. The experimental results show that the driver can maintain constant current output within the whole input and output variations, achieve good efficiency and realize current sharing under both balanced and unbalanced LED conditions. The dimming function can also be realized through frequency modulation method and burst mode control method.

As a conclusion, a single-stage $MC^3$ LED driver concept is proposed and implemented with two topologies. The proposed idea provides a simple, low-cost and efficient solution for indoor LED lighting application with multiple LED string configuration. It also has good current sharing capability and robustness to LED forward voltage variations or short failures.

# Acknowledgements

First of all, I would like to thank my advisor, Dr. Fred C. Lee. It is him who leads me into the world of power electronics. I have learned a lot from his profound knowledge and his rigorous research attitude during the past three years. I can never forget those days of struggling and learning. None of the results showing here would be possible without his help.

I am also grateful to my other committee members: Dr. Paolo Mattavelli and Dr. Daniel Stilwell, for their support, and suggestions throughout my study and research as well as the excellent classes they have taught which have become the foundation of my current and future works.

I would like to thank all the great staffs in CPES: Ms. Teresa Shaw, Ms. Linda Gallagher, Ms. Marianne Hawthorne, Ms. Teresa Rose, Ms Linda Long, Mr. David Gilham, Dr. Wenli Zhang and Mr. Douglas Sterk.

It takes courage to be here in CPES and it also takes courage to leave here for the coming future. The past three years had never been easy for me because of all the frustrations and all the struggling. I am proud that I finally make it to this point but I also feel sorry that I cannot stay any longer. It has been such a pleasure to work in CPES and it is such an honor to be part of the great family. I would like to thank all the people that have been part of my life: Dr. Ming Xu, Dr. Shuo Wang, Dr. Pengju Kong, Dr. Jian Li, Dr. Julu Sun, Dr. Chuanyun Wang, Dr. Yan Dong, Dr. Dianbo Fu, Dr. Yan Jiang, Dr. Yan Liang, Dr. Rixin Lai, Dr. Honggang Sheng, Dr. Michele Lim, Dr. Di Zhang, Dr. Puqi Ning, Dr. Brian Cheng, Dr. Xiaoyong Ren, Dr. Fang Luo, Dr. Xiao Cao, Dr. Sara

Ahmad, Dr. Qiang Li, Mr. Yi Sun, Mr. David Reusch, Mr. Shu Ji, Mr. Igor Cvetkovic, Mr. Zheng Luo, Mr. Pengjie Lai, Mr. Qian Li, Mr. Daocheng Huang, Mr. Zijian Wang, Mr. Zhiyu Shen, Mr. Dong Jiang, Mr. Ruxi Wang, Ms. Zheng Zhao, Ms. Ying Lu, Mr. Dong Dong, Mr. Zheng Chen, Mr. Mingkai Mu, Mr. Feng Yu, Mr. Yingyi Yan, Mr. Chanwit Prasantanakorn, Ms. Yiying Yao, Mr. Jing Xue, Ms. Zhuxian Xu, Mr. Yipeng Su, Mr. Marko Jaksic, Mr. Milisav Danilovic, Mr. Hemant Bishnoi, Mr. Justin Walraven, Mr. Weiyi Feng, Mr. Bo Wen, Mr. Wei Zhang, Mr. Shuilin Tian, Mr. Li Jiang, Mr Xuning Zhang, Mr. Jin Li, Mr. Pei-Hsin Liu, Mr. Zhiqiang Wang, Mr. Lingxiao Xue, Mr. Yin Wang, Mr. Zhemin Zhang, Mr. Bo Zhou, Mr. Tao Tao.

Last but not least, I want to thank my family, my father Jun Wu, my mother Daiying Wu and my twin brother Haojie Wu. Thank you for your consistent support and love during my study here. You raise me up, to more than I can be.

# Table of Contents

# List of Figures

# List of Tables

# Chapter 1. Introduction

## 1.1 Introduction of Light-Emitting Diodes (LEDs)

The history of lighting is as long as human being's history. In ancient times, since our ancestor learned how to generate lighting source by fire, the process of civilization has started. In the year of 1879, when Thomas Edison invented incandescent, human being entered into the electric era. Both technology and productivity have been growing explosively since then.

Edison's invention of incandescent is definitely a milestone in the exploration of the lighting sources. On the other hand, however, the incandescent also has several obvious drawbacks, such as short lifetime (750-1000 hours), low efficacy (3-16 lm/W) and fragile etc.

In 1978, fluorescent has been invented and gradually used to replace incandescent. A fluorescent lamp is a gas-discharge lamp which uses electricity to excite mercury vapor. The excited mercury atoms produce short-wave ultraviolet light that then causes a phosphor to fluoresce and produce visible light. Compared to incandescent, fluorescent lamps have the advantages of longer lifetime (5000 hours), higher efficacy (50-67 lm/W), and lower heat (about 70% less heat compared to incandescent lamps). However, fluorescent also has a fatal disadvantage – the health and safety issue. Mercury has been used during the manufacturing process of fluorescent lamps. If a fluorescent lamp is broken, a very small amount of mercury can contaminate the surrounding environment.

The broken glass is usually considered a greater hazard than the small amount of spilled mercury. Hence, the United States Environmental Protection Agency classifies fluorescent lamps as hazardous waste, and recommends that they be segregated from general waste for recycling or safe disposal.

Later, high-intensity discharge (HID) lamps have been invented. A high-intensity discharge (HID) lamp is a type of electrical lamp which produces light by means of an electric arc between tungsten electrodes housed inside a translucent or transparent fused quartz or fused alumina arc tube. Compared to incandescent and fluorescent lamps, HID lamps have the highest efficacy and usually illuminate streets, highways, parking lots, large commercial stores, industrial buildings etc. Similar to fluorescent lamps, the halogen used in HID leads to critical environmental and safety issues.

Due to various limitations and drawbacks of traditional lighting sources discussed above, a new, clean and efficient lighting source is urgently desirable and under investigation for a long time. Recently, light-emitting diodes (LEDs) has emerged as a promising lighting source for the future, which take an important role in the roadmap of lighting sources development as shown in Fig. 1.1.

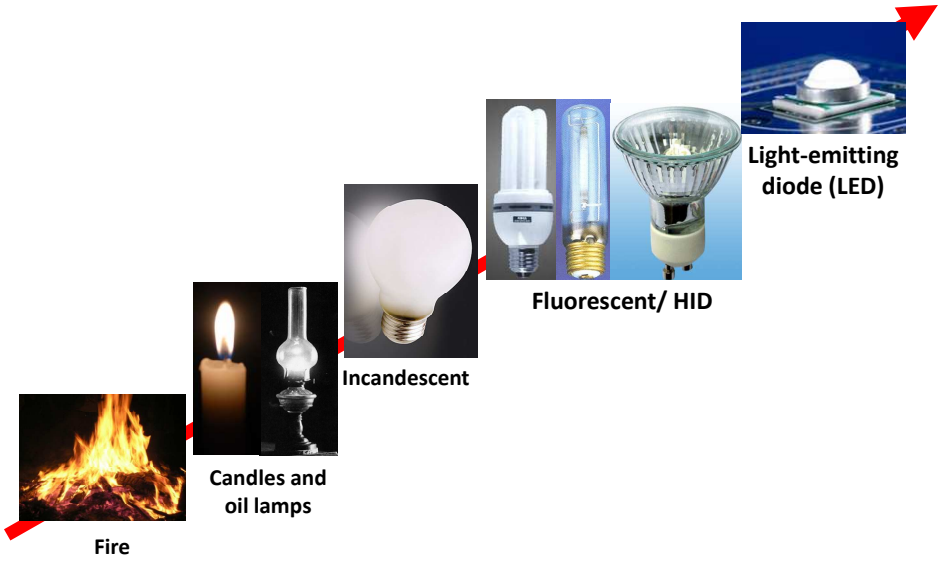


**Figure 1. 1 History of Lighting Sources**

A light-emitting diode (LED) is a semiconductor light source. When a LED is forward biased, electrons are able to recombine with electron holes within the device, releasing energy in the form of photons. This effect is called electroluminescence and the color of the light (corresponding to the energy of the photon) is determined by the energy gap of the semiconductor. The inner operation principle of LEDs is shown in Fig. 1.2.

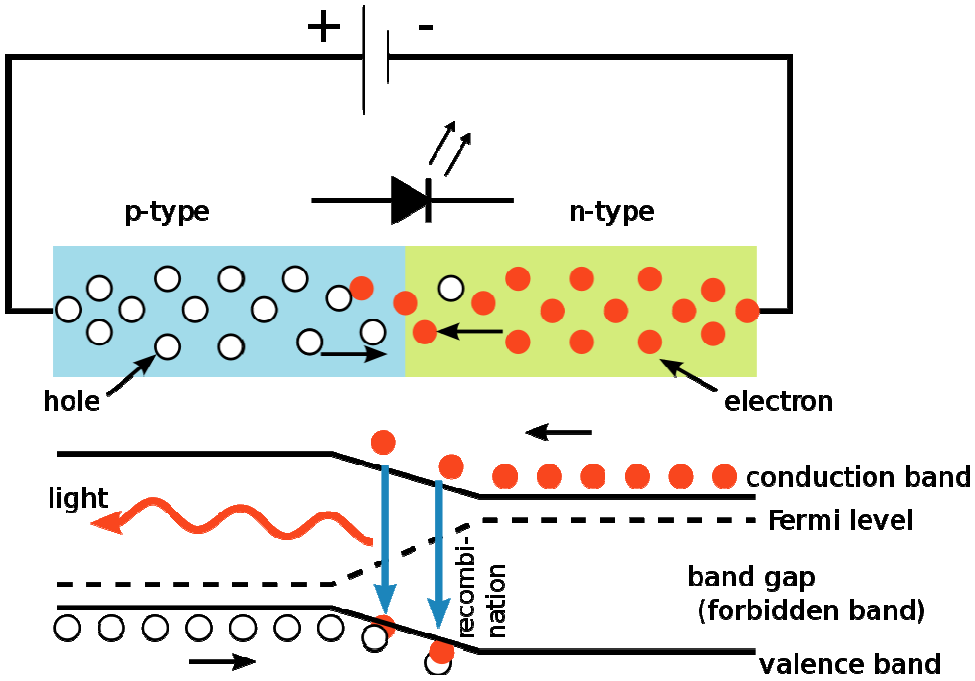


**Figure 1. 2 Inner Operation Principle of a LED**

First introduced as a practical electronic component in 1962, early LEDs can only emit low-intensity red light, but modern versions are available across the visible, ultraviolet and infrared wavelengths, with very high brightness and very high current. As a result, high brightness LED (HB-LED) has becoming more and more attractive to replace tradition lighting sources such as incandescent lamps, fluorescent lamps and HID lamps due to the following advantages [1]-[6]:

1. High efficacy

The efficacy of HB-LEDs keeps increasing rapidly. Nowadays the highest efficacy of commercial products has already reached 100 lm/W. In a report of solid-state lighting research and development provided by U.S. Department of Energy [7], the efficacy of HB-LEDs has potential to achieve a two-fold improvement over some of today's most

efficacious white-light sources. On the contrary, after decades of research and development, for the traditional three lighting sources - incandescent, fluorescent and HID - there is little room for significant, paradigm-shifting efficacy improvements, as shown in Fig. 1.3.

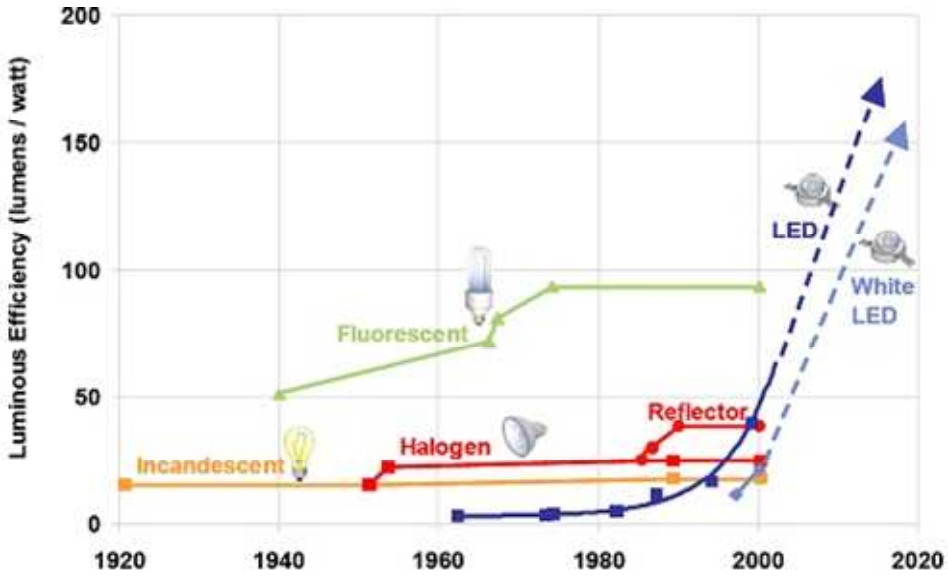


**Figure 1. 3 Historical and Predicted Efficacy of Lighting Source**

Actually, Cree just announces a white HB-LED with 231 lm/W in the laboratory in May 2011 [8], which breaks the highest LED efficacy record again. Although this level of performance is not yet available in commercial LED products, it is reasonable to believe that the performance improvements of LED may become even faster than the projections.

2. Long lifetime

Compared to traditional lighting sources, the LEDs have much longer lifetime (over 50,000 hours) and wider operating temperature range. Although at present the cost of LED is still high, considering the long lifetime, the LED's life-cycle cost is still

acceptable. Besides, from the long-term technology development point of view, the cost of LED will be continuously cut down, which makes LED become even more competitive in the future.

3. Quick On/Off time

LEDs light up very quickly, usually under several microseconds. This character of LEDs makes it very suitable in automotive application and backlighting application.

4. Wide color gamut

LEDs can provide a wider color gamut compared to previous cold cathode fluorescent lamps (CCFL) as LED’s color wavelengths have a higher purity level than fluorescent lamps. This character makes LEDs a good candidate in monitor or LCD flat panel TV's backlight systems [9]. As illustrated in Fig. 1.4, an LED backlight system claims a broader range of reds and greens for a more extensive color gamut and natural color expressions, compared to a CCFL backlighting system.

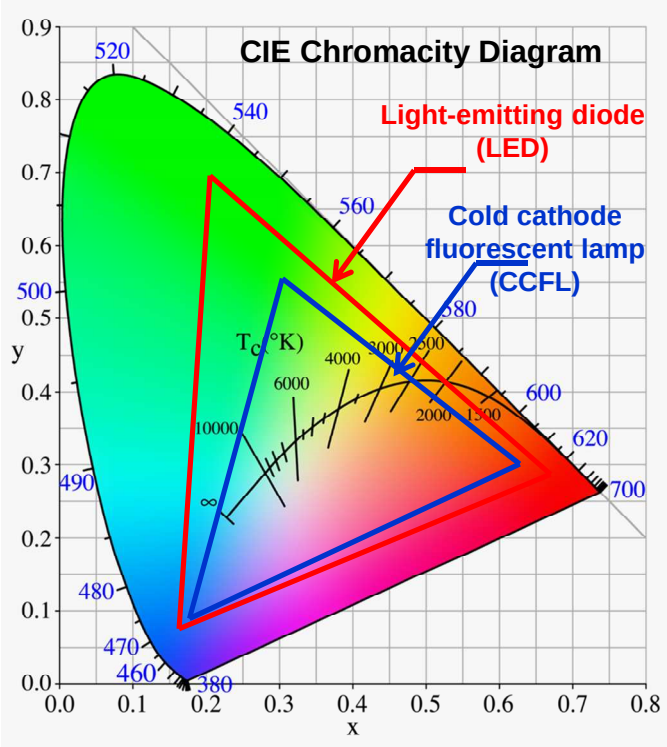


**Figure 1. 4 Color Gamut of LEDs**

5. Environmental friendliness

LEDs are mercury-free components and environmentally friendly, so that they can be disposed safely at the end of their lifetime.

As a lighting source, the brightness of LEDs is directly determined by its forward current. The LED i-v character under different junction temperatures is shown in Fig. 1.5. When driven by any voltage smaller than the threshold voltage, LED is reverse biased and forward current is zero. Only when the driving voltage exceeds threshold voltage, LED is switched on and forward current will increase quickly as forward voltage increases. The LED shows nonlinear character and is completely different from resistive load. In order to simplify the analysis, a piece-wise-linear LED model is widely used to

replace the real LED model. The cut-off voltage between LED's on-state and off-state is defined as LED's threshold voltage. The slope within the LED forward biased region is defined as LED’s dynamic resistance, which is usually a relatively small value. As a result, if driving LEDs with a voltage source, even a small voltage variation can cause large current change, which will affect the brightness of LEDs dramatically [10].

As a silicon-based device, LED shows negative temperature coefficient. In other words, the LED forward voltage will decrease when junction temperature increases. From this point of view, driving LEDs with a voltage source is not desirable either because even the voltage source can be kept constant, the temperature change will cause LED forward current to change under the same forward voltage.

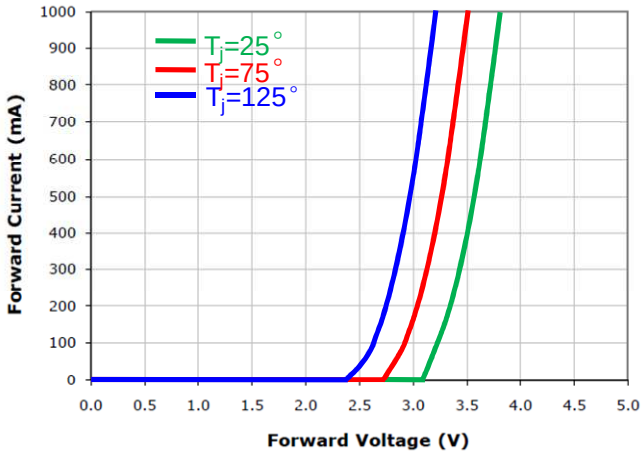


(a) Real model

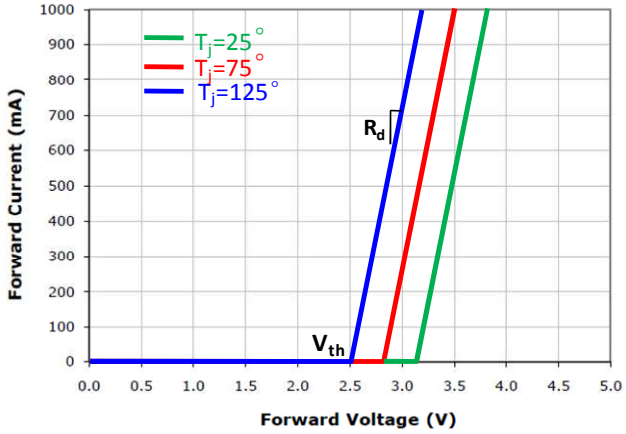


(b) Simplified piece-wise-linear model

**Figure 1. 5 LED i-v Character**

To describe the LED's nonlinear i-v character, the relationship between LED's forward current and voltage can be represented by the following piece-wise function:

$$I_o = \begin{cases} \dfrac{V_o - V_{th}}{R_d} & when\, V_o > V_{th} \\ 0 & when\, V_o \le V_{th} \end{cases}$$

In summary, based on the LED i-v character discussed above, a current source LED driver instead of voltage source is more desirable for good brightness control. Generally speaking, there are two common types of LED driver, as shown in Fig. 1.6.

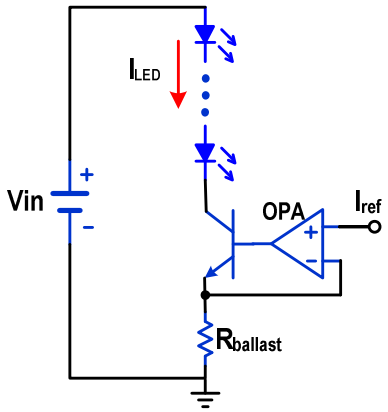


(a) Linear regulator

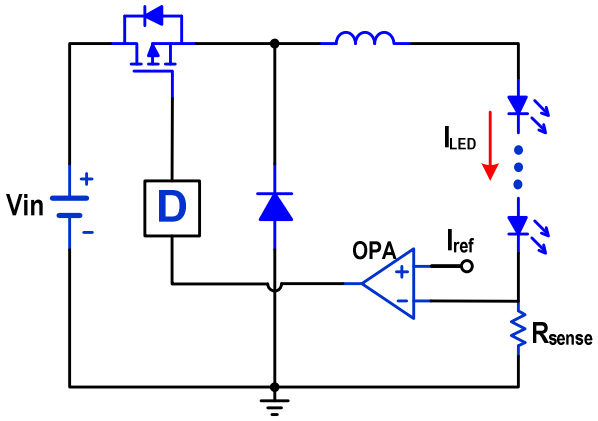


(b) Switch mode regulator

**Figure 1. 6 Two Types of LED Drivers**

The linear regulator is very simple and cost effective to provide current source and drive LEDs [11]. It also has the advantage of current sharing capability for multiple LED string configuration by using current mirror. However, the power dissipation on the

ballast resistor is large so that this type of LED driver is usually suitable for applications with LED forward current less than 100 mA.

Another widely used type of LED driver, the switch mode regulator, can provide independent accurate current control and achieve high efficiency as well [12]. This type of LED driver is suitable for applications with LED forward current from hundred milliameres up to several amperes. However, cost of this LED driving solution is high, especially for large LED luminaries with dozens or even hundreds of LED units in which multiple switch mode LED drivers are needed.

## 1.2 Review of Traditional LED Driver Solutions for Indoor Lighting

Based on the research from U.S. Department of Energy [13], total electric consumptions in U.S. are over 2390 TWh, 30% of which is for lighting. As a promising lighting source, the best opportunity and widest marketing for LEDs is various lighting applications, such as indoor lighting, outdoor lighting, industrial lighting, architectural lighting etc. Among these applications, the indoor lighting (including residential and commercial buildings) takes over 75% power consumptions. In this thesis, the LED driving solution for indoor lighting application is stressed and investigated thoroughly.

Fig. 1.7 shows some future indoor applications by using LED luminaries. As the total lumen demands for such applications increase, the number of LED units in the whole luminaries also increases, in some cases over 50 or even higher. The forward voltage of each LED unit is about 3.5V under several hundred milliamperes to one ampere current. If all the LED units are connected in series, the total string voltage will be several hundred volts, which is a big concern from the safety point of view. Moreover,

if open failure happens in one or more LED units, the whole LED luminaries needs to be shut down if there are no other open circuit protections.

(a) LED wall

(b) Decorative lighting

(c) Ceiling lamps

**Figure 1. 7 Examples of Future Indoor LED Luminaries**

Consequently, considering the reliability and safety issues, multi-channel LED configuration is widely used in these indoor LED luminaries, as shown in Fig. 1.8. Active current control with linear or switch regulator is necessary for precise current sharing for multi-channel LED configurations.

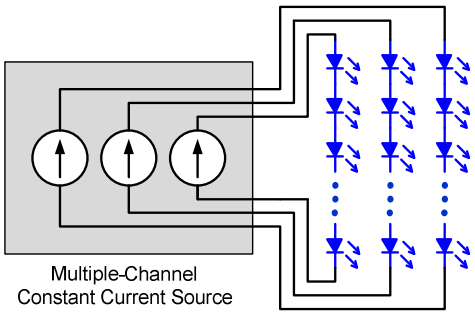


**Figure 1. 8 Multi-Channel LED Configuration**

How to generate multi-channel constant current ($MC^3$) sources and achieve current sharing are two major issues and challenges in this type of LED driver design. Some papers have been devoted to propose some driving solutions and current sharing methods [14]-[17]. There are also some commercial controllers to provide $MC^3$ solutions from main power management IC companies like Texas Instruments, Maxim Integrated Products, National Semiconductor, Intersil, MPS etc. The most popular $MC^3$ LED driver uses a two-stage structure, as shown in Fig. 1.9.

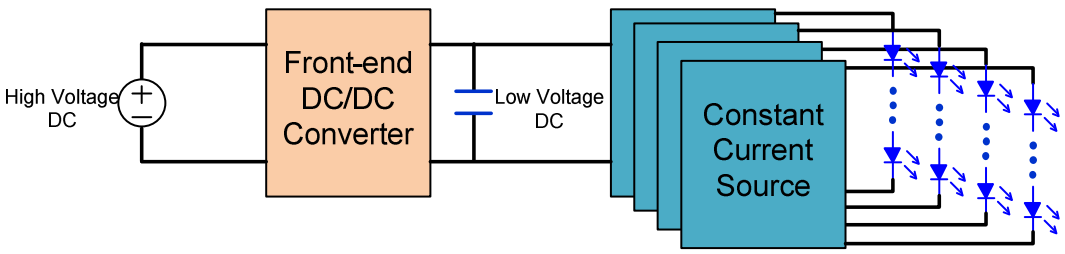


**Figure 1. 9 Traditional Two-stage $MC^3$ LED Driver Structure**

The first front-end DC/DC converter stage steps down the high voltage DC input to a low DC voltage level and usually also provides isolation. The second constant current source stage provides multiple constant current sources to drive several LED strings. Through a survey of commercial products, the traditional indoor LED driver solution can be classified into two types, as illustrated in Fig. 1.10.

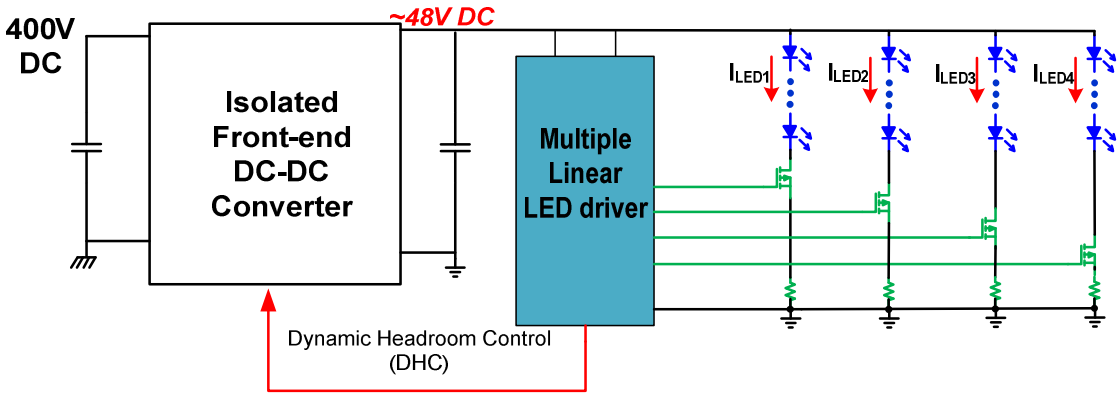


(a) Linear LED driver

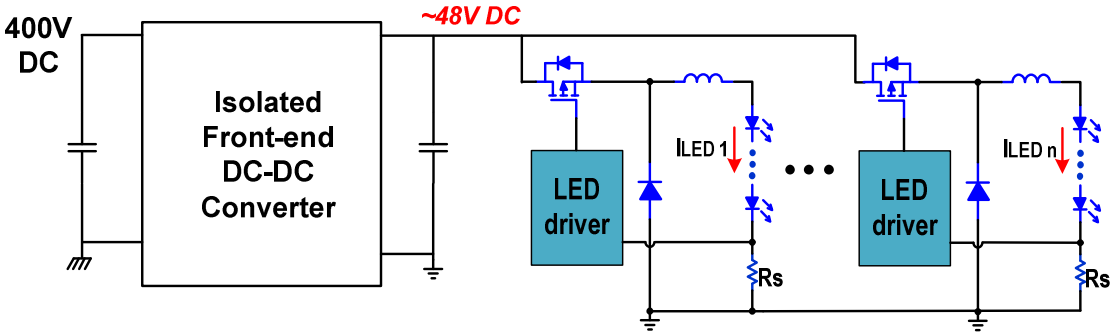


(b) Switch mode LED driver

**Figure 1. 10 Review of Traditional Indoor LED Driver Solutions**

The solution shows in Fig. 1.10 (a) is the most cost effective [18]-[20]. In order to improve the efficiency, the dynamic headroom control (DHC) is also proposed and used in some commercial products. The forward voltages of multiple LED strings are sensed and processed in real-time so that the voltage output level of the frone-end DC/DC stage is adaptively controlled to equal to the highest LED string voltage plus a certain headroom voltage. The independent current regulation can also be achieved in this solution. There are several commercial ICs such as TLC5690, LM3464, MAX16823 adopting this structure and control strategy. However, even though DHC is adopted, when facing with unbalanced LED string condition or LED short failure in some of the strings, in order to keep current regulation and current, the loss on the linear regulator will become huge and damage the driver's overall efficiency very much.

The switch mode LED driver solution in Fig. 1.10 (b) can overcome the drawbacks mention above [21]-[24]. In this solution, each LED string has completely independent current control; no matter how unbalanced one or more LED strings could be, other LED strings can always operate normally without any changes from the current control point of view. Hence this solution has the best robustness to the LED forward voltage variations and short failures. Also many commercial ICs can be used in this solution, such as TPS54160, LM3402, MP4688, MAX16832 etc. Obviously the system structure in this solution is complicated and the cost is high. Especially when the system of LED luminaries become larger and larger, the number of LED strings also increases. Each LED string needs a independent power stage as well as control circuit to provide current source, which will increase the total cost dramatically.

In summary, how to design a simple, low cost and efficient multi-channel constant current LED driver is a challenge. In this thesis, a single-stage $MC^3$ LED driver idea has been proposed and investigated through two different topologies (PWM half-bridge topology and LLC resonant topology), which will be addressed in details in Chapter 3 and Chapter 4.

## 1.3 Objectives and Thesis Outline

LEDs as a promising lighting source, have great opportunity and marketing prospective in many applications such as indoor & outdoor lighting, backlight, automotive, architectural lighting etc. The LEDs are preferred to be driven by current source and the driver should be designed carefully. From power electronics point of view, how to design a simple, low-cost and efficient LED driver is a challenge. This thesis focuses on the indoor lighting application with multiple LED string configuration and proposes a new single-stage multi-channel constant current ($MC^3$) LED driver to simplify the system architecture, improve efficiency and achieve current sharing capability.

The driving solution for an indoor LED luminaries with multiple strings based on the DC nano grid for future sustainable building initiative will be tackled in this thesis. The whole system structure is shown in Fig. 1.11.

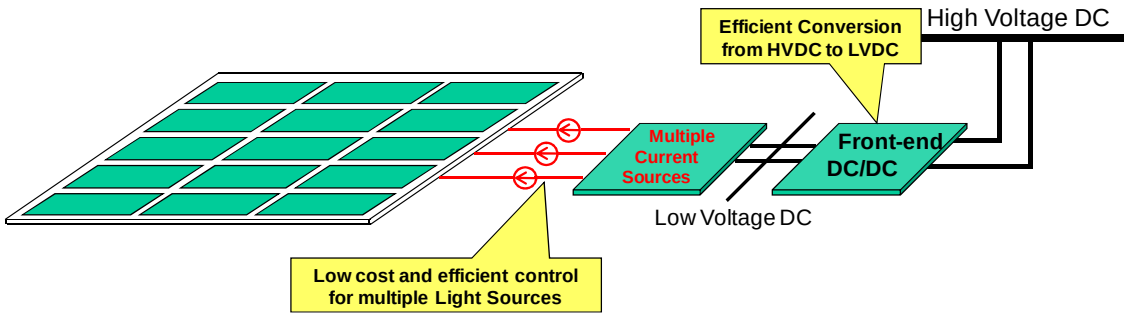


**Figure 1. 11 Example of Indoor LED Luminaries in DC Nano Grid**

On the left hand side, the flat luminaries emulate a future indoor LED luminaries with total 64 LED units, which are divided into four strings. The specifications of the system and LED luminaries are summarized in Table 1.1.

**Table 1. 1 Specifications of the DC Nano Grid and Indoor LED Luminaries**

| | |
|---|---|
| DC input voltage $V_{in}$ | 380V±20V |
| LED channel threshold voltage $V_{th}$ | 40V±5V |
| LED channel current $I_o$ | 1A |
| LED channel dynamic resistor $R_d$ | 10Ω |
| Total LED string number | 4 |
| Maximum current difference | <10% |

As shown in Fig. 1.11, the driving solution for this indoor LED luminaries application should have two basic functions: firstly, the driving solution provides the step-down function from a high voltage DC bus (~380V) to a mid level DC voltage with isolation; secondly, multiple constant current sources can be generated to driving multiple LED strings. Current sharing is also required between multiple current sources.

From the previous discussion and survey on traditional solutions, we can find out the drawbacks and bottlenecks of traditional solutions. As a result, a new driving solution is in great demand to provide a simple, low-cost and efficient solution. Generally speaking, there are three challenges for this $MC^3$ LED driver design:

1. Simplify the system architecture;

2. Achieve current sharing between multiple LED strings;

3. Good robustness to LED forward voltage variation & failure mode.

The outline of this thesis is as follows:

Chapter 1 introduces some basic concepts of LEDs and driving requirements. Then focusing on the indoor lighting application, some traditional solutions are reviewed and their advantages & disadvantages are discussed.

In order to simplify the system architecture, a single-stage $MC^3$ LED driver is proposed, using multiple transformer structure to provide multiple current sources. In Chapter 2, a PWM half bridge topology is used to realize the proposed concept. The circuit is analyzed in details and a mathematical solution is solved to describe the current cross regulation between multiple LED strings. Some factors which affect the current sharing are found out and analyzed. A simulation model is built by Simplis simulation tool to verify that the circuit has very good robustness to LED forward voltage variations and LED short failures. Some drawbacks of the single-stage $MC^3$ PWM LED driver are also discussed at the end of Chapter 2.

Chapter 3 proposes a new $MC^3$ LED driver by using LLC resonant converter to overcome the drawbacks of $MC^3$ PWM LED driver topology. Different from traditional front-end LLC converter, the proposed $MC^3$ LLC LED driver is controlled to provide current source output. LLC voltage and current gain characteristic is derived after considering the LED i-v character for the design purpose. A design procedure is proposed based on the modified LLC current gain characteristic. A 100kHz 4-channel $MC^3$ LLC LED driver is designed and tested to verify the design procedure and current sharing capability. Some dimming methods are also investigated.

Chapter 4 summarizes the conclusions and discusses some ideas for future work.

# Chapter 2. Proposed Single-stage $MC^3$ PWM LED Driver

## 2.1 Structure of Proposed Single-stage $MC^3$ PWM LED Driver

In traditional $MC^3$ LED driver solutions, a two-stage structure is widely used. Although by using such structure, independent current control and current sharing can be achieved between multiple LED strings, there are also some drawbacks. Firstly, both stages need one or more controllers. Especially in the second stage, each LED string needs a controller to control the output current individually. Therefore, this structure is complicated and expensive; furthermore, the two-stage solution also sacrifices the efficiency to some extent. On the other hand, the price of LED driver is very sensitive to the market. Low cost but efficient solution is in great demand.

In order to simplify the system structure, a single-stage $MC^3$ LED driver structure has been proposed, as shown in Fig. 2.1 [25]. Basically, the front-end DC/DC stage and multiple constant current source stage are combined together to be a single stage, which serves the same functions as both stages do in traditional solution at the same time.

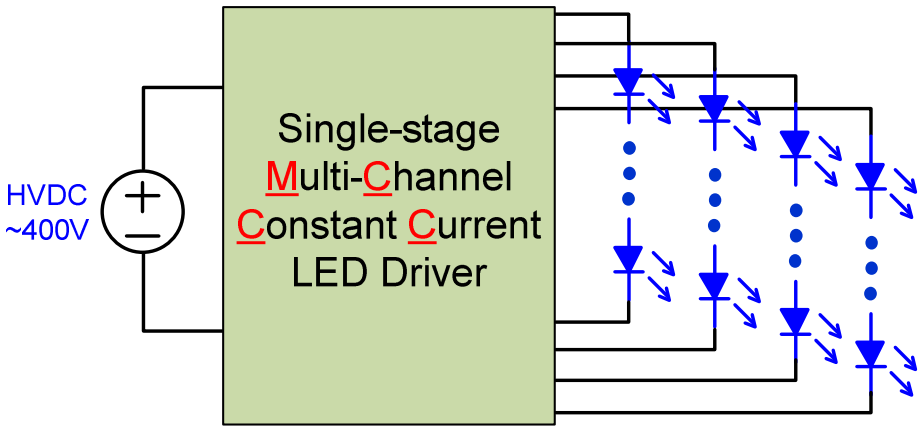


**Figure 2. 1 Structure of Proposed Single-stage MC$^3$ LED Driver**

The structure above just proposes an general idea of simplifying the system's complexity. The key point is how to implement this idea by some suitable topology structure. Essentially, this single-stage MC$^3$ LED driver is still a front-end DC/DC converter, which should have the step down function from high voltage DC bus to low voltage DC bus and provide isolation. At the same time, it should also have the function with multiple current source outputs.

When recalling the traditional DC/DC converter with multiple voltage sources outputs, the transformer structure shown in Fig. 2.2 (a) is very common [26][27]. By employing multiple secondary windings to the same primary winding of the transformer, multiple voltage source outputs can be generated. If the turns ratio of each secondary winding to primary winding is kept the same, the multiple outputs have the same voltage level.

Back to the requirement in the single-stage MC$^3$ LED driver, instead of multiple voltage source outputs, multiple current source outputs are needed to drive multiple LED

string, which is exactly a dual case. As a result, a dual circuit of multiple transformer structure with multiple current sources can be drawn in Fig. 2.2 (b).

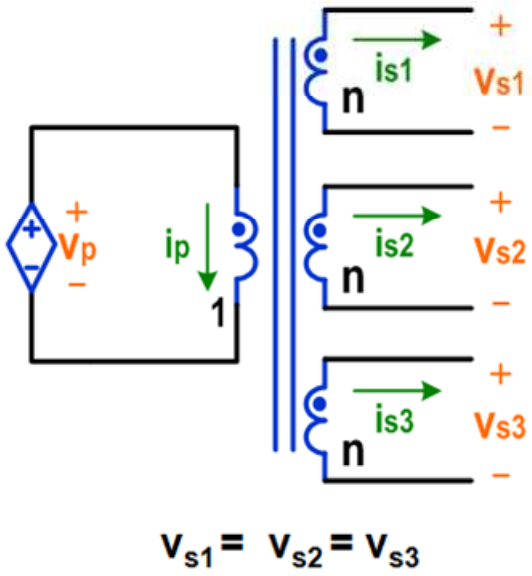


(a) Multiple voltage source outputs

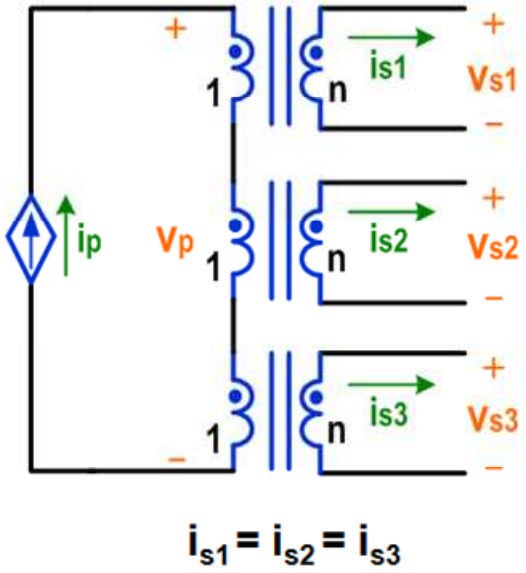


(b) Multiple current source outputs

**Figure 2. 2 Multiple Transformer Structure**

Different from multiple voltage source output case, multiple transformers with independent cores are used. The primary windings of each transformer are connected in series while the secondary windings are connected in parallel. It is easy to see that the primary windings of each transformer share the same current. If the turns ratio of each transformer is designed to be identical, each transformer's secondary current is forced to be identical too. By employing this multiple transformer structure, as long as the primary current is controlled to be current source, multiple current source outputs can be generated on each transformer's secondary side, which are connected in parallel and drive the load independently.

Taken PWM half-bridge topology as an example, the circuit schematic of the proposed single-stage $MC^3$ LED driver is illustrated in Fig. 2.3.

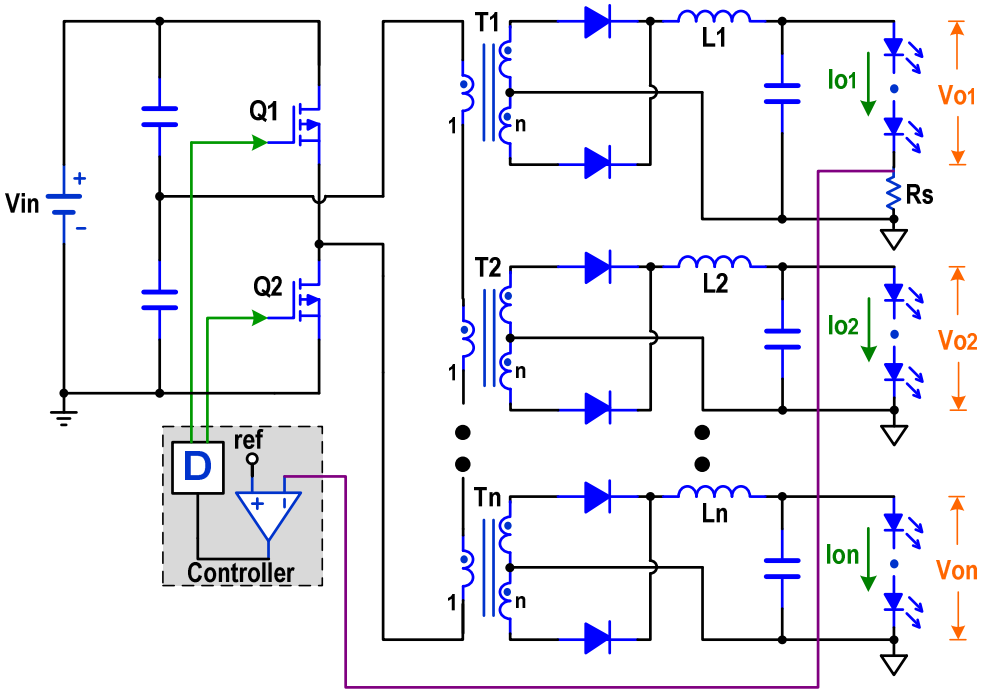


**Figure 2. 3 Circuit Schematic of a Single-stage $MC^3$ PWM LED Driver**

Compared to traditional PWM half bridge converter with single voltage source output, the multiple transformer structure is adopted for multiple output purpose. In order to provide current source to drive LEDs, one LED string current is sensed through a sensing resistor to control the primary side MOSFETs' duty cycle. Other LED strings' currents are cross regulated. By adopting this structure, the control scheme is simplified and only one controller is needed, which can also reduce the cost.

For this control scheme for multiple current source outputs, the key issue is the current sharing between different LED strings, especially when the LED strings are not perfectly balanced. In the next section, the detailed operating waveforms are analyzed and a mathematical solution is derived to quantify the current sharing capability.

## 2.2 Current Cross Regulation (CCR) Analysis

Theoretically, if the circuit is symmetrical and the component values have no tolerance, as long as one LED string's current is sensed and controlled, other LED strings' currents can be perfectly cross regulated. However, in practical application, the LED strings always have some mismatches, mainly because of two reasons:

1. LED i-v character variation

In the manufacturing of LED units, there is a variation of performance around the average values given in the technical data sheets, such as luminous flux (brightness), color and forward voltage. The LEDs also have negative temperature coefficient, which can cause its i-v character change in a certain range. As a result, even driven by the same forward current, the forward voltage of different LED units may vary within a certain range, which can cause mismatched LED string condition.

2. LED short failure

LED short failure can also occur sometimes during normal operating condition. When one or more LED units fail in short failure in one LED string, the forward voltage of that string will be lower than others'.

In practice, the mismatched LED string condition is pretty common and that will downgrade the current sharing capability. The current cross regulation under unbalanced LED string condition needs to be analyzed in details.

### 2.2.1 Analysis for two-string case

Taken a two-string $MC^3$ LED driver case for example, the circuit diagram and operation waveforms are shown in Fig. 2.4. Assuming mismatched LED strings ($V_{o1}>V_{o2}$), same output inductance ($L_1=L_2$) and CCM operation mode, ignoring the impact of transformer magnetizing inductance and leakage inductance, the output current cross regulation is analyzed in detail as follows.

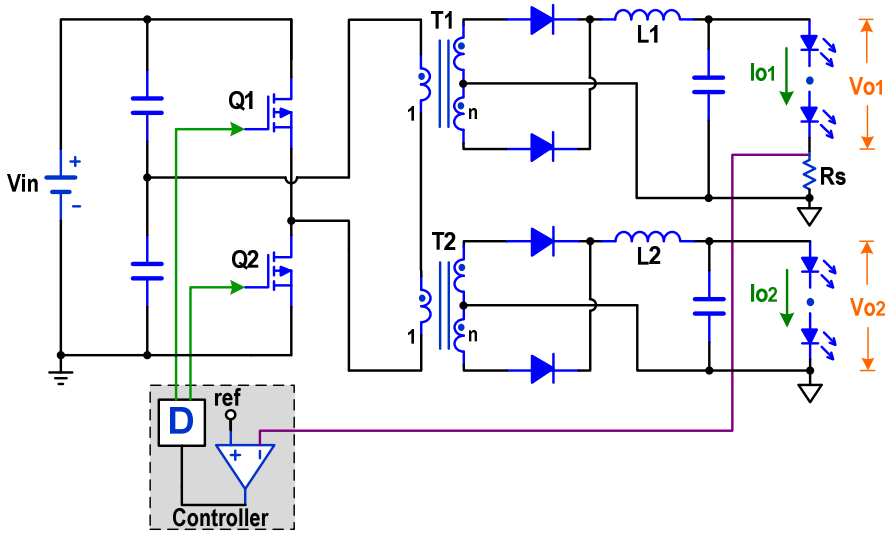


**Figure 2. 4 Example of a Two-string $MC^3$ PWM LED Driver for CCR Analysis**

The key waveforms at steady state are shown in Fig. 2.5. During one half switching cycle, the circuit has three operating modes and during the other half cycle those operating modes repeat. The equivalent circuits of each mode are shown in Fig. 2.6.

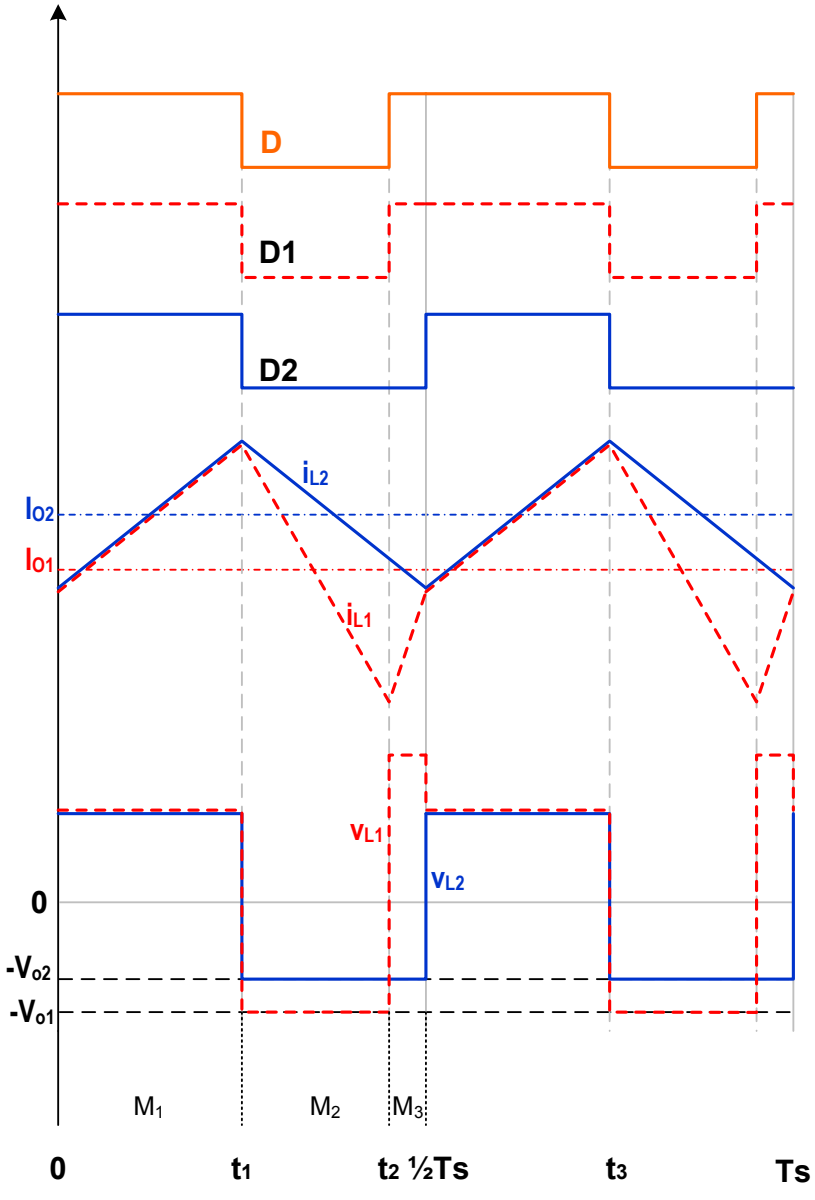


**Figure 2. 5 Key Waveforms at Steady State of a Two-string MC$^3$ PWM LED Driver**

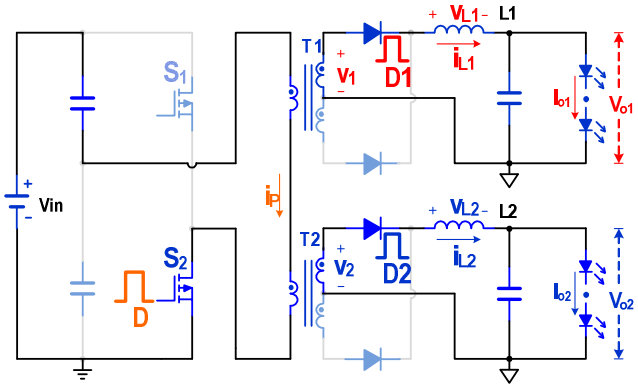


(a) Mode 1

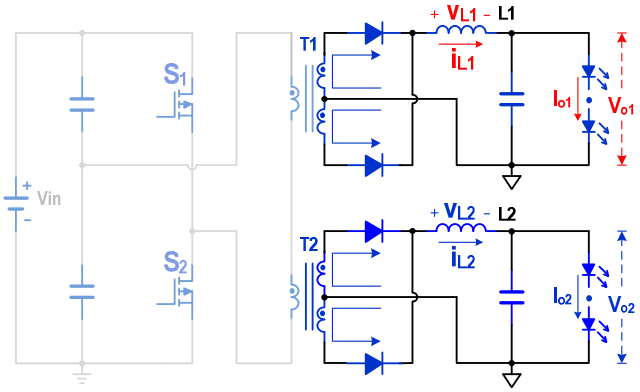


(b) Mode 2

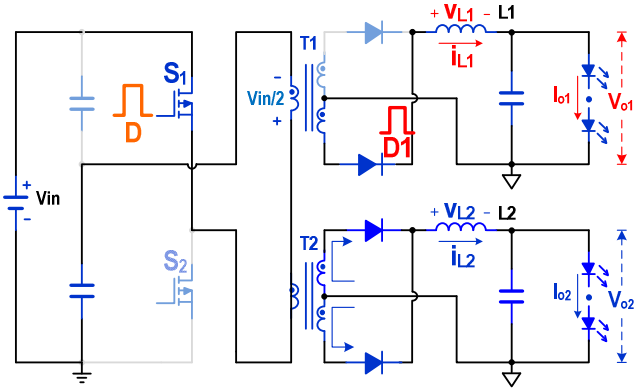


(c) Mode 3

**Figure 2. 6 Equivalent Circuits during One Half Switching Cycle**

Mode 1 [0~$t_1$]: one of primary side switches $S_2$ in the half bridge is turned on; input voltage is applied on both transformer $T_1$ and $T_2$. According to the multiple transformer structure, the primary side currents of two transformers are identical, and so do the secondary side currents. Therefore, during this period, the currents of inductor $L_1$ and $L_2$ are equal. The voltages applied on two output inductors are equal too. Set $V_1$ and $V_2$ as the secondary winding voltages of $T_1$ and $T_2$, and $V_{o1}$ and $V_{o2}$ as the output string voltages, then we can get the following equation for the output inductor currents:

$$L\frac{di_{L1}}{dt} = V_1 - V_{o1} \tag{2.1}$$

$$L\frac{di_{L2}}{dt} = V_2 - V_{o2} \tag{2.2}$$

$$i_{L1} = i_{L2} \tag{2.3}$$

Mode 2 [$t_1$~$t_2$]: both of primary side switches are turned off; all secondary side diodes are on for current freewheeling; both transformer $T_1$ and $T_2$ are shorted. During this period, the voltages applied on two output inductors equal to minus of the two string voltages respectively, which are different due to mismatched LED string condition. So for the currents of output inductor $L_1$ and $L_2$ we have:

$$L\frac{di_{L1}}{dt} = -V_{o1} \tag{2.4}$$

$$L\frac{di_{L2}}{dt} = -V_{o2} \tag{2.5}$$

Because the output string voltage are mismatched and $V_{o1}>V_{o2}$, the inductor currents $i_{L1}$ and $i_{L2}$ are different too and:

$$i_{L1} < i_{L2}$$

Mode 3 [$t_2$~$1/2T_s$]: at moment of $t_2$, another primary switch $S_1$ is turned on. Because the instantaneous inductor currents are different and $i_{L1} < i_{L2}$, the transformer $T_2$ is still shorted and all input voltage applied on transformer $T_1$. The diodes of LED string 2 are still freewheeling until the moment of $1/2T_s$, when the two inductors' current are equal. Therefore, the equivalent duty cycle $D_1$ and $D_2$ of diodes in two strings are not equal either and $D_1 > D_2$. During this period we have:

$$L\frac{di_{L1}}{dt} = V_s - V_{o1} \tag{2.6}$$

$$L\frac{di_{L2}}{dt} = -V_{o2} \tag{2.7}$$

Where Vs is the sum of two transformers' secondary side voltage:

$$V_s = V_1 + V_2$$

During this period, the inductor currents $i_{L1}$ and $i_{L2}$ are still different:

$$i_{L1} < i_{L2}$$

From $1/2T_s$ to $T_s$, the other half switching cycle starts, and the operation principle and waveforms are the same except the polarity changes.

Define $I_{o1}$ and $I_{o2}$ are the DC average output currents of two LED strings (which also equal to the average output inductor current), and $\Delta I_{max}$ represents the current difference between two LED strings. From equations above, we can derive:

$$\Delta \mathrm{I}_{\max} = I_{o2} - I_{o1} \tag{2.8}$$

$$\Delta \mathrm{I}_{\max(2)} = \frac{1}{2 \cdot f_s \cdot L} \cdot \left(D_1 - D_2\right) \cdot \left(V_s - V_{o1} - V_{o2}\right) \tag{2.9}$$

Where $D_1$ and $D_2$ represent the conduction time during one switching cycle for secondary rectifier diodes in LED string 1 & 2:

$$D_1 = \frac{1}{2} \frac{V_{o1} + V_{o2}}{V_s}$$

$$D_2 = \frac{V_{o2}}{V_s - V_{o1} + V_{o2}}$$

From the equation (2.9), we can find out that the current cross regulation is related to the different conduction time of two diodes $D_1$ and $D_2$, which is also determined by the difference between LED strings' output voltage $V_{o1}$ and $V_{o2}$. The larger the LED strings' voltage difference is, the worse current cross regulation between multiple LED strings will be. Moreover, the switching frequency and output inductance also impact the current cross regulation, which will be discussed in the following sections.

### 2.2.2 Analysis for n-string case

The similar analysis method can also be extended to the N-string $MC^3$ PWM LED driver, as shown in Fig. 2.3. Still considering the mismatched LED string condition, we assume that the voltages of each LED string satisfy the equation below:

$$V_{o1} > V_{o2} > V_{o3} > \cdots > V_{on}$$

The definition of $\Delta I_{max}$ is the current difference between the LED string with maximum current and the LED string with minimum current. For a N-string case, the mathematical equation of $\Delta I_{max}$ can be derived and extended from (2.9), which is shown as (2.10).

$$\Delta I_{\max(n)} = \frac{1}{2 \cdot f_s \cdot L} \cdot \left( \Delta D_1 + \frac{\Delta D_2}{2} + \cdots + \frac{\Delta D_{n-1}}{n-1} \right) \cdot \left( V_s - \sum_{j=1}^{n} V_{oj} \right) \qquad (2.10)$$

Where $D_k$ still represents the conduction time during one switching cycle for the secondary rectifier diode in LED string k:

$$D_k = \frac{1}{2} \cdot \left( 1 - \frac{V_s - \sum_{j=1}^{n} V_{oj}}{V_s - \left[ V_{o1} + V_{o2} + \cdots + V_{o(k-1)} - (k-1) \cdot V_{ok} \right]} \right)$$

$$\Delta D_k = D_k - D_{k+1}$$

The equation (2.10) provides a general model to describe the current cross regulation between multiple LED string outputs mathematically. By using this model, factors which affect current cross regulation can easily be found out and analyzed.

### 2.2.3 Factors affecting current cross regulation

In practice, for the multi-channel LED application, the tolerance of current difference between multiple strings is usually less than 10%. In order to verify the current sharing capability and current cross regulation of proposed circuit, a simulation model of a 4-string $MC^3$ PWM LED driver is built by Simplis simulation tool. The circuit diagram is shown in Fig. 2.7.

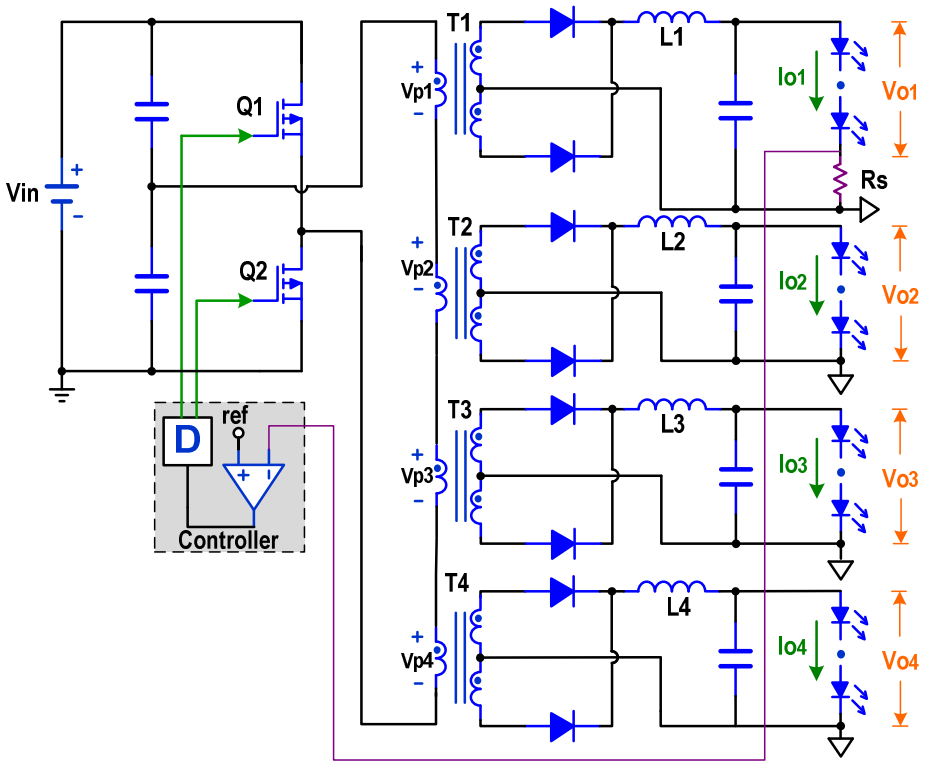


**Figure 2. 7 Simulation Verification of a 4-string $MC^3$ PWM LED Driver**

The input voltage is 400 V DC. The LED string current is 1 A and the LEDs numbers of each string are specially set as 13, 14, 15 and 16 are about to emulate the unbalanced LED string condition. The output inductance is 30uH and switching frequency is chosen to be 300 kHz.

The circuit is simulated in Simplis and the output inductor current waveforms are shown in Fig. 2.8.

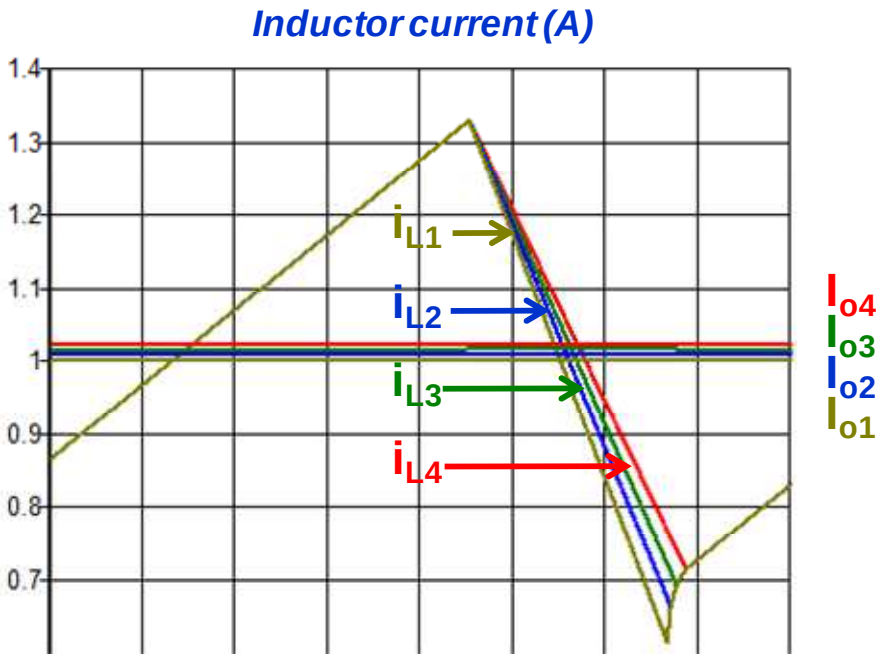


**Figure 2. 8 Simulation Waveforms of 4-string Output Inductor Current**

The simulation clearly shows the inductor current difference during Mode 2 and Mode 3 as discussed in previous section. Since the current of LED string 1 is controlled, the simulation result shows $I_{o1}$=1.000A as expected. Although 4 LED strings are unbalanced, the maximum current difference (between LED string 1 and string 4) is only 20 mA, only 2% of full load current.

Based on the mathematical solution derived in previous section, the LED string current can also be calculated. The results are summarized in Table 2.1.

**Table 2. 1 Current Cross Regulation for 4-string MC$^3$ PWM LED Driver**

| | LED Number | Vo (V) | Io (A) |
|---|---|---|---|
| String 1 | 16 | 49.1 | 1.000 |
| String 2 | 15 | 45.9 | 1.008 |
| String 3 | 14 | 42.6 | 1.014 |
| String 4 | 13 | 39.4 | 1.021 |
| $\Delta I_{max}$ (%) | 2.1% | | |

The calculation results shows the maximum current difference is 21 mA, matching with the simulation results very well.

From the equation (2.10), we notice that there are another two factors which affect the current cross regulation - the switching frequency and output inductance. So the current cross regulation is also calculated with two different switching frequency and output inductor values, as shown in Table 2.2.

**Table 2. 2 Factors Affecting Current Cross Regulation ($f_s$ & L)**

| | | | String 1 | String 2 | String 3 | String 4 |
|---|---|---|---|---|---|---|
| LED Number | | | 16 | 15 | 14 | 13 |
| Voltage (V) | | | 49.1 | 45.9 | 42.6 | 39.4 |
| fs=300 kHz | L=30 uH | Current (A) | 1.000 | 1.008 | 1.014 | 1.021 |
| | | $\Delta I_{max}$ (%) | | | | **2.1%** |
| | L=60 uH | Current (A) | 1.000 | 1.004 | 1.007 | 1.011 |
| | | $\Delta I_{max}$ (%) | | | | **1.1%** |
| fs=600 kHz | L=30 uH | Current (A) | 1.000 | 1.004 | 1.007 | 1.011 |
| | | $\Delta I_{max}$ (%) | | | | **1.1%** |
| | L=60 uH | Current (A) | 1.000 | 1.002 | 1.004 | 1.006 |
| | | $\Delta I_{max}$ (%) | | | | **0.6%** |

From the table above, we can see that higher switching frequency or larger output inductance can help improve the current cross regulation and reduce the current difference between multiple LED strings. In all the four cases in Table 2.2, the maximum current difference is only 2.1%, showing the proposed circuit has good current sharing capability even with unbalanced LED string conditions.

## 2.3 System Robustness to Unbalanced LED Conditions

In previous section, the current cross regulation of proposed circuit has been verified for a slightly unbalanced LED condition. However, in practice, the unbalance conditions

of LED string load could be even more severe. For example, there may be more LED units failing in short in one string; or even worse, several LED strings may have LED units failing in short at the same time. Either condition may further downgrade the current cross regulation between multiple LED strings.

In the section, the system robustness is studied for several severe unbalanced LED conditions. Still taken a 4-string $MC^3$ PWM LED driver shown in Fig. 2.7 as example, the input voltage is 400 V. Each LED string has 16 LED units in series under normal operating condition and string current is 1 A. The switching frequency is 300 kHz and output inductance is 30 uH. In order to emulate some severe unbalanced LED conditions, two assumptions have been made:

1. One or more LED strings have LEDs in short failure;

2. The number of short LEDs in failure strings are equal.

Then three unbalanced LED conditions are simulated: only one LED string fails in short; two LED strings fail in short; three LED strings fail in short. During the simulation, the number of short LEDs in each failure string gradually increases and the maximum current difference is plotted in Fig. 2.9.

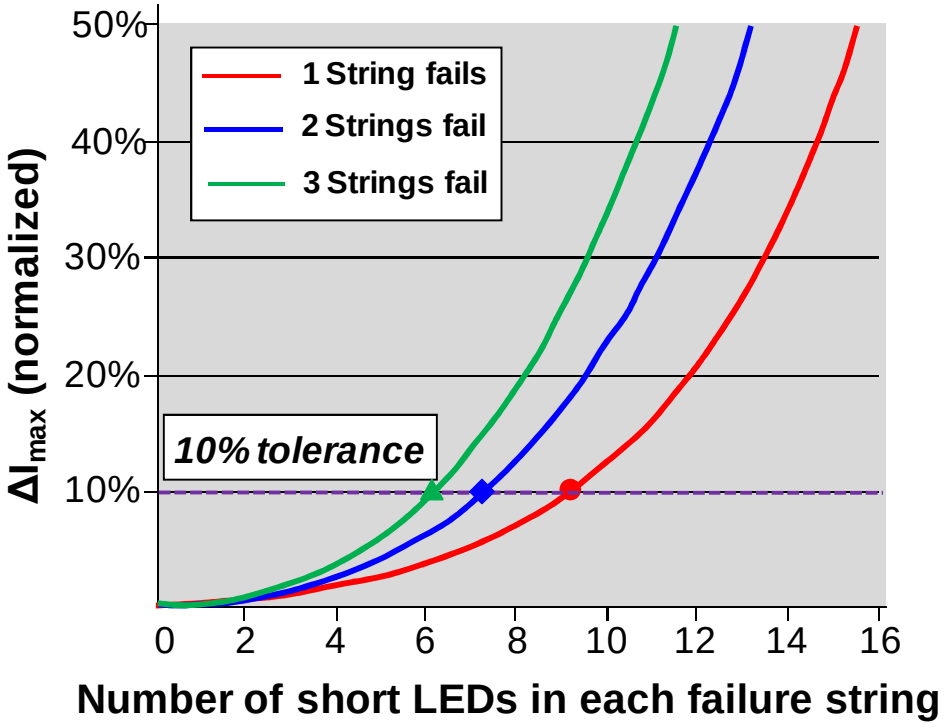


**Figure 2. 9 System Robustness to Unbalanced LED Conditions**

For only one string in short failure case, when there are 9 LEDs failing in short failure, the maximum current difference is still under 10% tolerance. That means even more than half of the whole string fails in short, the current sharing can still satisfy 10% difference requirement.

When two or three strings fails in short, the current cross regulation will become worse because of more severe unbalanced condition. However, the simulation results in Fig. 2.9 shows the circuit still has good robustness. For the case with two strings in short failure, the maximum current difference can be obtained under 10% with 7 LEDs in short failure. The worst case is when there are three strings in short failure at the same time. Even under such severe condition, the maximum current difference can be obtained under 10% with 6 LEDs in short failure.

## 2.4 Limitations of Proposed Single-stage $MC^3$ PWM LED Driver

Although comparing to the traditional two-stage $MC^3$ LED driver, the proposed single-stage $MC^3$ PWM LED driver has many advantages such as, simpler structure, higher efficiency, low cost, easy control scheme etc., this circuit still have some drawbacks and limitations, such as:

1. Hard switching topology

Because the proposed $MC^3$ PWM half bridge LED driver is a hard switching topology, the switching loss is higher compared to other soft switching PWM circuits and resonant converters. This feature will also limit the potential of further pushing to higher efficiency and achieving higher density.

2. Bulky transformer and output inductor

Due to the structure of proposed circuit, for each LED string, one transformer and one output inductor are needed to provide current source. Furthermore, in order to improve current cross regulation between multiple LED strings, larger output inductor is desirable because it can reduce the current difference. As a result, the whole system may become bulky, especially when the total number of LED strings increases. This is another limitations of achieving high power density for the proposed $MC^3$ LED driver structure.

How to overcome the limitations above and improve the performance of $MC^3$ LED driver is still challengeable. Considering that such limitations are related to the PWM half bridge topology, probably we need to investigate some new topologies with different features, which will be discussed in Chapter 3.

## 2.5 Summary

A single-stage $MC^3$ LED driver structure is proposed to simplify the complexity of multiple LED driving scheme, reduce cost and improve efficiency. Multiple transformer structure is used to provide multiple current source outputs. Compared to traditional two-stage $MC^3$ LED driver solutions, the proposed structure can not only achieve high efficiency, but also simplify the system complexity and reduce cost.

A PWM half bridge topology is chosen to implement the proposed concept. In order to analyze the current cross regulation under unbalanced LED conditions, a general model is derived. From the derived model it can be noticed that unbalanced LED conditions will cause different conduction time of secondary rectifier diodes and hence downgrade the current cross regulation. Moreover, switching frequency and output inductor also can affect currnt sharing between multiple LED strings. Through simulation verification for various unbalanced conditions, the proposed circuit shows good robustness to LED forward voltage variation and short failure.

Finally, some drawbacks and limitations of proposed single-stage $MC^3$ PWM LED driver are discussed. Such limitations are related to the internal character of PWM half-bridge topology. In order to overcome those limitations and further improve efficiency of the $MC^3$ LED driver, a new topology are investigated to implement the multiple transformer structure in the next chapter.

# Chapter 3. Proposed $MC^3$ LLC Resonant LED Driver

## 3.1 Structure of Proposed $MC^3$ LLC Resonant LED Driver

In Chapter 2, a single-stage $MC^3$ PWM LED driver has been proposed to replace traditional two-stage solutions in order to simplify the system architecture, reduce cost and improve efficiency. The proposed circuit has also been simulated and verified to have good current sharing capability and robustness. However, it still has several drawbacks which have been discussed in the last part of previous chapter.

In order to overcome the drawbacks discussed above, instead of PWM half bridge topology, a LLC resonant converter is used to implement the proposed single-stage $MC^3$ LED driver concept. The circuit schematic of proposed $MC^3$ LLC resonant LED driver is shown in Fig. 3.1 (taken a 4-string case as example).

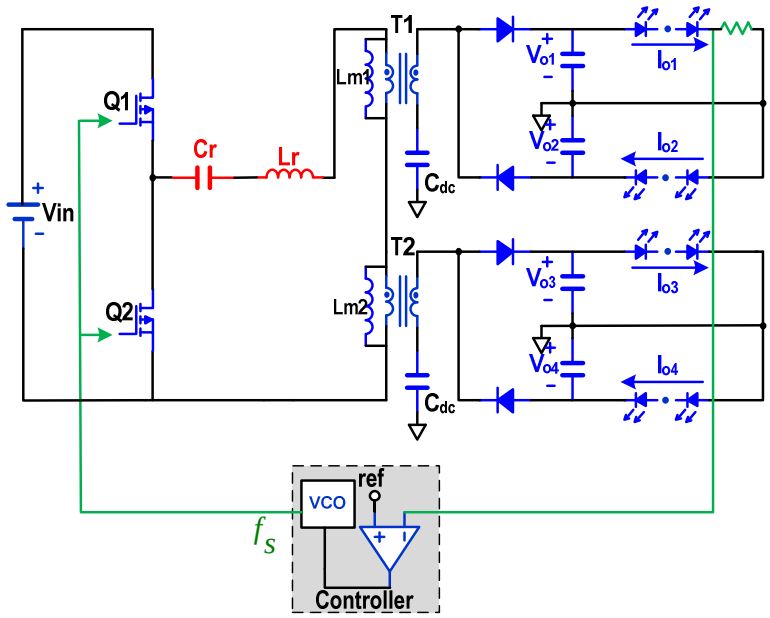


**Figure 3. 1 Circuit Schematic of a Single-stage MC$^3$ LLC Resonant LED Driver**

Compared to the MC$^3$ PWM LED driver, the MC$^3$ LLC resonant LED driver have several characters and advantages [28][29]:

1. The LLC resonant converter has the ZVS capability from the primary side MOSFETs from zero to full load range, and the turn off current is also low. The switching loss is reduced compared to PWM hard switching topology, so the converter has the potential to operate at higher efficiency and achieve higher power density.

2. The output inductor in LLC resonant converter is eliminated. For the application with multiple LED strings, by eliminating output inductors, the cost can be reduced and the power density can also be improved.

3. The transformers adopt voltage-doubler configuration on the secondary side so that each transformer drives two LED strings at the same time and the number of transformers can be reduced by half.

4. The multiple transformer structure is still utilized to provide multiple current source outputs, which has already been discussed in Chapter 2. Besides, a DC block capacitor is also utilized to achieve precise current sharing between two LED strings driven by the same transformer through voltage-doubler configuration, which is first proposed in [30]. The dc block cap $C_{dc}$ is in series with the transformer's secondary winding and used to balance the forward voltage difference between two LED strings. In order to analyze the function of this DC block capacitor, a simplified LLC equivalent circuit with two LED strings are shown in Fig. 3.2.

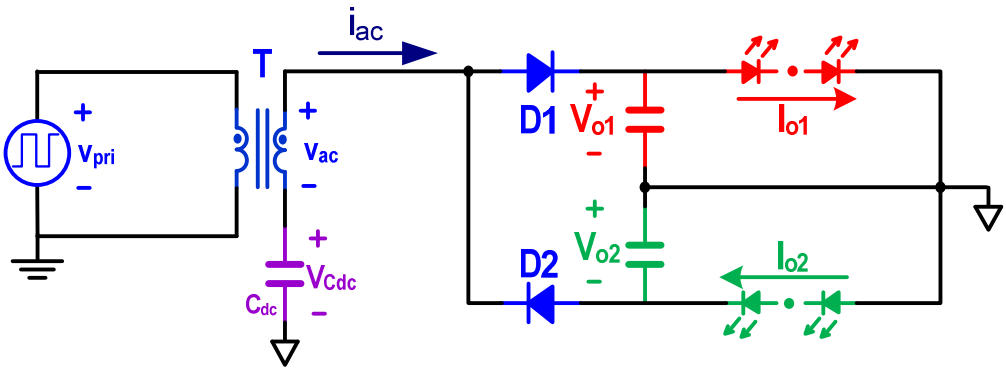


**Figure 3. 2 Simplified LLC LED Driver with Two LED Strings**

Depending on the switching frequency of LLC converter, there are two typical operating conditions: when switching frequency is lower or equal to the resonant frequency, the transformer secondary side current is continuous, as shown in Fig. 3.3 (a); when switching frequency is higher than the resonant frequency, the transformer secondary side current is discontinuous, as shown in Fig. 3.3 (b).

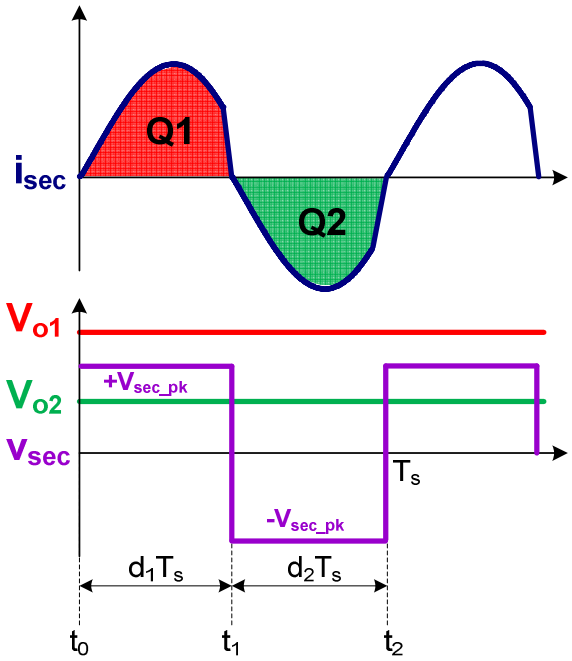


(a) $f_s<f_o$

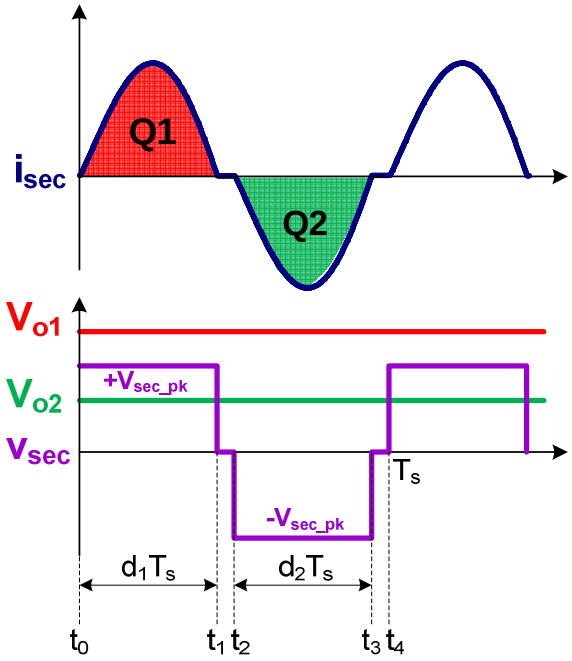


(b) $f_s>f_o$

**Figure 3. 3 Typical Waveforms of LLC LED Driver with DC Block Cap**

The detailed analysis and choice of the DC block capacitor can be found in [31]. Considering the charge balance of DC block capacitor during one switching cycle, the charge quantity for each half cycle must be equal ($Q_1$=$Q_2$). The DC average current in each LED string can be derived in (3.1) and (3.2):

$$I_{o1} = \frac{Q_1}{T_s} \tag{3.1}$$

$$I_{o2} = \frac{Q_2}{T_s} \tag{3.2}$$

Obviously due the charge balance of DC block capacitor, the currents in both LED strings are forced to be identical, as in (3.3):

$$I_{o1} = I_{o2} \tag{3.3}$$

The average voltage across $C_{dc}$ can be derived based on the volt-second balance of the transformer [7] and the result is shown in (3.4):

$$V_{Cdc} = \frac{V_{o1} - V_{o2}}{2} \tag{3.4}$$

When two LED strings are balanced, their forward voltages are equal and the average voltage across $C_{dc}$ is zero. However, if they are unbalanced, the strings' forward voltage difference will be undertaken by $C_{dc}$ and the average voltage on $C_{dc}$ is no longer zero, but one half of the voltage difference between two LED strings.

The operation principle of proposed MC$^3$ LLC LED driver is shown in Fig. 3.4 with the typical operation waveforms. Assuming the converter operates at resonant frequency, the resonant tank current is pure sinusoid and the magnetizing current is triangle wave. The transformer's secondary side current $i_{ac}$ is approximately sinusoid wave current and the DC average current of rectified $i_{ac}$ equals to LED load current. The transformer's secondary side voltage, $v_{ac}$, is square wave voltage, which amplitude equals to the output voltage $V_o$. When the output capacitor is large enough, the ripples on the output voltage and current are negligible.

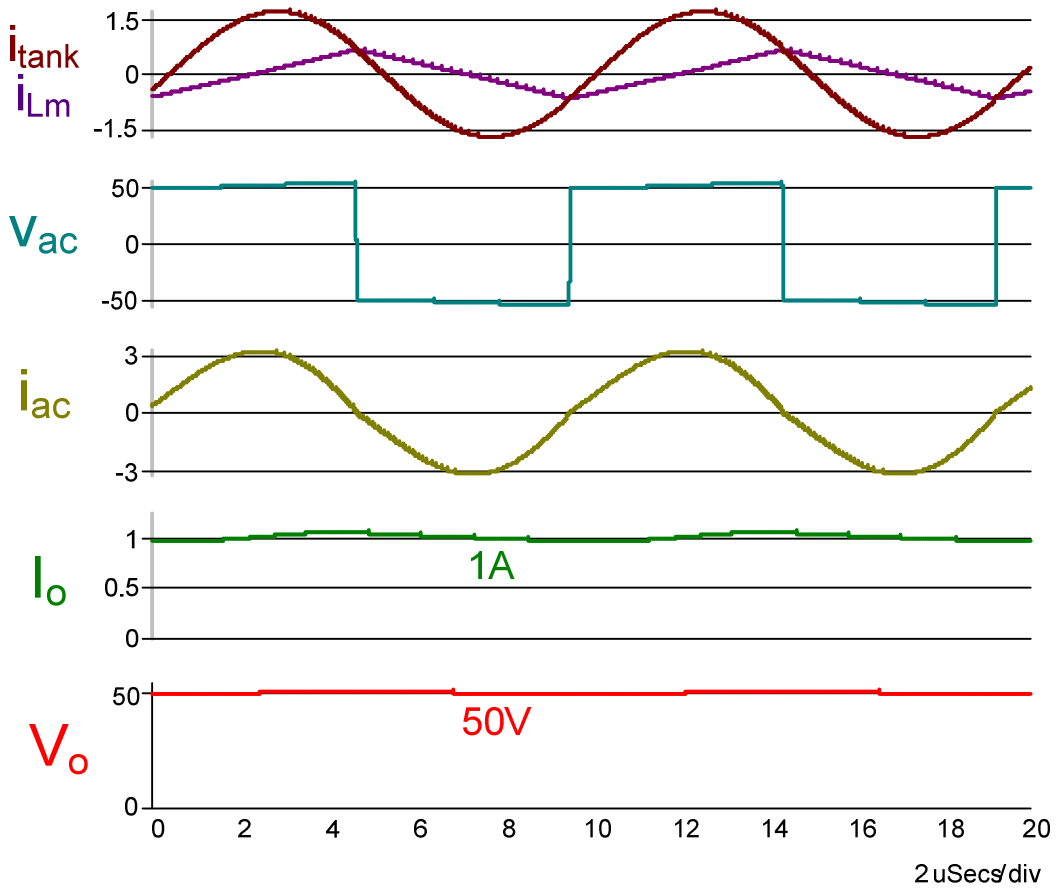


**Figure 3. 4 Simplis Simulation Waveforms of MC$^3$ LLC LED Driver ($V_o$>$V_{th}$)**

When designing the LLC converter as LED driver, the output current, instead output voltage in LLC front-end converter, is controlled. Furthermore, the LED load character is quite different from the resistance load. As a result, the traditional LLC voltage gain characteristic is not suitable to reflect the converter's operation principle and needs to be modified.

Due to the negative temperature coefficient of LEDs shown in Fig. 1.5, the LED forward voltage may vary (e.g. ±10%), even driven by constant current. The PFC output also has certain voltage ripples. As a result, designing a constant current LED driver with wide input and output voltage ranges is required and challengeable. Proper design procedure is also investigated based on the modified LLC current gain characteristic with LED load in the next section.

## 3.2 LLC Voltage and Current Gain Characteristic with LED Load

### 3.2.1 Review of LLC voltage gain characteristic with resistive load

The LLC voltage gain characteristic with resistive load and its operation range have been discussed in many papers [32][33] and widely used in LLC front-end DC/DC converter design. Taken the LLC front-end DC/DC converter with resistive load as example, the circuit diagram is shown in Fig. 3.5.

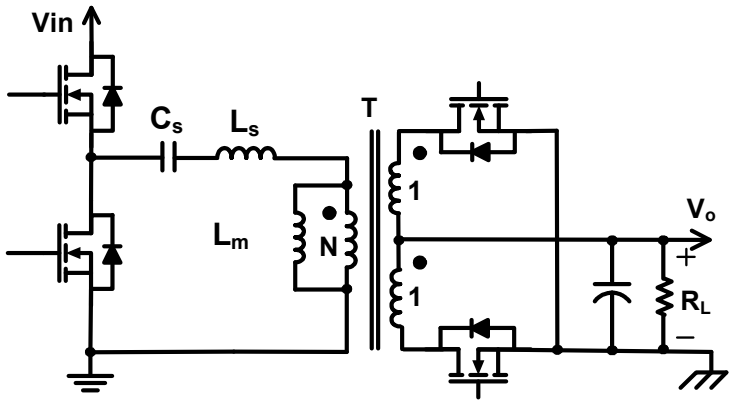


**Figure 3. 5 LLC Front-end DC/DC Converter with Resistive Load**

Based on the Fundamental Harmonic Approximation (FHA), the resistive load can be modeled as an equivalent ac resistance $R_{ac}$, as in equation (3.5). The AC equivalent circuit then can be drawn in Fig. 3.6 and solved.

$$R_{ac} = \frac{8N^2}{\pi^2} R_L \tag{3.5}$$

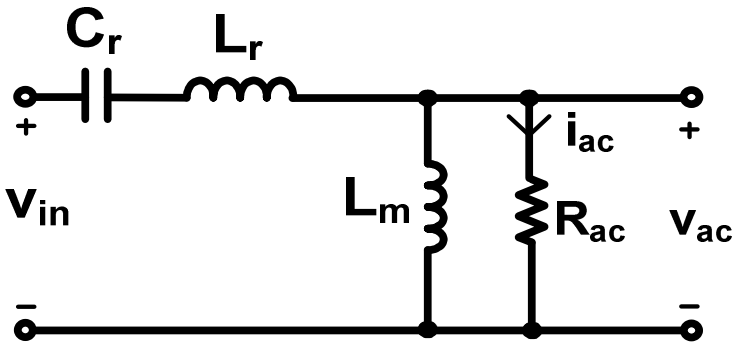


**Figure 3. 6 AC Equivalent Circuit based on FHA**

For different load conditions, the LLC voltage gain characteristic can be expressed by equation (3.6):

$$M_V = \left| \frac{V_o}{V_{in} / 2N} \right| = \left| \frac{1}{1 + \frac{1}{L_n}(1 - \frac{1}{f_n^2}) + j \cdot Q \cdot (f_n - \frac{1}{f_n})} \right| \tag{3.6}$$

$$Q = \frac{\sqrt{L_r / C_r}}{R_{ac}} = \frac{\sqrt{L_r / C_r}}{\frac{8N^2}{\pi^2} R_L}$$

Where Q is a function of load resistor. Different Q values represent different load conditions.

The LLC voltage gain curves can be plotted in Fig. 3.7. Each curve represents the relationship between the voltage gain and the switching frequency for a specific load condition.

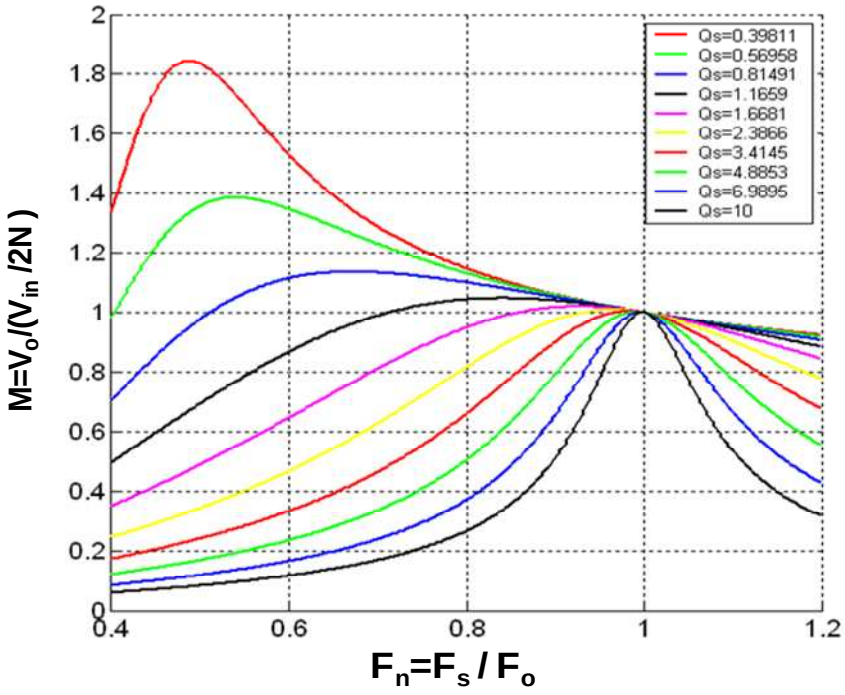


**Figure 3. 7 LLC Voltage Gain Characteristic w/ Resistive Load**

The LLC voltage gain characteristic is still used in [34] [35] in order to analyze the operation principle and design LLC LED driver. However, in LLC LED driver, the load is LEDs instead of resistor, which has completely different nonlinear character. Since the LED current is controlled, LED cannot be modeled as a constant resistor any more when the LED forward current changes. Consequently the previous definition of quality factor Q is no longer valid either. That means the LLC voltage gain characteristic can't reflect the operating principle and steady state character of LLC LED driver either correctly nor directly.

Considering the unique nonlinear character of LED load, the load condition needs to be redefined and the AC equivalent circuit also needs to be modified, which will be discussed in details in the following section. After obtaining the AC equivalent circuit for LLC converter with LED load, the modified LLC voltage and current characteristics can be derived.

### 3.2.2 AC equivalent circuit of LLC converter with LED load

As discussed before, the LED load shows nonlinearity and cannot be modeled as a constant resistor any more. So first of all, the character of LED needs to be analyzed in details and its equivalent load expressions need to be derived.

Using simplified piece-wise-linear model, the i-v curve of Cree X-lamp XP-E White LED is shown in Fig. 3.8.

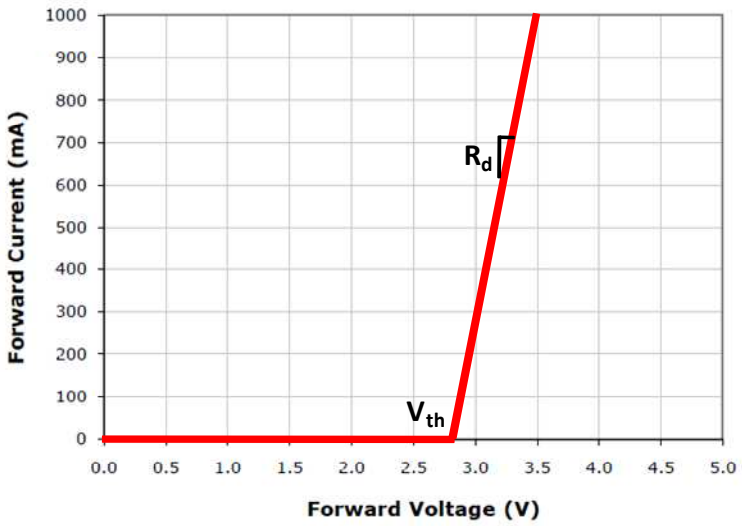


**Figure 3. 8 Cree X-lamp XP-E White LED i-v Character (piece-wise-linear model)**

The LED's threshold voltage $V_{th}$ represents the boundary between LED's on state and off state. When LED's forward voltage is smaller than threshold voltage, LED is off and forward current keeps zero. Only if LED's forward voltage exceeds threshold voltage, LED starts to conduct current and its i-v relationship follows the curve shown in Fig. 3.8. As a result, to describe the LED's nonlinear i-v character, the relationship between LED's forward current and voltage can be represented by the following piece-wise function:

$$I_o = \begin{cases} \dfrac{V_o - V_{th}}{R_d} & when\, V_o > V_{th} \\ 0 & when\, V_o \le V_{th} \end{cases} \tag{3.7}$$

Then the AC equivalent circuit of LLC converter with LED as shown in Fig. 3.9 will be analyzed.

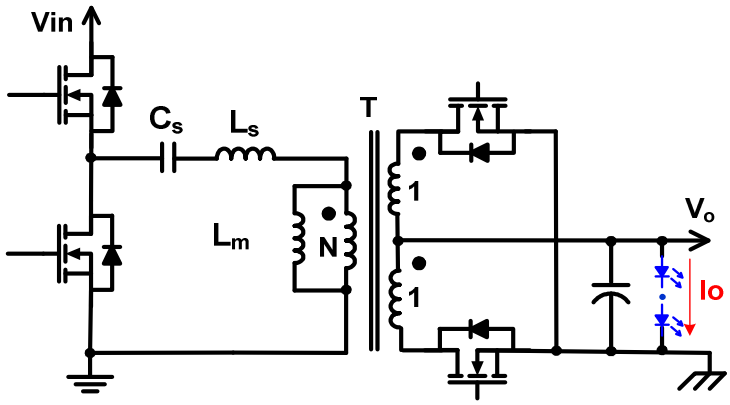


**Figure 3. 9 LLC Converter with LED Load (when $V_o$>$V_{th}$)**

From the simulation waveform, we can assume that the ripples of LED's forward voltage $V_o$ and current $I_o$ are negligible. As a result, the input excitation of resonant tank is square wave voltage source as well as the transformer secondary side voltage is square wave voltage sink. The following equivalent circuit can be used.

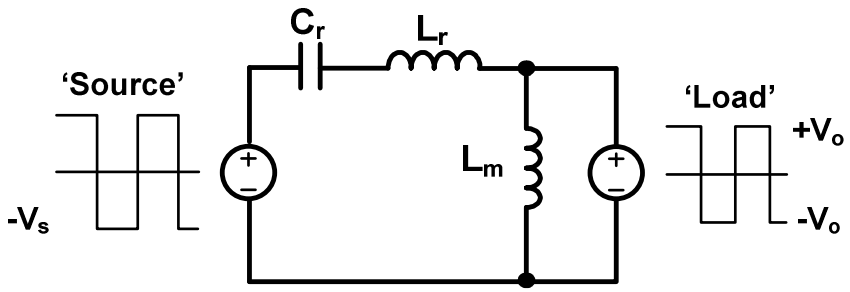


**Figure 3. 10 Equivalent Circuit of LLC Converter with LED Load (when $V_o$>$V_{th}$)**

This equivalent circuit is the same as the one used in the analysis of traditional LLC DC/DC converter with resistive load, but the load character is different and requires careful analysis.

Using the equivalent circuit for transformer secondary rectifier and LED load as shown in Fig. 3.11 (a), we can derive the AC equivalent resistor for LED load.

According to previous assumptions, $V_{ac}$ is square wave voltage and $I_{ac}$ is sinusoid wave current. Based on Fundamental Harmonic Approximation (FHA), only fundamental harmonics transfer energy. As shown in Fig. 3.11 (b), the fundamental harmonic $V_{ac}^{F}$ of square wave voltage $V_{ac}$ and sinusoid wave current $I_{ac}$ are responsible to transfer energy to the load.

Since the amplitude of square wave voltage $V_{ac}$ equal to the output voltage $V_o$, we can easily calculate its fundamental harmonic using Fourier Series:

$$v_{ac}^{F} = \frac{4N}{\pi} \cdot V_O \cdot \sin(\omega_s t) \tag{3.8}$$

Since the output capacitors only absorb AC current, the DC average value of rectified sinusoid wave current $I_{ac}$ equals to the LED load current $I_o$:

$$i_{ac} = \frac{\pi}{2N} \cdot I_O \cdot \sin(\omega_s t) \tag{3.9}$$

Based on the energy equivalence point of view, the load can be modeled as a AC equivalent resistor, as shown in Fig. 3.11 (b). The definition of AC equivalent resistor is:

$$R_{ac} = \frac{v_{ac}^{F}}{i_{ac}}$$

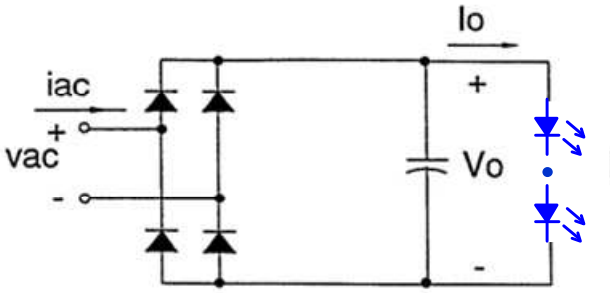


(a) Equivalent circuit

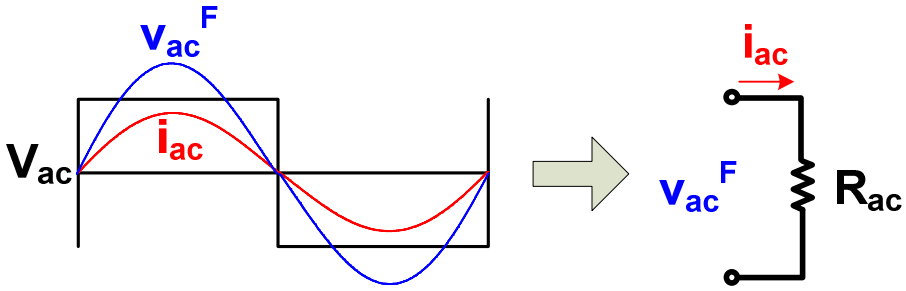


(b) Waveforms of $V_{ac}$ & $I_{ac}$ and definition of $R_{ac}$

**Figure 3. 11 Derivation of AC Equivalent Resistor for LED Load**

On the other hand, since in this case, the load is LED which has non-linear character and its i-v relationship follows the piece-wise function as shown in equation (3.7). Replacing $V_{ac}^{F}$ & $I_{ac}$ by equation (3.8) & (3.9) and combining the LED's i-v relationship from equation (3.7) in the definition of $R_{ac}$, we can derive the complete expression of AC equivalent resistor of LED load in LLC converter:

$$R_{ac} = \frac{v_{ac}^{F}}{i_{ac}} = \begin{cases} \frac{8N^2}{\pi^2}\left(\frac{V_o}{V_o - V_{th}}\right) \cdot R_d & when\ V_o > V_{th} \\ \infty & when\ V_o \le V_{th} \end{cases} \quad (3.10)$$

The AC equivalent resistor of LED load is no longer a function of constant resistor, but reflects LED's non-linear character. Then we can modify the AC equivalent circuit of LLC converter with LED load, as shown in Fig. 3.12.

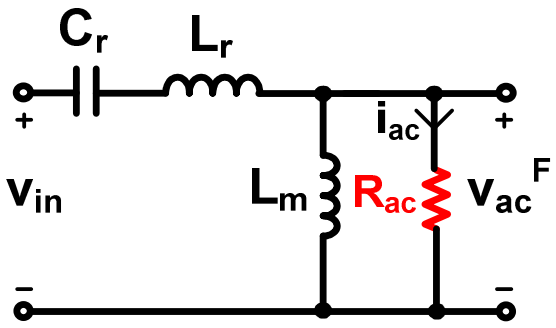


**Figure 3. 12 AC Equivalent Circuit of LLC Converter with LED Load**

This AC equivalent circuit seems the same as the one of LLC DC/DC converter with resistive load, but the definition of $R_{ac}$ is completely different. Here the equation (3.10) should be used to represent LED load character. Then the LLC voltage and current characteristics with LED load can be derived based on this equivalent circuit.

### 3.2.3 Derivation of LLC voltage & current gain characters with LED load

In the previous section, we have already derived the AC equivalent circuits of LLC converter with LED load. It is important to mention that because of the nonlinear character of LED load, two different AC equivalent circuits should be analyzed independently to reflect LED load's nonlinearity - when $V_o > V_{th}$, LED is in on state and $R_{ac}$ is a finite value and follows LED's i-v relationship; when $V_o < V_{th}$, LED is in off state and forward current is zero, the circuit operates as in no load condition.

By solving the AC equivalent circuit in Fig. 3.12, the modified LLC voltage gain characteristic with LED load can be derived:

$$M_V(f_n, L_n, Q) = \left|\frac{V_o}{V_{in}/2N}\right| = \begin{cases} \frac{1}{K} \cdot \frac{Q^2(f_n - \frac{1}{f_n})^2 + \sqrt{Q^4(f_n - \frac{1}{f_n})^4 - \left[\left(1 + \frac{1}{L_n}(1 - \frac{1}{f_n^2})\right)^2 + Q^2(f_n - \frac{1}{f_n})^2\right]\left[Q^2(f_n - \frac{1}{f_n})^2 - K^2\right]}}{\left[1 + \frac{1}{L_n}(1 - \frac{1}{f_n^2})\right]^2 + Q^2(f_n - \frac{1}{f_n})^2} & when\ V_o > V_{th} \\ \left|\frac{1}{1 + \frac{1}{L_n}(1 - \frac{1}{f_n^2})}\right| & when\ V_o \le V_{th} \end{cases} \quad (3.11)$$

$$K = \frac{V_{in}/2N}{V_{th}} \quad (3.12)$$

When $K$ is a number slightly larger than 1. If ignoring the input variation, we can assume it to be a constant value.

Three key design parameters - resonant frequency, inductor ratio and characteristic factor - are defined as follows:

$$f_o = \frac{1}{2\pi\sqrt{L_r C_r}}$$

$$L_n = \frac{L_m}{L_r}$$

$$Q = \frac{\sqrt{L_r / C_r}}{\frac{8N^2}{\pi^2} R_d}$$

Where $R_d$ is the dynamic resistance of LED load.

The definition of characteristic factor is different from the one used in LLC voltage gain characteristic with resistive load. In order to model the LED load characteristic, the dynamic resistor is used to reflect the load's incremental change while LED forward current is regulated.

Taken normal operating condition in Table 1.1 as an example, the modified LLC voltage gain curves with LED load can be plotted by using equation (3.11), as shown in Fig. 3.13 (choose $L_n$=3):

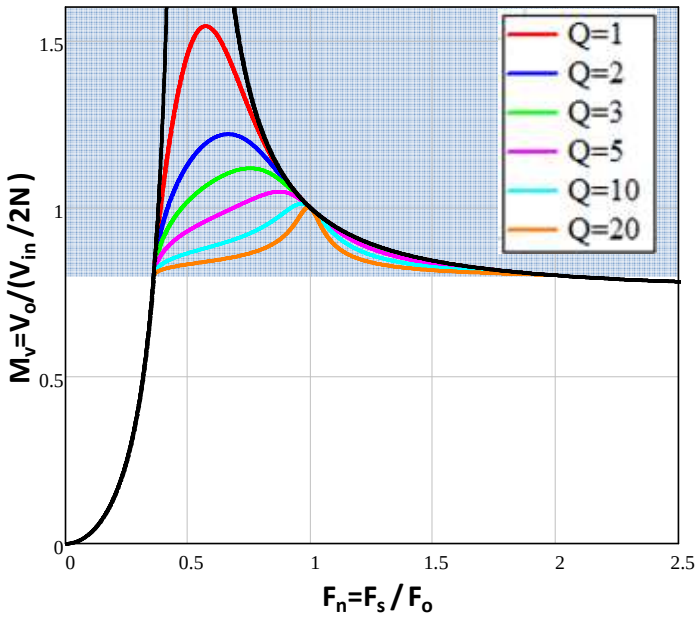


**Figure 3. 13 LLC Voltage Gain Curves with LED Load**

It is clearly shown that after considering the nonlinearity of LED load, there is a boundary ($V_o$=$V_{th}$) in the modified LLC voltage gain curves which represents the boundary condition of LED's on & off states. Above the boundary, a series of voltage gain curves can be plotted by using the first equation in (3.11) with different Q values. On the other hand, below the boundary, LED load is in off state and the circuit operates

as in LLC's no load condition. The voltage gain curve can be plotted by using the second equation in (3.11), as the black curve. Obviously, under normal condition, LED strings conduct current to emit light, so the light blue region in Fig. 3.13 is the operation region for LLC LED driver to provide current source to the LED load.

Similarly, using the same AC equivalent circuit in Fig. 3.12, we can also derive the LLC current gain characteristic with LED load. Especially for LLC LED driver, the LED forward current instead of voltage needs to be controlled. From this point of view, the LLC current gain characteristic is even more desirable and useful to properly design the circuit.

The LLC current gain characteristic with LED load can be solved as the following equation:

$$M_I(f_n, L_n, Q) = \left|\frac{I_o}{I_n}\right| = \begin{cases} \frac{1}{K-1} \cdot \frac{-\left[1+\frac{1}{L_n}(1-\frac{1}{f_n^2})\right]^2 + \sqrt{\left[1+\frac{1}{L_n}(1-\frac{1}{f_n^2})\right]^4 - [\left[1+\frac{1}{L_n}(1-\frac{1}{f_n^2})\right]^2 + Q^2(f_n - \frac{1}{f_n})^2] \cdot (\left[1+\frac{1}{L_n}(1-\frac{1}{f_n^2})\right]^2 - K^2)}}{\left[1+\frac{1}{L_n}(1-\frac{1}{f_n^2})\right]^2 + Q^2(f_n - \frac{1}{f_n})^2} & when\ V_o > V_{th} \\ 0 & when\ V_o \le V_{th} \end{cases} \quad (3.13)$$

When $I_n = \frac{V_{in\_nom} / 2N - V_{th\_nom}}{R_d}$ is normalization factor of LED load current. It is defined as the output current at resonant point under normal input and output condition. The definition of K is the same as modified voltage gain characteristic, which can represent both input and output variations.

Under normal condition, we can also plot the LLC current gain curves by using equation (3.13), as shown in Fig. 3.14 (choose $L_n$=3):

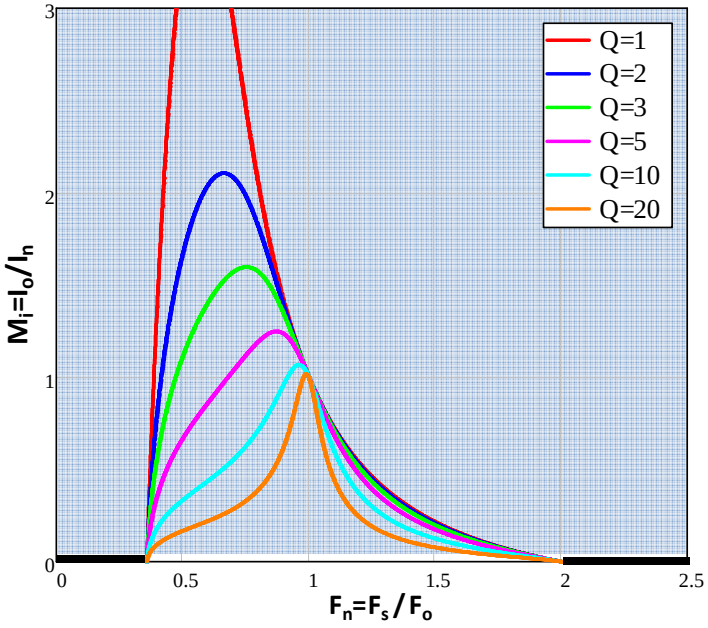


**Figure 3. 14 LLC Current Gain Curves with LED Load**

Because the nonlinearity of LED load character has been considered, the LLC current gain characteristic also has two different equations corresponding to the LED on & off states. When $V_o>V_{th}$, LED is in on state and the current gain is larger than zero. A series of current gain curves can be plotted by using the first equation in (3.13) with different Q values. On the other hand, when $V_o<V_{th}$, LED is in off state and there is no current output. So the current gain equal to zero, as shown in black curve in Fig. 3.14.

### 3.2.4 Comparison: LLC voltage & current gain characters with LED load

After considering the LED load's nonlinear character, we have derived the LLC voltage and current gain characteristics. Some definitions of normalization factors are summarized and compared in the following table:

**Table 3.1 Definitions of Normalization Factors**

| | $f_n$ | $L_n$ | Q |
|---|---|---|---|
| Voltage gain | $f_n = \frac{f_s}{f_o}$ | $L_n = \frac{L_m}{L_r}$ | $Q = \frac{\sqrt{L_r / C_r}}{\frac{8N^2}{\pi^2} R_d}$ |
| Current gain | $f_n = \frac{f_s}{f_o}$ | $L_n = \frac{L_m}{L_r}$ | $Q = \frac{\sqrt{L_r / C_r}}{\frac{8N^2}{\pi^2} R_d}$ |

Obviously, the LLC voltage and current gain characteristics with LED load have the uniform definitions of these normalization factors.

The LLC voltage and current gain curves with LED load are compared in Fig. 3.15.

It is clearly shown that both LLC voltage gain curves and current gain curves with LED load are divided into parts:

When $V_o > V_{th}$, LED is in on state. A series of voltage gain curves and current gain curves can be plotted with different Q values, respectively;

When $V_o < V_{th}$, LED is in off state. For the voltage gain, it will follow the curve representing no load condition. For the current gain, since the LED forward current is zero, the current gain curve stays along the horizontal axis.

In summary, the LLC voltage and current gain curves with LED load are identical from both mathematical and physical meaning point of views. They can also be exactly mapped between each other.

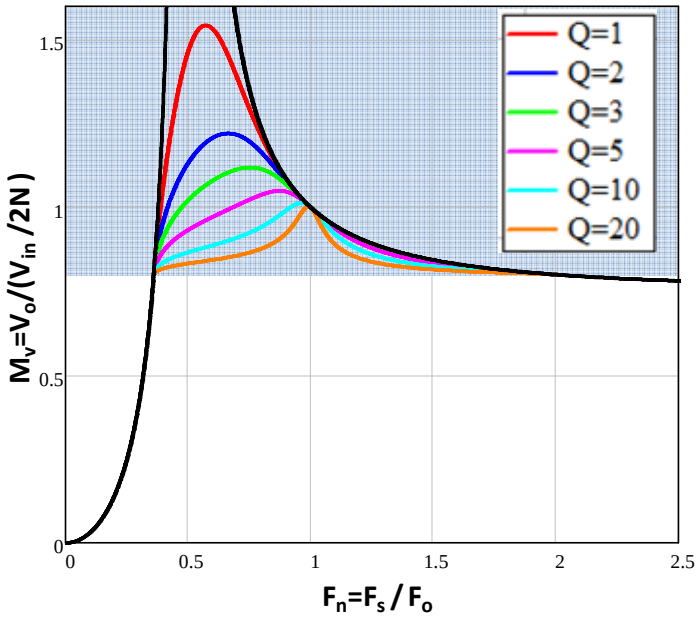


(a) voltage gain curves

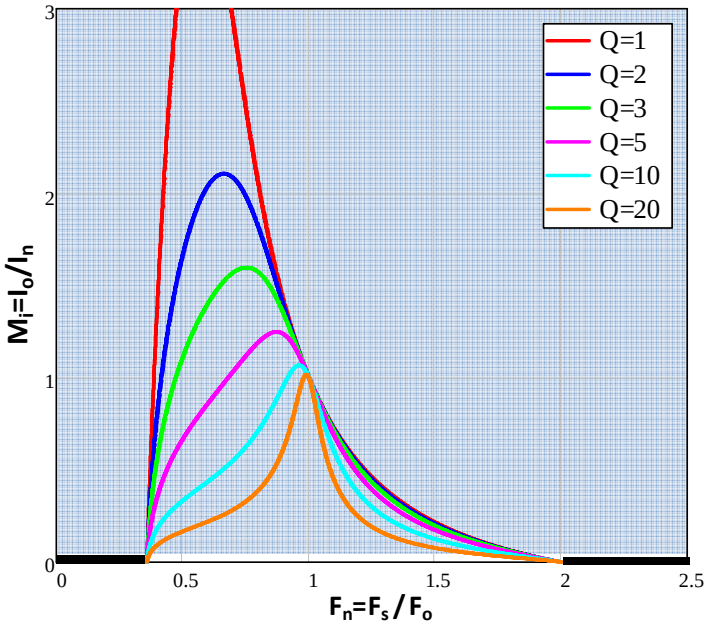


(b) current gain curves

**Figure 3. 15 Comparison between LLC Voltage & Current Gain Curves with LED load**

When LLC converter operates as a LED driver, it's controlled to provide current source for the LED load. In other words, the output current, instead of output voltage in LLC front-end DC/DC converter, is our control target. Consequently, the LLC current gain characteristic is more desirable and useful, which reflect the relationship between the control variable (switching frequency) and the output variable (LED load current).

Using the Simplis simulation tool, the LLC LED driver is simulated with different resonant tank conditions (different Q values) and the simulated current gain curves can also be plotted. The calculated and simulated LLC current gain curves are compared in Fig. 3.16 (choose $L_n$=3).

We can see that the simulated current gain curves roughly match with the calculated ones, especially around the resonant frequency because the fundamental harmonic approximation is valid at resonant frequency. In the following design procedure, the LLC current gain characteristic with LED load as in equation (3.13) will be used.

We can also notice that although the relationship between LED forward voltage and current are nonlinear, they still have monotonic increasing function. As a result, similar to LLC voltage gain curve, in Fig. 3.16, when switching frequency is higher than resonant frequency, the converter runs in ZVS region. On the other hand, when switching frequency is lower than resonant frequency, the peak point of each current gain curve represents the boundary of ZVS and ZCS regions.

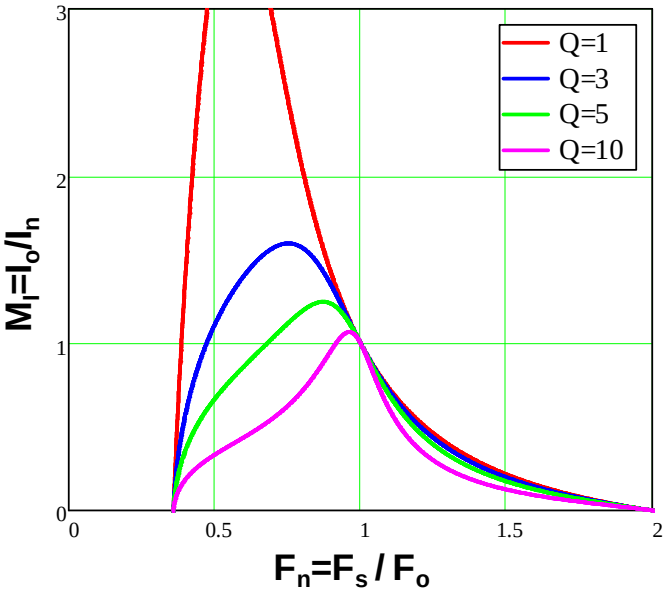


(a) calculated current gain curves

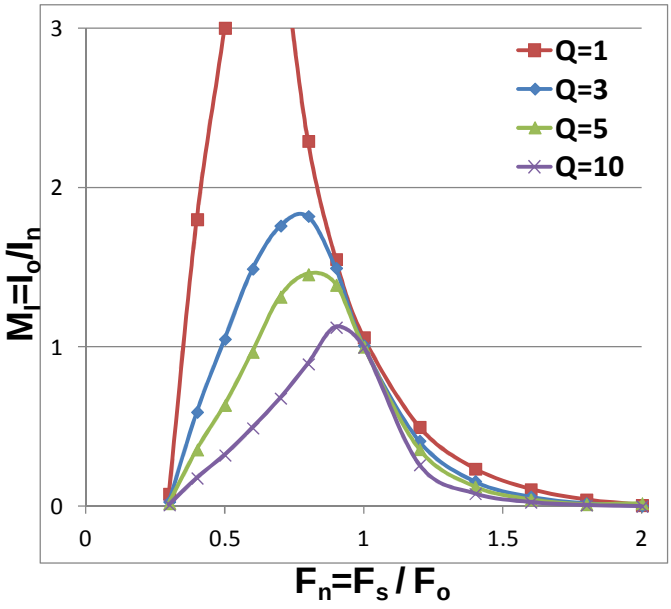


(b) simulated current gain curves

**Figure 3. 16 Comparison between Calculated and Simulated LLC Current Gain Curves**

### 3.2.5 Operation region of $MC^3$ LLC LED driver under dimming condition

In indoor LED luminaries application, besides full load current output capability, the $MC^3$ LED driver should also be dimmable. That means the LED driver should have the capability to dim the output current to be the level lower than full load current condition so that the LED's output lumens can be adjusted.

For the proposed $MC^3$ LLC LED driver, one straightforward way to realize dimming function is through frequency modulation. From the LLC current gain curves we can notice that under normal condition, the current gain equal to one at resonant frequency, which means the LED driver can provide 100% load current. If the switching frequency increases and the converter operates above resonant frequency, the current gain will reduce so that the average output current can be dimmed.

For different $L_n$ and Q values, series of LLC current gain curves can be plotted and compared, as shown in Fig. 3.17:

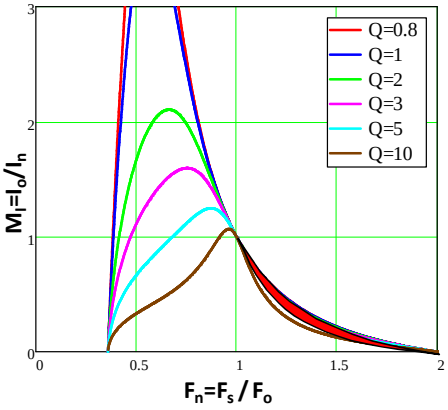


(a) $L_n$=3

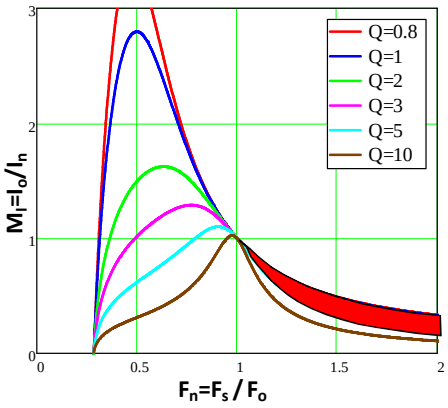


(b) $L_n$=5

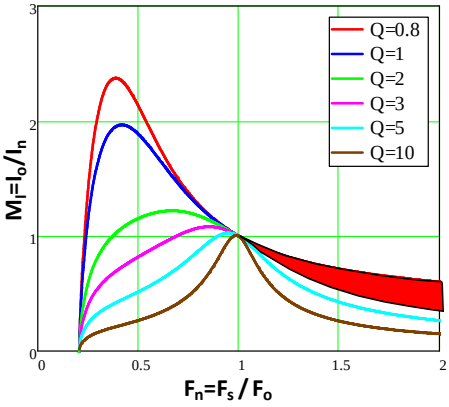


(c) $L_n$=10

**Figure 3. 17 Comparison of LLC Current Gain Curve with Different $L_n$ & Q**

In this figure above, the red zone represents the converter's operation region under dimming condition (from 100% load current to 0% load current). Comparing these three current gain curves we can notice that the smaller the $L_n$ value, the narrower the switching frequency range under dimming condition. Obviously, narrower switching frequency range is more desirable. As a result, from the dimming function point of view, smaller $L_n$ is preferred.

In summary, modified LLC voltage and current gain characteristics with LED load have been derived by considering LED's nonlinear i-v character. For design purpose, the LLC current gain characteristic is more straightforward and hence used in the following design example.

## 3.3 Design Example of MC$^3$ LLC Resonant LED Driver

As for the MC$^3$ LLC LED driver, the design targets include two aspects:

- Firstly, the LED driver's efficiency at normal operating condition (which is also the most common operating condition) should be optimized;
- Secondly, both input voltage and LED output forward voltage have certain variations; the MC$^3$ LLC LED driver should have the capability to provide 100% constant current output within the whole input and output ranges.

Compared to the optimal design procedure proposed in [33], the design and optimization of transformer's turns-ratio, dead time and magnetizing inductance in the MC$^3$ LLC LED driver are quite similar to the LLC front-end DC/DC converter design. However, the design of resonant tank (also $L_n$ & Q) should be based on the LLC current gain characteristic with LED load derived in previous section.

Taken a four-string MC$^3$ LLC LED driver as example, the circuit diagram is shown in Fig. 3.18. The design specifications are summarized in Table 3.2.

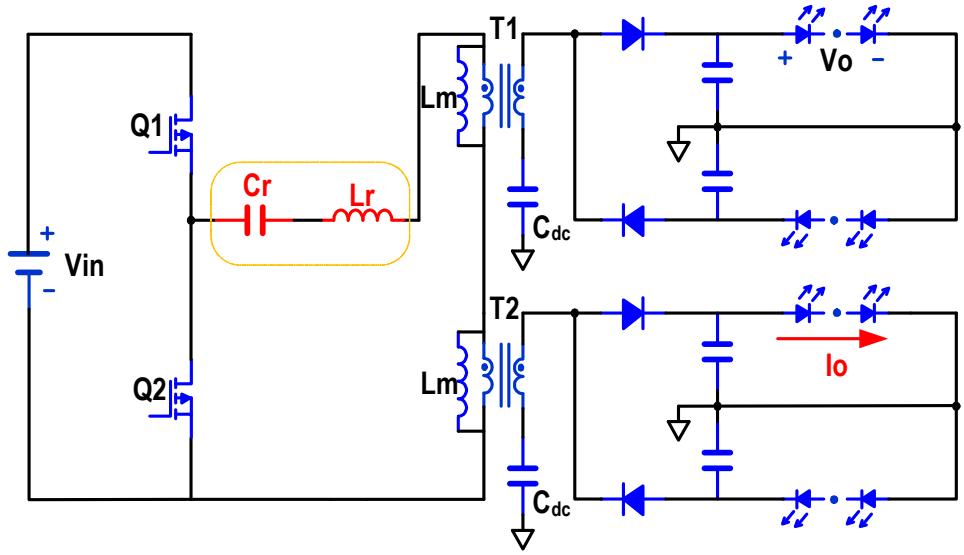


**Figure 3. 18 Design Example of a 4-string MC$^3$ LLC LED Driver**

**Table 3.2 Design Results of a 100 kHz, 200 W, 4-string MC$^3$ LLC LED Driver**

| | |
|---|---|
| DC input voltage $V_{in}$ | 380V±20V |
| LED channel threshold voltage $V_{th}$ | 40V±5V |
| LED channel current $I_o$ | 1A |
| LED channel dynamic resistor $R_d$ | 10Ω |
| Switching frequency $f_s$ | 100kHz |

To complete the MC$^3$ LLC LED driver design, there are totally four design parameters and three design steps.

***1. Transformer's turns ratio***

The transformer's turns ratio is the first parameter which need to be designed. The transformer's turns ratio directly determine the converter's operation point under normal input and output condition. As discussed before, the LED driver is desired to achieve high efficiency under normal condition. Consequently, the design of transformer's turns ratio should make the converter operate close to resonant frequency under normal condition, which is the most efficient operating point of LLC resonant converter.

***2. Dead-time $T_d$ and transformer's magnetizing inductance $L_m$***

In paper [33], the relationship between dead-time and total conduction loss (both primary & secondary side) is derived. Then the dead-time can be chosen to minimize the total conduction loss. The value of magnetizing inductance is determined based on the dead time and $C_{oss}$ of primary side MOSFET in order to achieve ZVS operation.

***3. Resonant tank design ($L_n$ & Q)***

After transformer's turns ratio and magnetizing inductance have been determined, the only parameters remaining for design is the resonant tank inductor and capacitor. The definitions of inductor ratio $L_n$ and quality factor Q are shown in the following equations:

$$L_n = \frac{L_m}{L_r}$$

$$Q = \frac{\sqrt{L_r / C_r}}{\frac{8N^2}{\pi^2} R_d}$$

We can see that since the resonant tank inductor $L_r$ and capacitor $C_r$ have certain relationships with $L_n$ and Q. As long as the value of $L_n$ and Q can be determined, the values of Lr and Cr can be easily calculated correspondingly.

Based on the LLC current gain characteristic with LED load, the impact of different combinations of $L_n$ and Q can be analyzed. Only certain combinations of $L_n$ and Q can maintain the constant current output capability within the whole input and output range, which is the design criteria for the resonant tank design.

The detailed design procedure is discussed in Appendix. Following the proposed design procedure, a prototype of 100 kHz, 200 W, 4-string $MC^3$ LLC LED driver is designed and tested to verify the constant current output and dimming capabilities of the proposed circuit. Assuming the input voltage has $\pm 5\%$ variation and LED threshold voltage have $\pm 10\%$ variation (the detailed specifications are listed in Table 3.2), the design results are summarized in Table 3.3.

**Table 3.3 Design Results of a 100 kHz, 200 W, 4-string MC$^3$ LLC LED Driver**

| | |
|---|---|
| DC input voltage $V_{in}$ | 380V |
| LED channel voltage $V_o$ | 50V |
| LED channel current $I_o$ | 1A |
| Input voltage $V_{in}$ variation | ±5% |
| LED threshold voltage $V_{th}$ variation | ±10% |
| Switching frequency $f_s$ | 100kHz |
| Transformer turns ratio | 24:12 (PQ26/20 3C96) |
| Magnetizing inductor | 800uH |
| Inductor ratio | 5 |
| Resonant inductor | 160uH (RM8/ILP 3C96) |
| Resonant capacitor | 16nF |
| Primary Power MOSFETs | STD13NM60N |
| Secondary Schottky Diodes | PDS4150 |

The hardware is tested under various LED load conditions and the experimental results are shown in the next section.

## 3.4 Experimental Results

### 3.4.1 Operation waveforms under normal condition

Firstly, the designed LED driver is tested under normal condition: $V_{in\_nom}$=380V, $V_{o\_nom}$=50V. The four LED strings are balanced (forward voltage difference is less than 0.5V). The waveforms of primary side MOSFET gate driving signal, drain-to-source

voltage and resonant tank current are shown in Fig. 3.19. The four LED strings' currents are shown in Fig. 3.20.

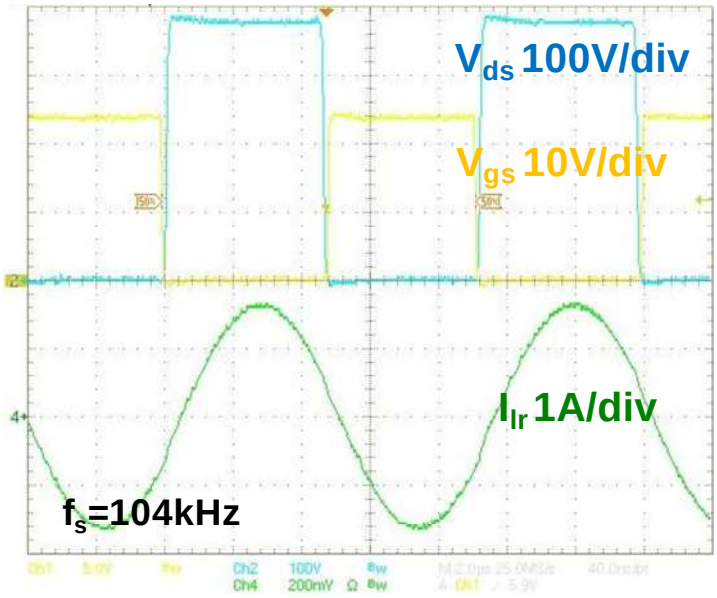


**Figure 3. 19 Operating Waveforms when ($V_{in\_nom}$, $V_{o\_nom}$)=(380V, 50V)**

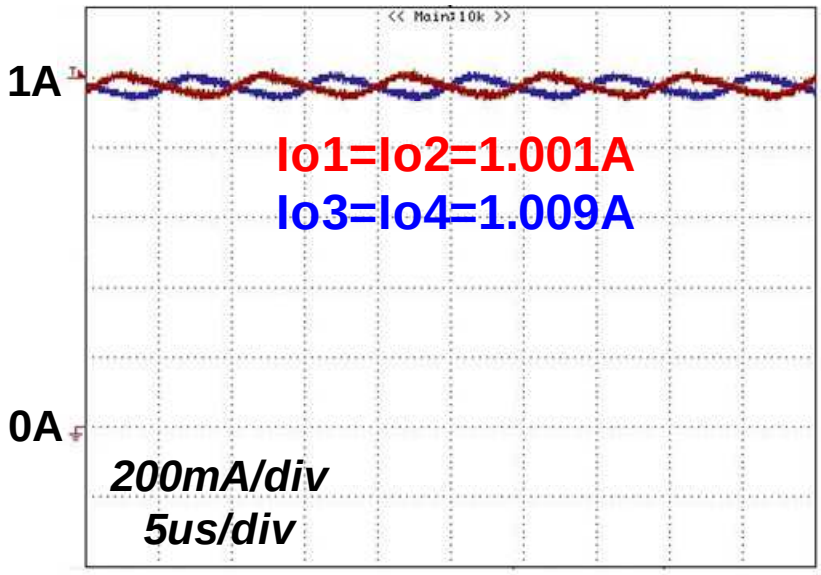


**Figure 3. 20 LED String Current Waveforms when ($V_{in\_nom}$, $V_{o\_nom}$)=(380V, 50V)**

Fig. 3.19 shows that in order to regulate the LED string current to be 1A, the LLC resonant converter runs at $f_s$=104 kHz, slightly below the resonant frequency, which meets the design target. Fig. 3.20 shows the four LED strings current waveforms. Due to DC block cap, LED string 1 and string 2's currents are almost the same (so do LED string 3 & string 4), which are 1.001A and 1.009A respectively. The current difference is only 0.8%. The circuit shows very good current sharing capability under normal condition with balanced LED strings.

### 3.4.2 Operation waveforms with input & output variations

As the circuit's specification shows in Table 3.2, both input voltage and LED string's forward voltage have some variations. The circuit is also tested with two boundary conditions:

1. $V_{in\_max}$=400V, $V_{o\_min}$=45V;

2. $V_{in\_min}$=360V, $V_{o\_max}$=55V.

The operation waveforms under two boundary conditions are shown in Fig. 3.21.

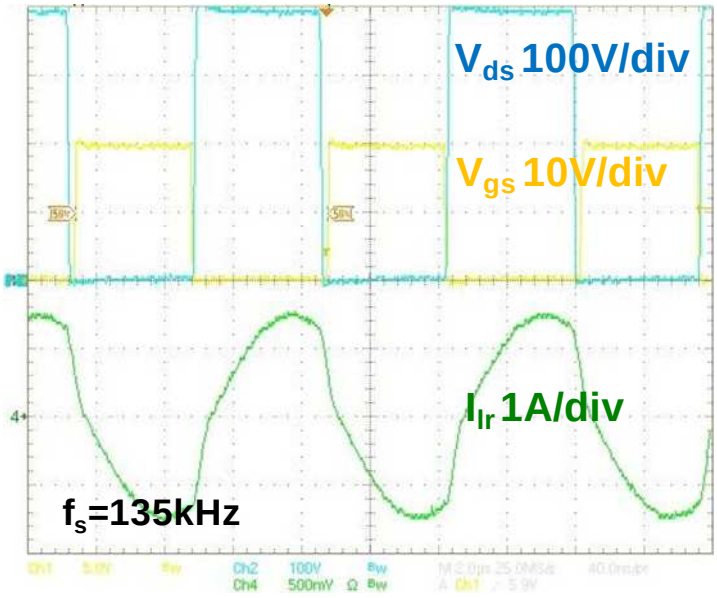


(a) ($V_{in\_max}$, $V_{o\_min}$)=(400V, 45V)

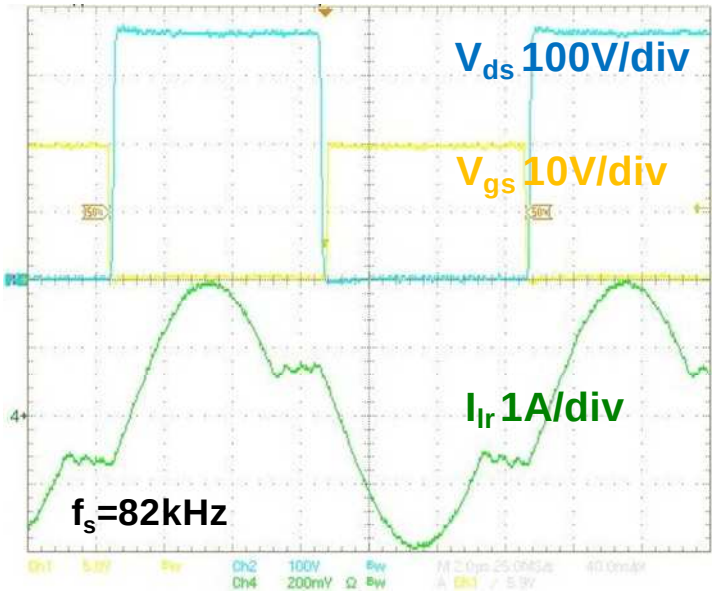


(b) ($V_{in\_min}$, $V_{o\_max}$)=(360V, 55V)

**Figure 3. 21 Operating Waveforms with Input & Output Variations**

Fig. 3.21 (a) shows that when $V_{in\_max}$=400V, $V_{o\_min}$=45V, the LLC LED driver increases the switching frequency to 135 kHz to maintain 1A LED string current output.

Fig. 3.21 (b) shows that $V_{in\_min}$=360V, $V_{o\_max}$=55V, the LLC LED driver needs to decrease the switching frequncy to 82 kHz in order to boost the current gain. The circuit still has the capability of providing 100% LED string current.

Under these two boundary conditions, the four LED strings' currents are summarized in Table 3.4. The maximum current difference is 1.3% and the circuit shows good current sharing capability within the whole input and output voltage variations.

**Table 3.4 Experimental Results of Current Sharing with Input & Output Variations**

| | $V_{in\_max}$=400V, $V_{o\_min}$=45V | $V_{in\_min}$=360V, $V_{o\_max}$=55V |
|---|---|---|
| LED string 1&2 | 1.001A | 1.002A |
| LED string 3&4 | 1.011A | 1.015A |
| Current difference | **1.0%** | **1.3%** |

Assuming the LED string forward voltage under normal condition ($V_{o\_nom}$=50V), the efficiency within the whole input voltage variation is tested and plotted in Fig. 3.22.

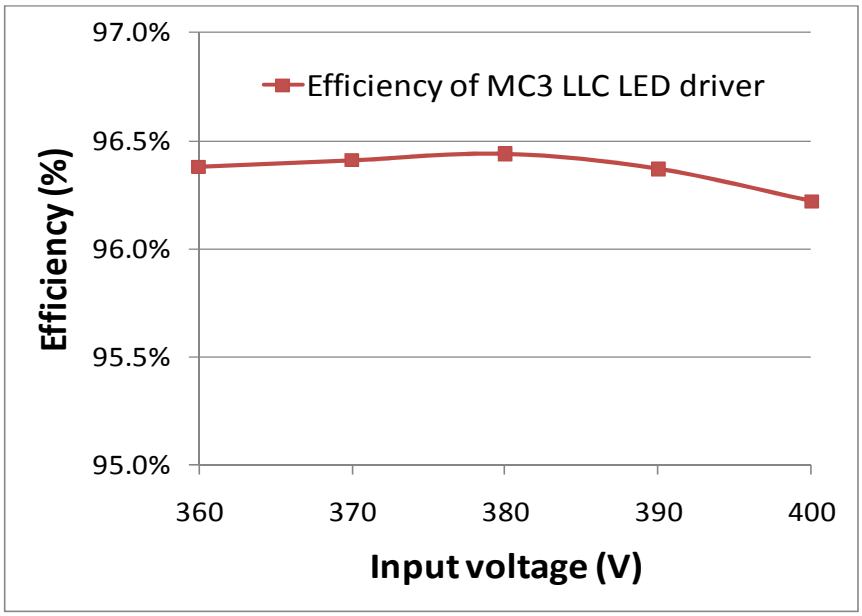


**Figure 3. 22 Efficiency with Input Voltage Variation**

Since the circuit is designed to operate slightly below resonant frequency at normal condition, the highest efficiency can be achieved when $V_{in\_nom}$=380V & $V_{o\_nom}$=50V, which is 96.4%. During the whole input voltage range from 360V to 400V, the overall efficiency of $MC^3$ LLC LED driver is above 96.2%. only 0.2% efficiency drop comparing to normal condition.

### 3.4.3 System robustness to LED short failure

Previous experimental results show that the proposed circuit has very good current sharing capability under balanced LED string condition. However, the current sharing under unbalanced LED string condition still needs investigation. One extreme unbalanced condition has been chosen - when LED string 4 is completely in short failure and other three strings work normally. The circuit diagram is shown in Fig. 3.23. The forward voltages of four LED strings are 50V, 50V, 50V and 0V, respectively.

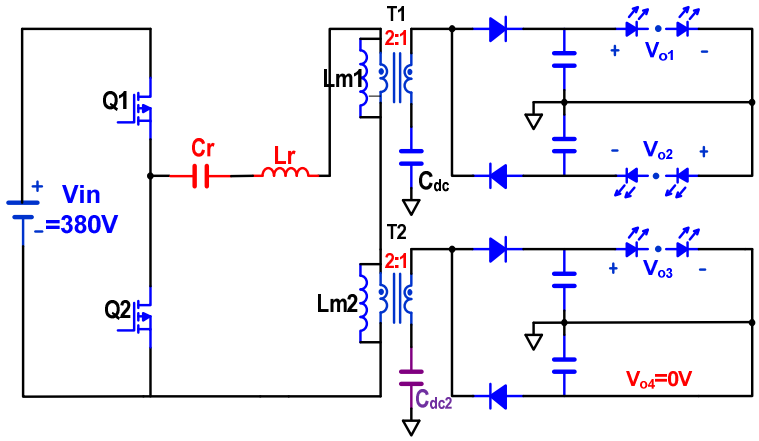


**Figure 3. 23 MC$^3$ LLC LED Driver with One LED String in Short Failure**

The operation waveforms are shown in Fig. 3.24. In this case, the switching frequency increases to 160 kHz to regulate 1A LED string current. Because the voltage difference between LED string 3&4 are 50V, the average voltage on DC block cap $C_{dc2}$ is no longer zero, but equal to 25V which is one half of the two strings' voltage difference. The experimental results confirm the analysis of DC block cap at the beginning of this chapter.

The three normal LED string currents are: $I_{o1}=I_{o2}=0.999A$; $I_{o3}=1.021A$. Even with one LED string in short failure, the circuit can still regulate the load current and achieve current sharing (only 2% current difference).

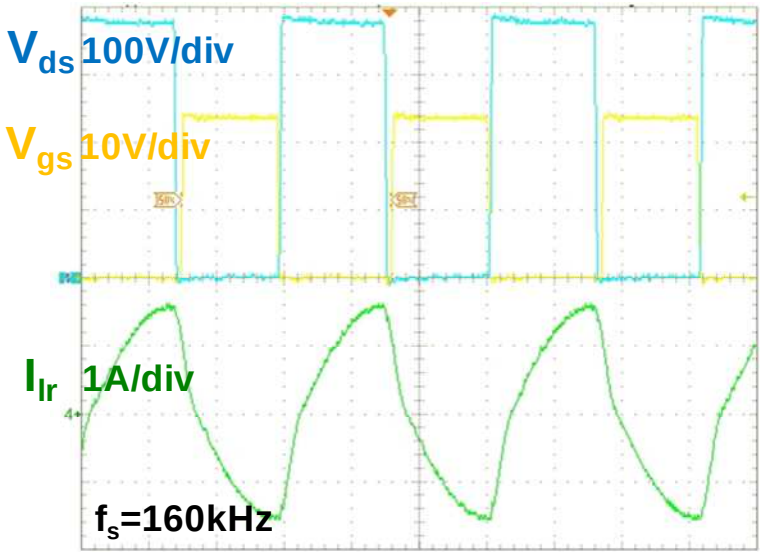


(a)

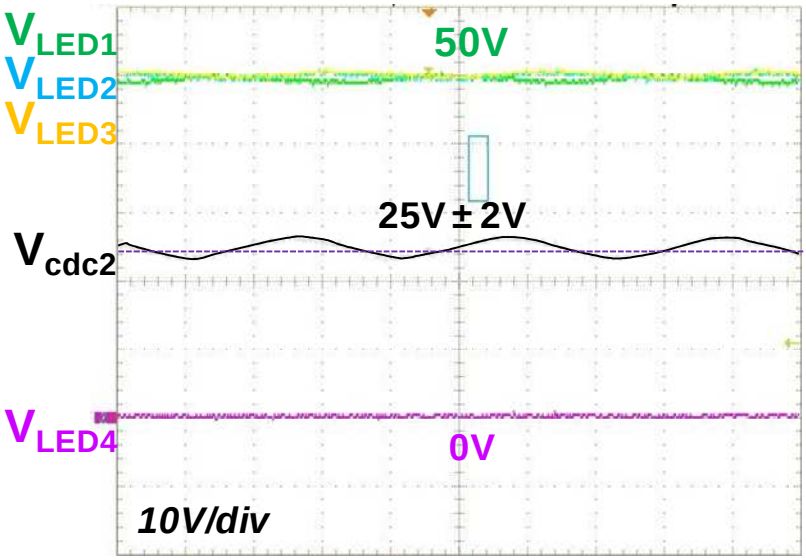


(b)

**Figure 3. 24 Operation Waveforms with One LED String in Short Failure**

## 3.5 Dimming Methods of MC$^3$ LLC LED Driver

### 3.5.1 Frequency modulation dimming method of MC$^3$ LLC LED driver

As discussed before, the analog dimming function of proposed MC$^3$ LLC LED driver can be implemented by frequency modulation. The control diagram is shown in Fig. 3.25.

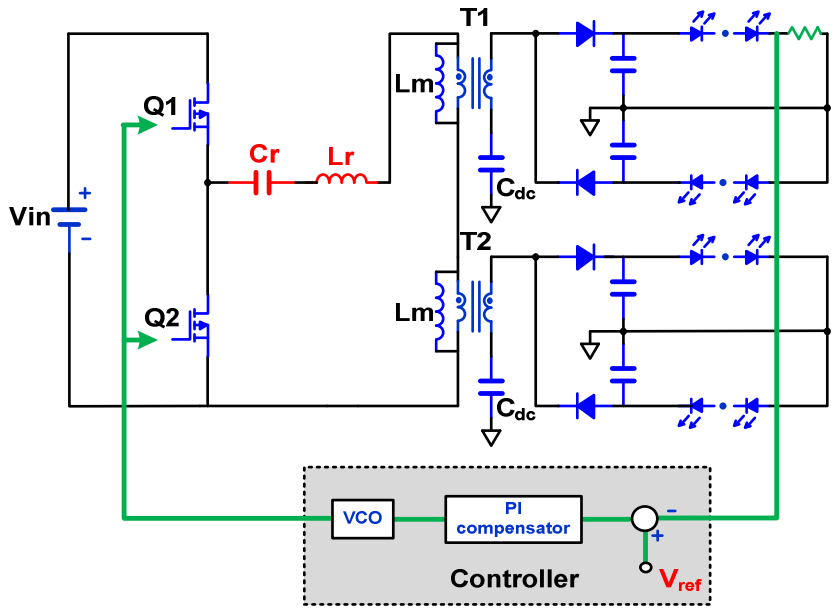


**Figure 3. 25 Frequency Modulation Dimming Method of MC$^3$ LLC LED Driver**

In frequency modulation dimming method, LED load current is sensed and compared with the reference. To dim LED load current, the reference will be changed from 5V to 0V, which represent the different dimming ratio. Then the switching frequency can be modulated in order to regulate LED load current.

Assuming normal input & output threshold voltage condition ($V_{in\_nom}$=380V, $V_{th\_nom}$=40V), the experimental waveforms under different dimming ratios are summarized in Fig. 3.26.

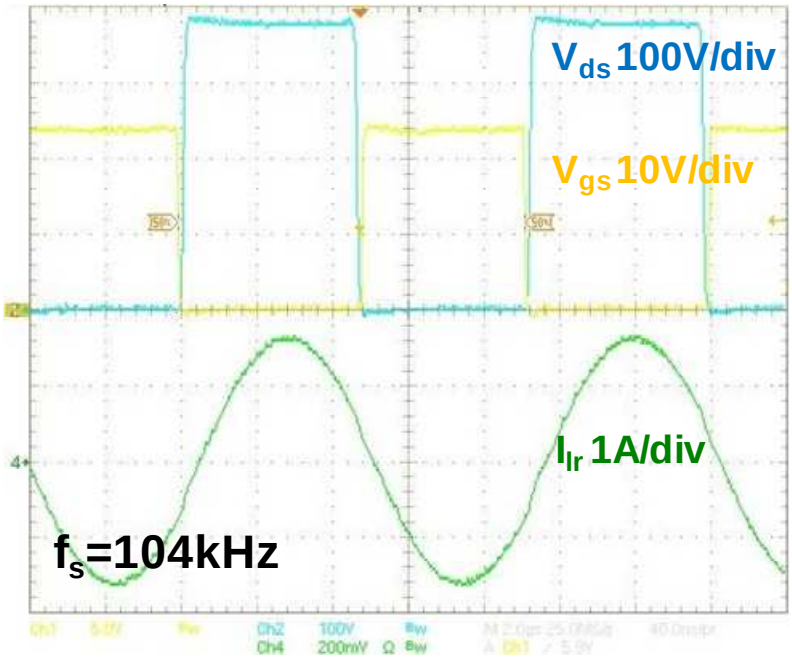


(a) dimming ratio=100% (fs=104kHz)

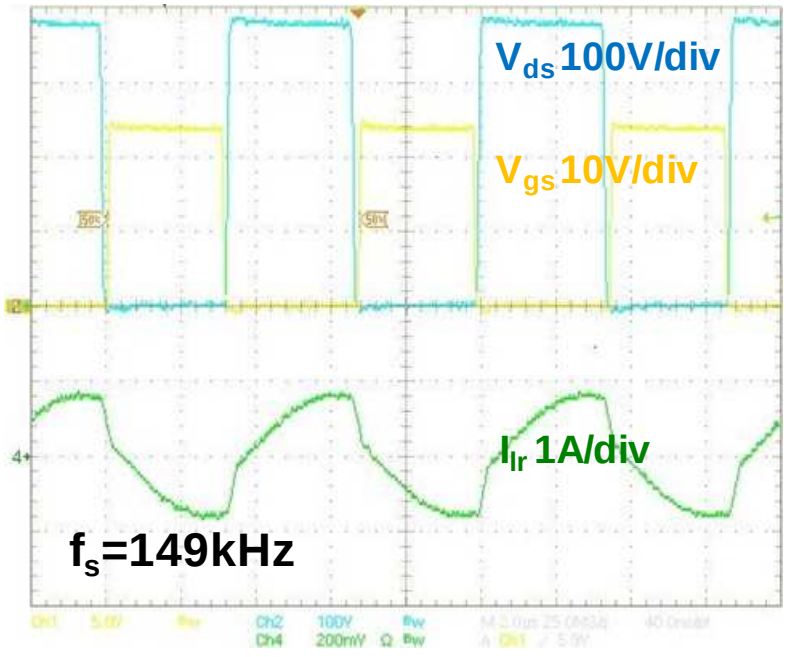


(b) dimming ratio=50% (fs=149kHz)

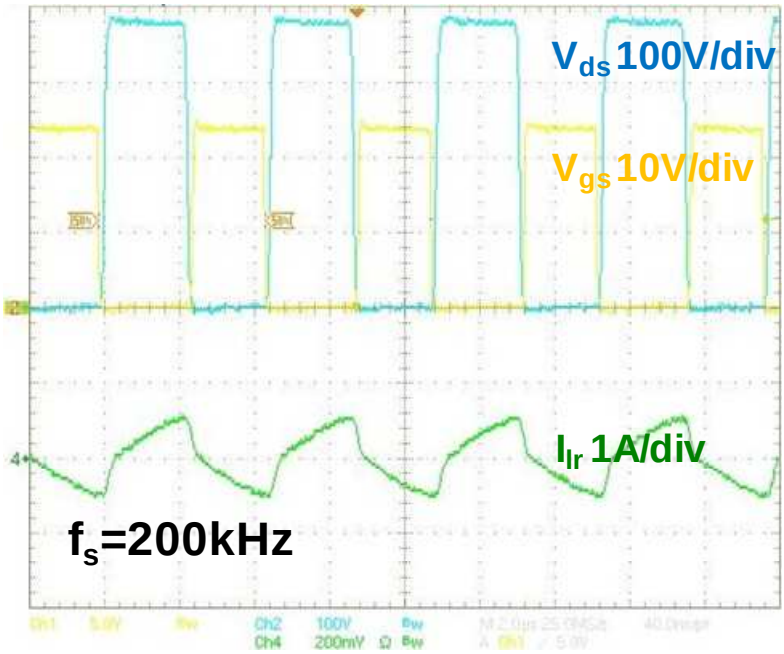


(c) dimming ratio=26% (fs=200kHz)

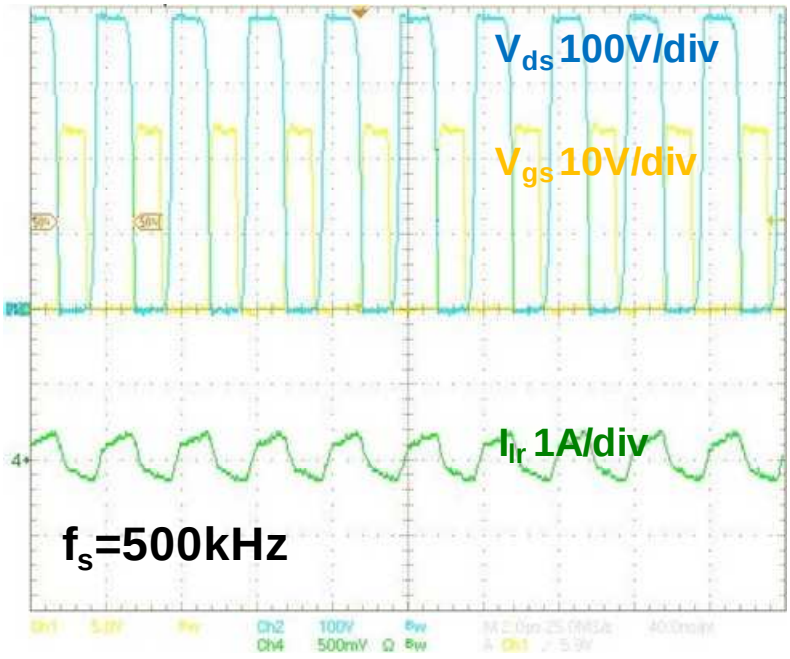


(d) dimming ratio=17% (fs=500kHz)

**Figure 3. 26 Operating Waveforms with Dimming Conditions**

The efficiency with different dimming ratio is plotted in Fig. 3.27.

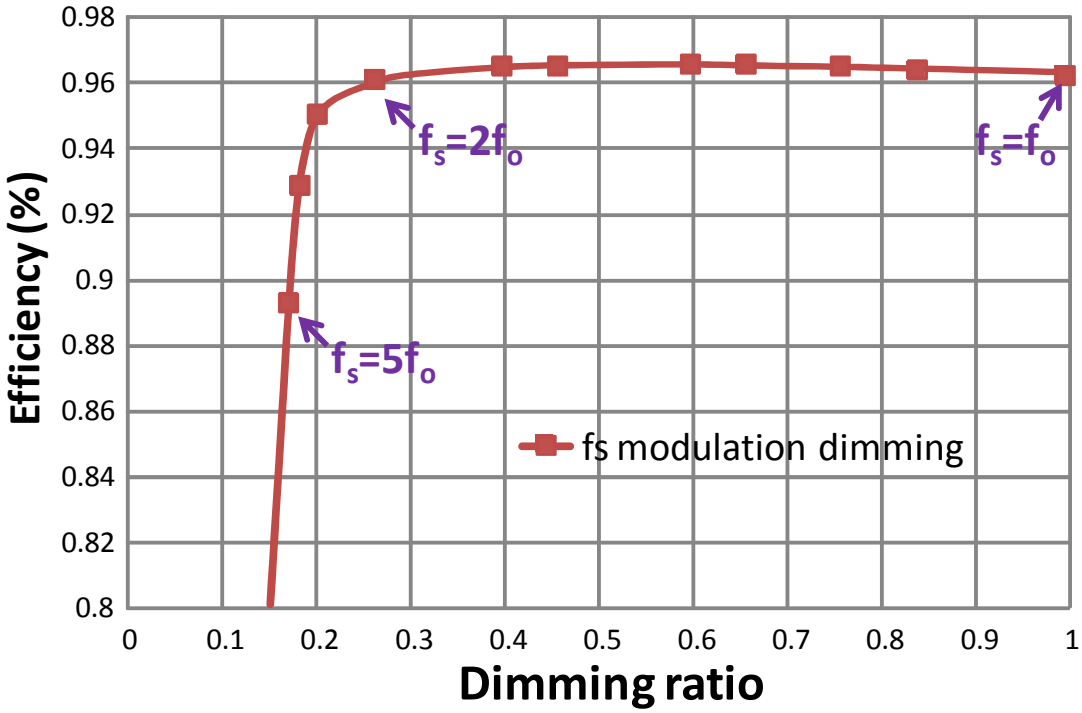


**Figure 3. 27 Efficiency under Dimming Conditions by Frequency Modulation Dimming**

From the efficiency curve above we can see that there are still some drawbacks of the frequency modulation dimming method. First of all, it is difficult to achieve full range dimming (from 0% to 100%) and the frequency needs to be pushed very high for low dimming ratio conditions. Secondly, the efficiency will drop dramatically to achieve low dimming ratio because the ZVS operation may be lost under low dimming ratio condition and the switching loss increase dramatically with higher frequency.

In order to overcome the drawback of frequency modulation dimming method, another dimming method is investigated in the next section, by which the converter can always operate close to resonant frequency and thus the efficiency under dimming condition can be improved.

### 3.5.2 Burst mode dimming method of MC$^3$ LLC LED driver

In traditional front-end LLC DC/DC converter, in order to improve light load efficiency, burst mode control is widely used. In paper [36], a novel burst mode control solution is proposed for the highest efficiency. Inspiring from previous burst mode control used in front-end LLC DC/DC converter, a burst mode dimming method for MC$^3$ LLC LED driver is generated. The control scheme is shown in Fig. 3.28.

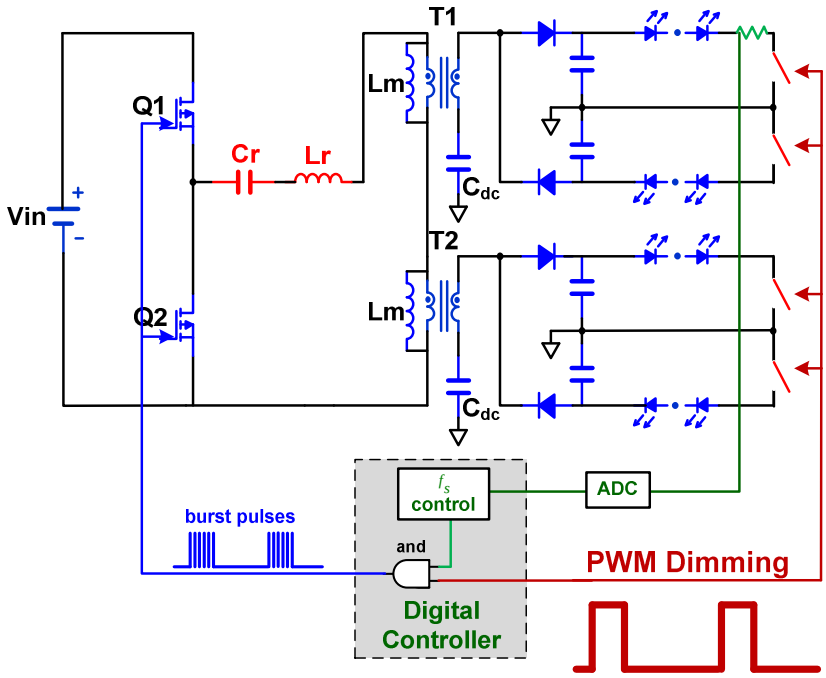


**Figure 3. 28 Burst Mode Dimming Method of MC$^3$ LLC LED Driver**

In this control scheme, the LED current is sensed and controlled always equal to full load current. As a result, the converter always operates close to resonant frequency, like under normal condition. However, a external switch is added in series with each LED string. A PWM dimming signal is applied to this external switch to control the on/off of LED strings. Simultaneously, the same PWM dimming signal is also applied to the

digital controller to generate burse pulses of primary switches. When PWM dimming signal is high, LED strings are on and the converter operates at resonant frequency; when PWM dimming signal is low, LED strings are off and the primary switches stop working. The average current of LED strings can be easily controlled by the duty cycle of PWM dimming signal.

The proposed burst mode dimming method is implemented by FPGA digital controller and the experimental waveforms are shown in Fig. 3.29.

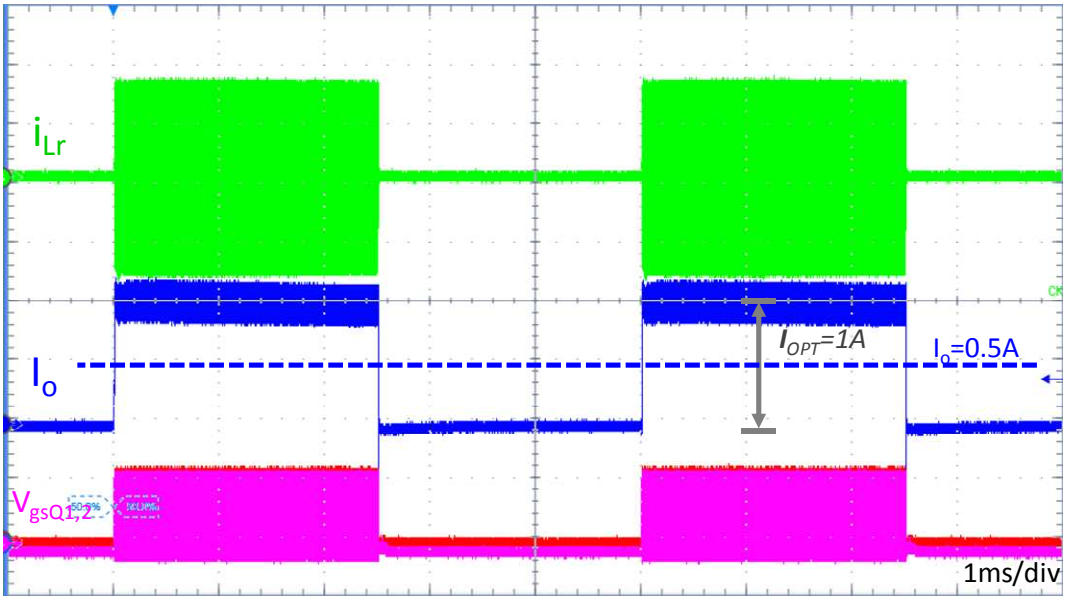


(a) Dimming ratio=50% (Io=0.5A)

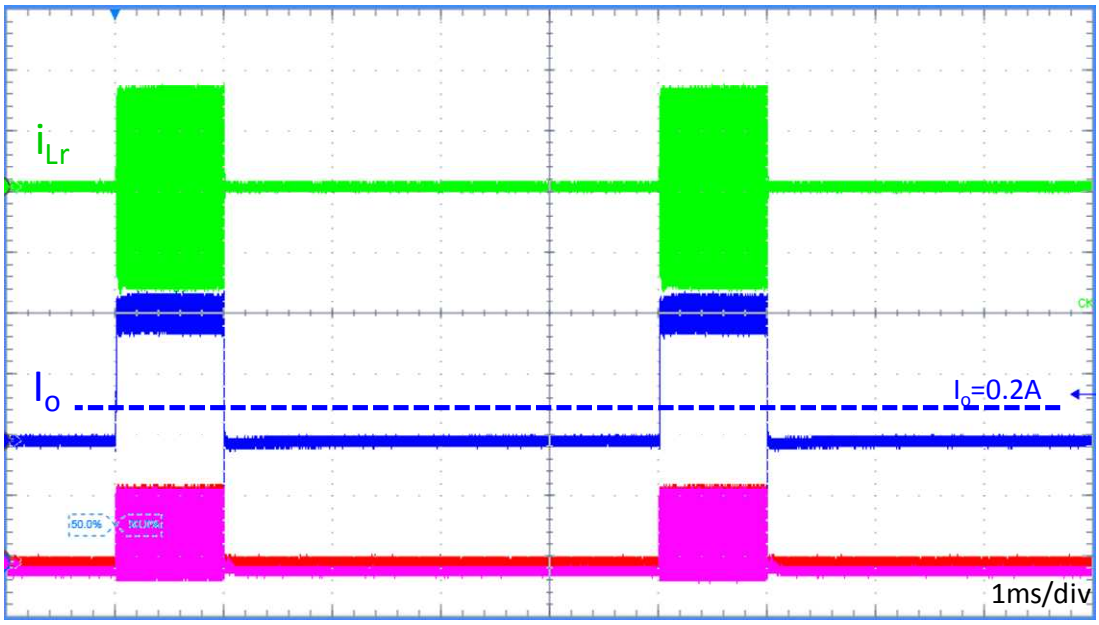


(b) Dimming ratio=20% (Io=0.2A)

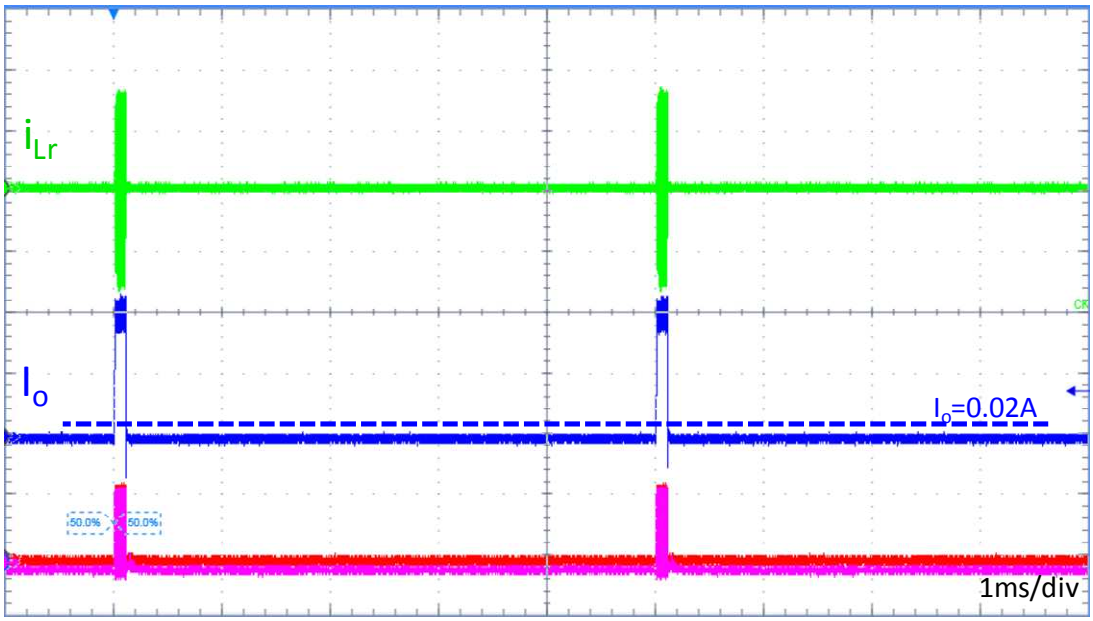


(c) Dimming ratio=2% (Io=0.02A)

**Figure 3. 29 Experimental Waveforms of Burst Mode Dimming Method**

It is clearly shown that the converter can always operate close to resonant frequency, which is the most efficient operation point of MC$^3$ LLC LED driver. The LED load's average current can be controlled by the duty cycle of PWM dimming signal. Consequently, no matter what dimming ratio is required, high efficiency (similar to full load condition) can be achieved. Another benefit of the proposed burst mode dimming method is that ultra low dimming ratio can also be achieved, only by adjusting PWM dimming signal's duty cycle.

The dimming efficiency by using burst mode dimming method has been measured and plotted in Fig. 3.30. We can see the efficiency under low diming ratio condition can be improved dramatically.

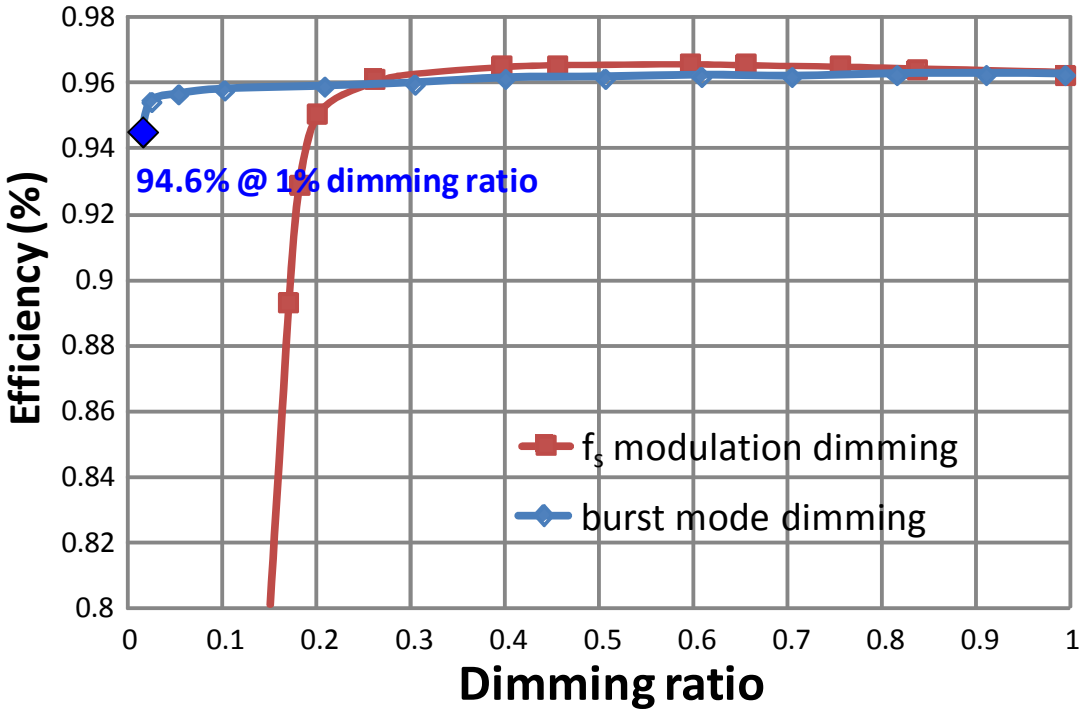


**Figure 3. 30 Efficiency under Dimming Conditions by Burst Mode Dimming (projected)**

## 3.6 Summary

A $MC^3$ LLC resonant LED driver for multiple LED driving application is proposed to achieve simple system structure, low cost, high efficiency and good current sharing. In the proposed circuit, multiple transformer structure and DC block cap are utilized to achieve current sharing among multiple LED strings.

LED load has unique nonlinear character, which is quite different from resistive load. Traditional LLC voltage gain characteristic is no long suitable in this $MC^3$ LLC LED driver. The modified LLC voltage and current gain characteristic is derived by considering the LED i-v character, which reflect the character of LLC converter with current source output. Based on the LLC current gain characteristic with LED load, a design procedure of $MC^3$ LLC LED driver is developed.

A 100 kHz 200 W 4-string $MC^3$ LLC LED driver is designed and tested to verify the proposed circuit and design procedure. The experimental results show that the circuit can provide constant current output within wide input and output variations. Under unbalanced LED condition, even one LED string totally in short failure, the circuit can still operate properly and achieve good current sharing.

Two dimming methods for $MC^3$ LLC LED driver is proposed and investigated. Frequency modulation is easy to implement but also has drawbacks such as wide frequency range and poor efficiency for low dimming ratio. Burst mode control method can overcome such drawbacks and improve the dimming efficiency very well. Not only ultra low dimming ratio can be achieved by burst mode dimming, but also the efficiency at low dimming ratio is still very high (e.g. 94.6% efficiency at 1% dimming ratio)

# Chapter 4. Conclusion

## 4.1 Summary

As a promising lighting source for future lighting application. LEDs become a hot topic and attract a lot of attentions of replacing traditional lighting sources. With the increase of total power of LED luminaries, multi-channel constant current ($MC^3$) LED driver is needed.

In order to overcome the drawbacks of traditional two-stage multiple LED driver solutions, a single-stage $MC^3$ LED driver concept has been proposed. Multiple transformer structure is used to provide multiple current source outputs. A PWM half bridge topology is chosen to implement the proposed concept first. In order to analyze the current cross regulation under unbalanced LED conditions, a general model is derived. Through simulation verification for various unbalanced conditions, the proposed circuit shows good robustness to LED forward voltage variation and short failure. However, the $MC^3$ PWM LED driver still has some drawbacks and needs further improvements.

The LLC resonant topology is chosen to further improve the efficiency, reduce cost and save components of the LED driver. Besides multiple transformer structure, a DC block capacitor in transformer's secondary side is also used to balance two LED strings' currents.

LLC voltage and current gain characteristic is derived by considering the LED i-v character for design purpose. Both of them can be exactly mapped between each other. Based on the modified current gain curve, a design procedure of LLC LED driver is developed, in order to provide constant current output within the whole line and load changes. A 100 kHz 200 W 4-string $MC^3$ LLC LED driver is designed and tested to verify the proposed circuit and design procedure. The proposed circuit shows good current sharing capability for both balanced and unbalanced LED load conditions. Two dimming methods are also proposed and verified by experiment.

## 4.2 Future Works

In this thesis, two methods for dimming control of $MC^3$ LLC LED driver is proposed and investigated. Frequency modulation is easy to implement but also has drawbacks such as wide frequency range and poor efficiency for low dimming ratio. Burst mode control method can overcome such drawbacks and improve the dimming efficiency very well.

The feasibility of burst mode dimming method has already been demonstrated through experiment. By using the state plane analysis and optimal pulse width control method proposed in [36], the fast transient response from zero current to 100% current and vice versa can also be achieved. In some LED application, fast transient response is in great demand. Hence how to implement this concept into the control of $MC^3$ LLC LED driver is also a good topic for future work.

In some LED applications, a PWM type current through LED is unacceptable because of some frequency interfering concerns with other devices such as remote

controller. So the burst mode dimming method may not be a good choice. Instead, a DC current is more desirable. As a result, besides frequency modulation dimming methods, other dimming methods should be investigated. Potential candidates may include: adding a notch filter into the resonant tank; PWM control (e.g. phase-shift PWM control and asymmetric PWM control etc.) and also some combinations between them.

# Appendix. Design Procedure of MC$^3$ LLC Resonant LED Driver

Fig. A.1 shows the circuit schematic of proposed single-stage MC$^3$ LLC resonant LED driver. For a good design of MC$^3$ LLC LED driver, it should fulfill two targets:

- Firstly, the LED driver's efficiency at normal operating condition (which is also the most common operating condition) should be optimized;
- Secondly, both input voltage and LED output forward voltage have certain variations; the MC$^3$ LLC LED driver should have the capability to provide 100% constant current output within the whole input and output ranges.

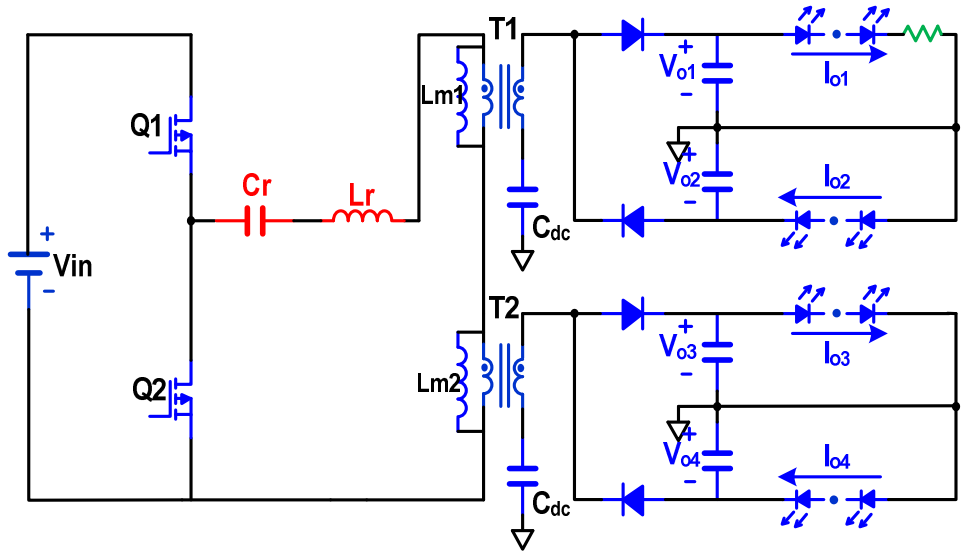


**Figure A. 1 Circuit Schematic of MC$^3$ LLC Resonant LED driver**

There are four key design parameters for this MC$^3$ LLC resonant LED driver - transformer's turns ratio, transformer's magnetizing inductance, resonant inductor & capacitor.

Compared to the optimal design procedure proposed in [33], the design and optimization of transformer's turns-ratio and magnetizing inductance in the $MC^3$ LLC LED driver are quite similar to the LLC front-end DC/DC converter design. However, the design of resonant tank (also $L_n$ & Q) should be based on the LLC current gain characteristic with LED load derived in Chapter 3 in order to achieve peak current gain requirement under ($V_{in\_min}$, $V_{th\_max}$) condition.

The design procedure can be divided into three steps and the design criteria for each step will be discussed in details as follows.

***1. Transformer's turns ratio N***

The transformer's turns ratio is the first parameter which needs to be designed. The transformer's turns ratio directly determines the converter's operation point under normal input and output condition. On the other hand, the LED driver is desired to achieve high efficiency under normal condition. Consequently, the design of transformer's turns ratio should make the converter operate close to the resonant frequency under normal condition, which is the most efficient operating point of LLC resonant converter.

The converter's current gain at normal condition can be expressed by equation (A.1), which is a function of transformer's turns ration N. In order to operate at resonant frequency, N should be properly designed so that the current gain at normal condition equals to one.

$$M_I = \frac{(\frac{V_{in\_nom}}{4N} - V_{th\_nom}) / R_d}{I_o} \approx 1 \qquad \text{(A.1)}$$

Obviously, given certain design specifications (e.g. given $V_{in\_nom}$ & $V_{th\_nom}$), the turns ratio N can be calculated. However, the calculation result is possibly not a integer. Then the ceiling function is used to choose the smallest following integer as the design of transformer's turns ratio. By choose the turns ratio number in this way, the benefit is that under normal condition, the converter could operate very close but slightly below the resonant frequency. As a result, both primary side MOSFETs and secondary side diodes can achieve ZVS turn-on and ZCS turn-off. Especially for the secondary side diodes, ZCS operation can minimize the reverse recovery loss.

For example, when normal input voltage and LED's threshold voltage are 380V and 40V respectively, the turns ratio N can be calculated in equation (A.2) by using the ceiling function:

$$N = \left\lceil \frac{V_{in\_nom}}{4(V_{th\_nom} + I_o \cdot R_d)} \right\rceil = \lceil 1.9 \rceil = 2 \tag{A.2}$$

Based on the designed turns ratio, the LLC current gain curves can be drawn in Fig. A.2. We can see that the operating point at normal condition is very close and slightly below the resonant point, which meets our design objective.

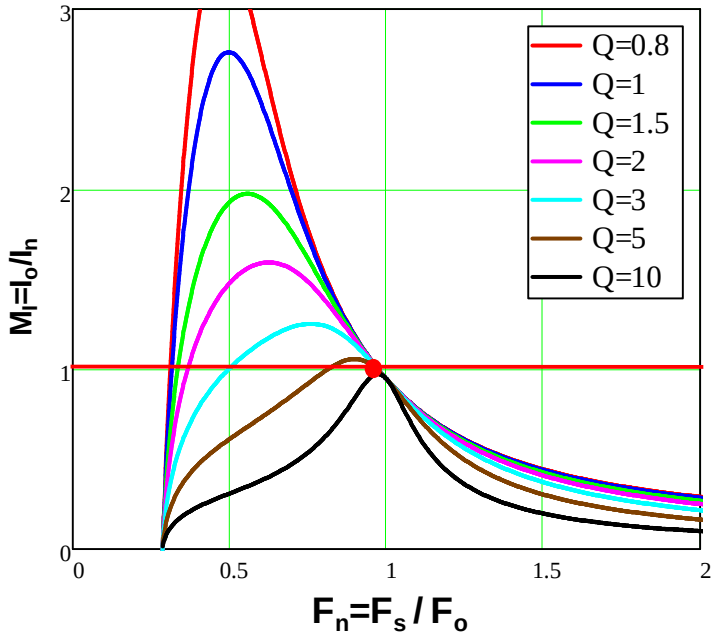


**Figure A. 2 LLC Current Gain Curves under Normal Condition**

### *2. Dead-time $T_d$ and transformer's magnetizing inductance $L_m$*

Before selecting transformer's magnetizing inductance value, the dead-time should firstly be optimized. In paper [33], the relationship between dead-time and converter's primary side and secondary side conduction loss has been derived. Based on the circuit specifications, we can draw the curves of primary side and secondary side RMS currents as a function of dead-time, as shown in Fig. A.3 and Fig. A.4 respectively.

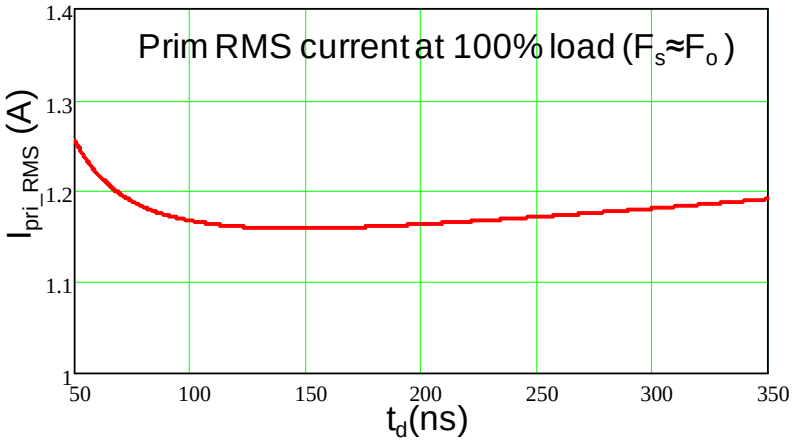


**Figure A. 3 Relationship between Primary RMS Current and Dead-time**

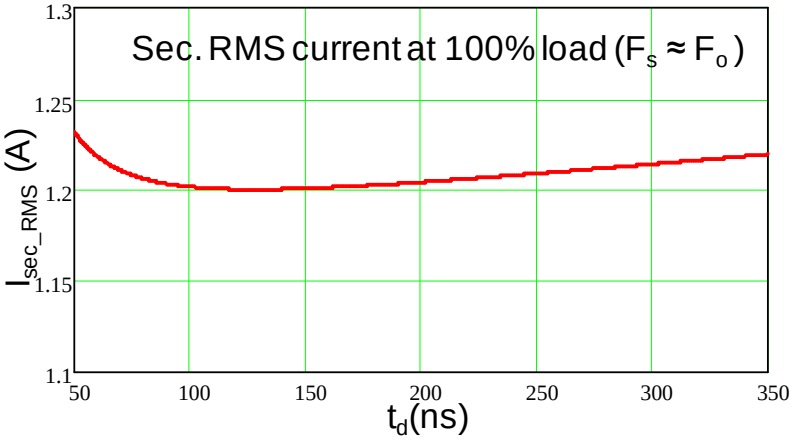


**Figure A. 4 Relationship between Secondary RMS Current and Dead-time**

Then by using the on-resistance of primary side MOSFETs and forward voltage of secondary side diodes, the relationship between total conduction loss and dead-time can be drawn in Fig. A.5.

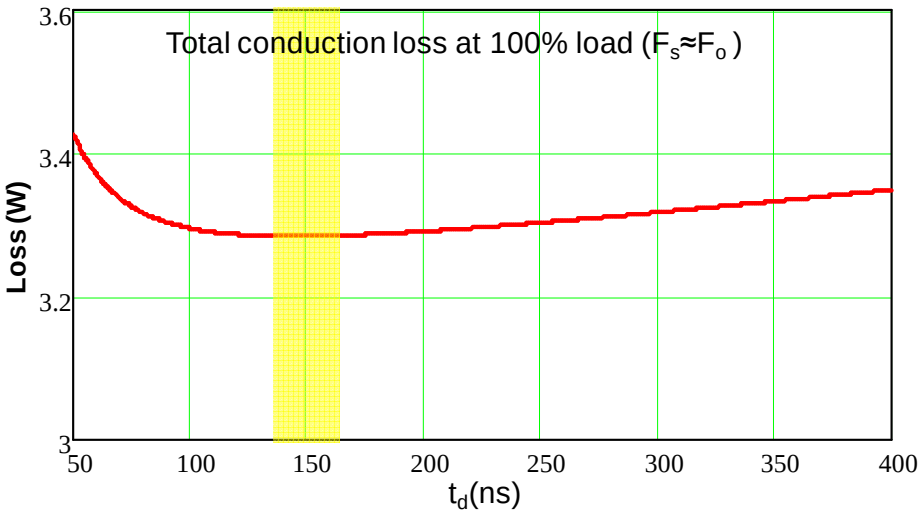


**Figure A. 5 Relationship between Total Conduction Loss and Dead-time**

From Fig. A.5 we can see the relationship between converter's total conduction loss and dead-time shows a U-shape. As a result, a optimum dead-time range can be found out so that the lowest conduction loss can be achieved. Then the corresponding optimized dead-time can be determined. In the prototype design, 150ns dead-time has been chosen.

The dead-time optimization is critical for the selection of transformer's magnetizing inductance. The magnetizing inductance value can determine the amplitude of magnetizing current during dead-time directly, which is used to fully discharge primary side MOSFETs' junction capacitor so that ZVS turn-on can be achieved.

The relationship between magnetizing inductance and magnetizing current during dead-time can be calculated in equation (A.3).

$$I_M = \frac{2NV_o}{L_m}\frac{T_o}{4} \tag{A.3}$$

Which is used to discharge the junction capacitor of primary side MOSFETs, as shown in Fig. A.6.

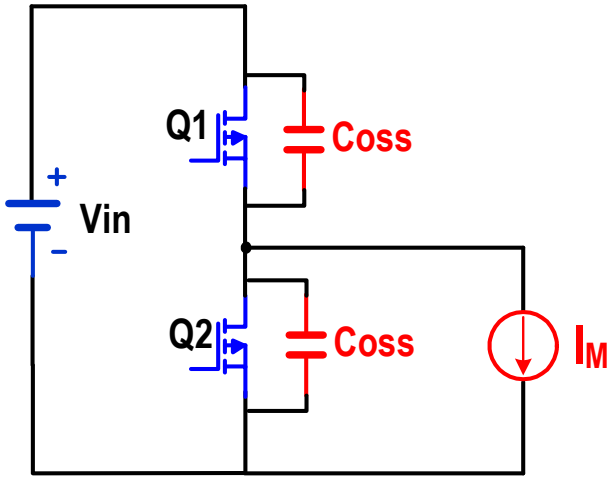


**Figure A. 6 ZVS Requirement for Magnetizing Inductance Design**

In order to achieve ZVS, during dead-time period, the following equation has to be satisfied:

$$I_M t_d \geq 2C_{oss}V_{in} \tag{A.4}$$

Combining equation (A.3) and (A.4), the selection criteria for magnetizing inductance $L_m$ can be found in equation (A.5)

$$L_m \leq \frac{T_o \cdot t_d}{16C_{oss}} \tag{A.5}$$

In the prototype design, for 100 kHz switching frequency and 150ns dead time, together with 150 pF $C_{oss}$ of the MOSFET (STD13NM60N), the value of magnetizing inductance can be easily calculated and around 800 uH (the sum of two transformers' magnetizing inductances).

### *3. Resonant tank design ($L_n$ & Q)*

After transformer's turns ratio and magnetizing inductance have been determined, the only parameters remaining for design is the resonant tank inductor and capacitor. The definitions of inductor ratio $L_n$ and quality factor Q are shown in the following equations:

$$L_n = \frac{L_m}{L_r}$$

$$Q = \frac{\sqrt{L_r / C_r}}{\frac{8N^2}{\pi^2} R_d}$$

We can see that since the resonant tank inductor $L_r$ and capacitor $C_r$ have certain relationships with $L_n$ and Q. As long as the value of $L_n$ and Q can be determined, the values of Lr and Cr can be easily calculated correspondingly. The impact of $L_n$ and Q on the circuit's character needs to be investigated so that some design criteria can be found.

For different $L_n$ and Q values, the shapes of current gain curves will change and hence impact the operation region under dimming conditions. Current gain curves with different $L_n$ and Q values under normal condition are compared in Fig. A.7.

Comparing these three cases with different $L_n$ values, although under normal condition the converter always operates at the resonant point, the choice of $L_n$ does impact the operation region under dimming condition: the smaller the $L_n$ value, the narrower the switching frequency range under dimming condition.

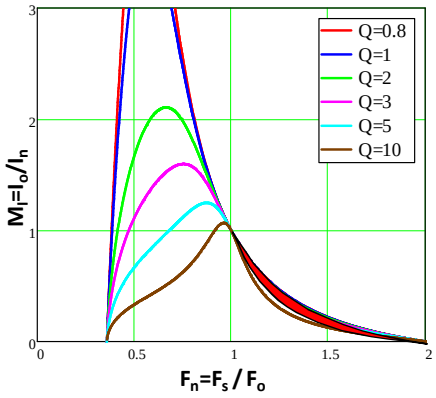


(a) $L_n$=3

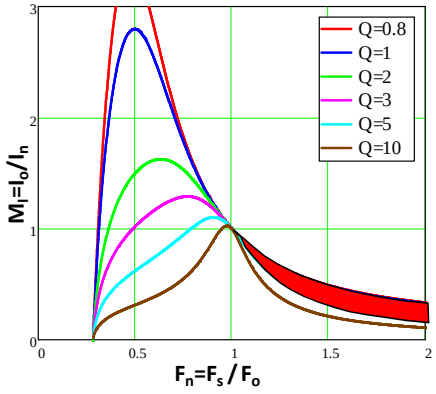


(b) $L_n$=5

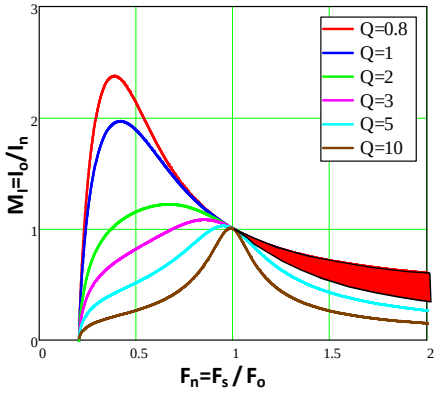


(c) $L_n$=10

**Figure A. 7 Impact of $L_n$ & Q on LLC Current Gain Curves under Normal Condition**

From the dimming operation point of view, the first criteria for $L_n$ and Q design can be generated:

- Smaller $L_n$ is preferred because narrower switching frequency range can be achieved.

Furthermore, in this $MC^3$ LLC LED driver design, the variations of input voltage and output LED threshold voltage also need to be considered. The current gain curves under normal condition and two boundary conditions are shown in Fig. A.8 (choose $L_n$=5 as an example).

Obviously, when either input voltage or LED threshold voltage varies, the converter have to modulate the switching frequency to maintain constant current output. Under the normal condition, the converter operates close to the resonant point to provide 100% LED load current and high efficiency can be achieved. Under ($V_{in\_max}$, $V_{o\_min}$) condition, the LLC converter increases the switching frequency to reduce the current gain in order to keep constant current output. On the contrary, under ($V_{in\_min}$, $V_{o\_max}$) condition, the LLC converter decreases the switching frequency to boost the current gain in order to keep constant current output.

From Fig. A.8 (c), we can notice that for some $L_n$ & Q designs, the peak current gain can't reach to one anymore (e.g. when Q>3), which means the LLC converter will lose the capability of providing 100% constant current under ($V_{in\_min}$, $V_{o\_max}$) condition. As a result, ($V_{in\_min}$, $V_{o\_max}$) condition is the worst case condition for the design of $L_n$ and Q. The impact of $L_n$ and Q on peak current gain under worst case condition ($V_{in\_min}$, $V_{o\_max}$) are shown and compared in Fig. A.9.

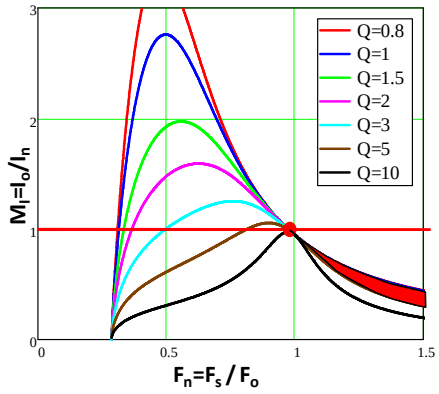


(a) Normal condition: ($V_{in\_nom}$, $V_{th\_nom}$)

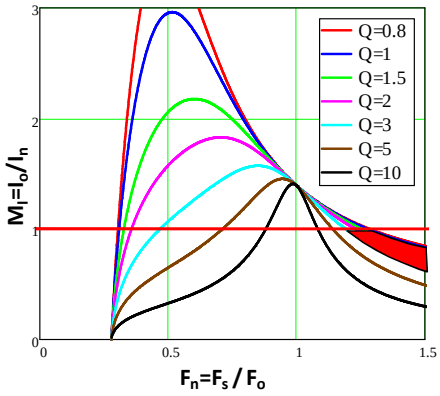


(b) Boundary condition 1: ($V_{in\_max}$, $V_{th\_min}$)

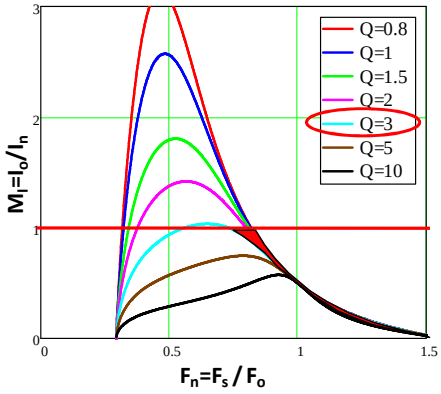


(c) Boundary condition 2: ($V_{in\_min}$, $V_{th\_max}$)

**Figure A. 8 Impact of Input & Output variations on LLC Current Gain Curves**

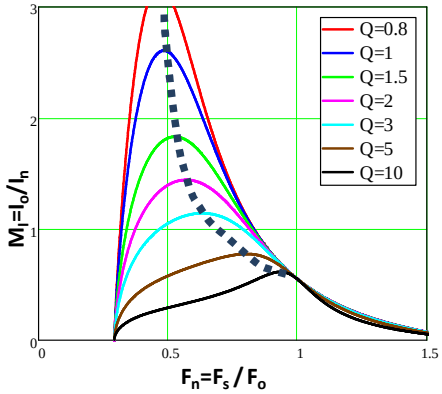


(a) Ln=5

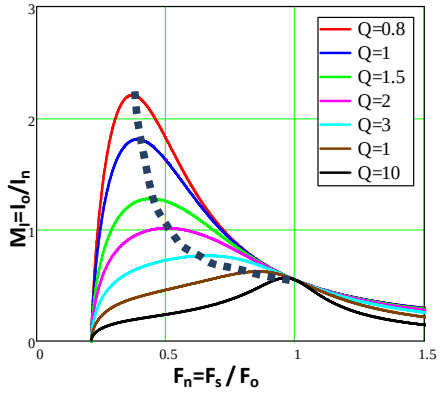


(b) Ln=10

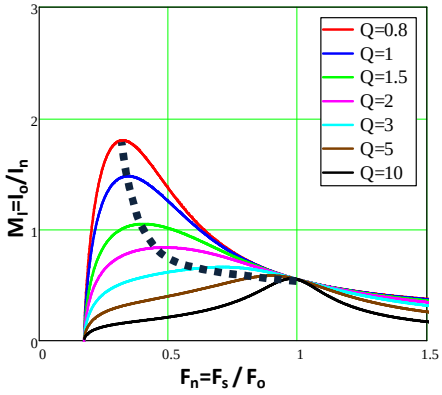


(c) Ln=15

**Figure A. 9 Impact of $L_n$ & Q on LLC Peak Current Gain**

From a series of current gain curves shown in Fig. A.9, it is clearly shown that the impact of $L_n$ and Q on the converter's peak current gain. For different $L_n$ and Q, the peak current gains which can be achieved are quite different. Only some certain combinations of $L_n$ and Q values can achieve required peak current gain and maintain constant current output under this worst case condition ($V_{in\_min}$, $V_{o\_max}$).

In order to determine all the valid combinations of $L_n$ and Q values, a peak current gain surface for different $L_n$ and Q values (blue surface) are calculated and plotted in Fig. A.10. Using a flat surface (yellow surface) to cut with the achieved peak current gain surface, a intersection line (red line) can be found out. Only for those $L_n$ and Q values above the red line, the achieved peak current gain is higher than 1 and the converter can maintain 100% current output within the whole input and output ranges.

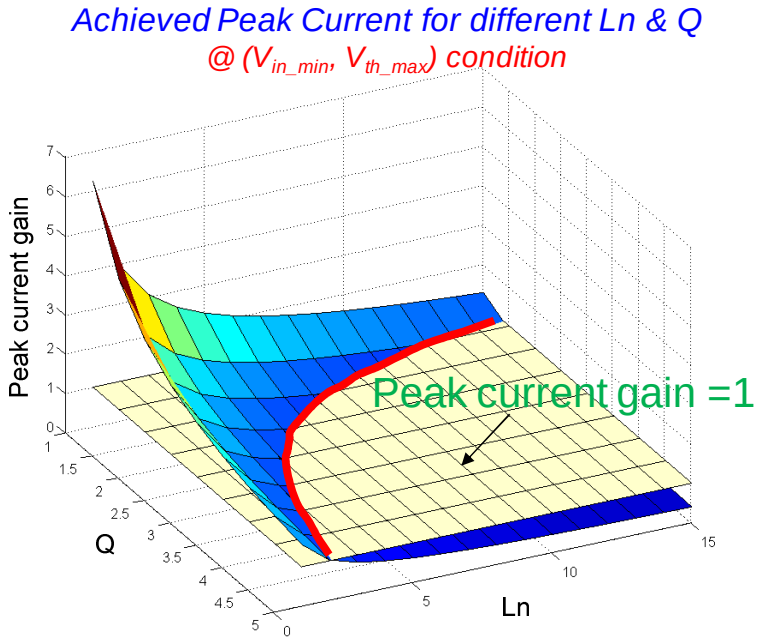


**Figure A. 10 Achieved Peak Current Gain for Different $L_n$ & Q**

For easy understanding and design purpose, we can plot the 2-D projection of the red line as in Fig. A.11. In order to achieve peak current gain larger than one, the design of $L_n$ and Q should be chosen on the left-upper side of the red line.

However, if only considering this peak current gain requirement, there are still infinite choices of $L_n$ and Q values. The question is how we can choose the proper $L_n$ and Q values from all the possible choices. Other constraints are need to be investigated in order to narrow down the design choices.

If we take a look at the definition of $L_n$ and Q, the following equation can be easily derived:

$$L_n \cdot Q = \frac{2\pi f_o}{\frac{8N^2}{\pi^2} R_d} \cdot L_m \tag{A.6}$$

It can be seen that after the transformer's turns ratio and magnetizing inductance are designed in the first two steps, the product of $L_n$ and Q is no longer an arbitrary value, but has to keep constant, as in (A.6). In other words, once the $L_n$ value is chosen, the corresponding Q value has already been determined.

In the prototype design, for the required magnetizing inductance of 800uH, the product of $L_n$ and Q has also been determined, which is 15. Then a hyperbolic line (purple line), which represent the constant product of $L_n$ and Q, can be added into Fig. A.11. The design of $L_n$ and Q can be further narrowed down, which locates along the purple line, but above the intersection point. In other words, in order to satisfy the peak current gain requirement, the design of $L_n$ has a minimum value.

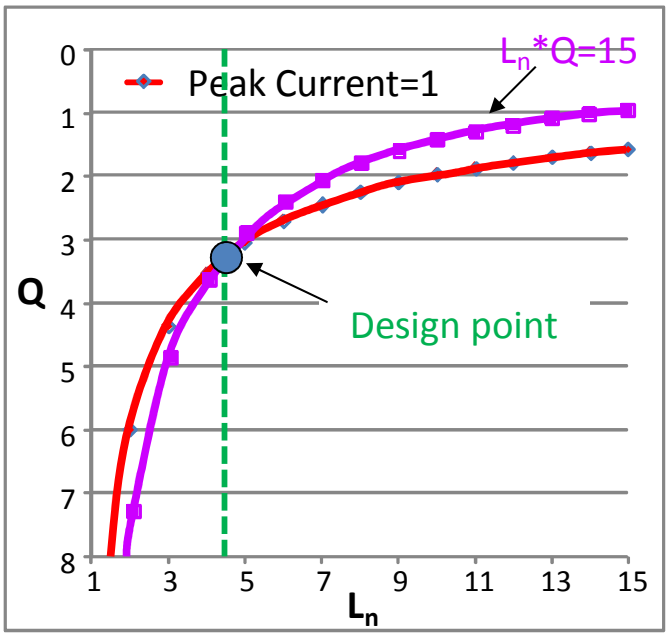


**Figure A. 11 Design Choices of $L_n$ & Q**

Recalling the previous analysis about the impact of $L_n$ and Q on dimming operation, there are totally two criteria for $L_n$ and Q design:

- $L_n$ has a minimum value in order to satisfy the peak current gain requirement;
- Smaller $L_n$ is preferred because narrower switching frequency range can be achieved under dimming condition.

Combining these two design criteria, it is very easy to determine that the intersection point is the desired design choice. In the prototype design, the design values of $L_n$ and Q are 5 and 3, respectively.

It is also possible than there is no intersection point between peak current gain curve (red line) and constant product curve of $L_n$ & Q (purple line), as shown in Fig. A.12.

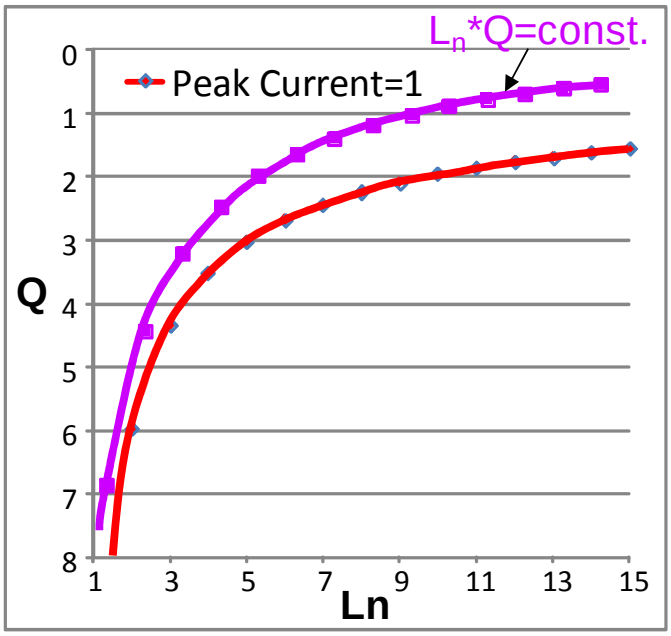


(a)

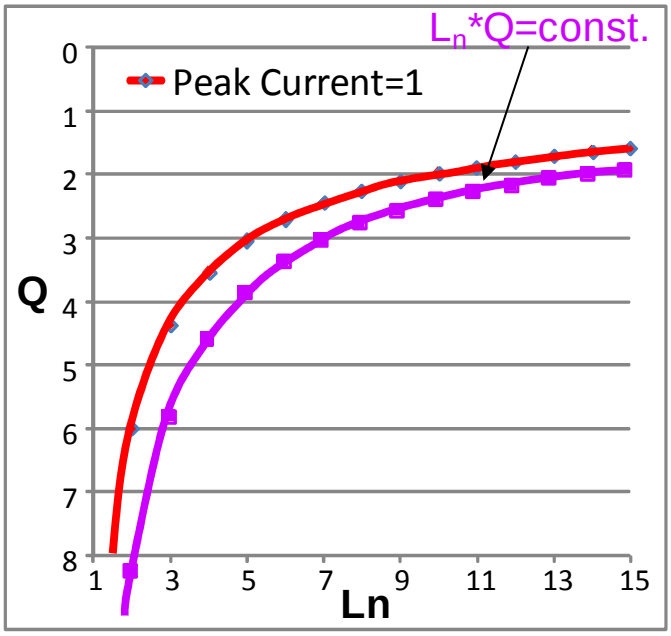


(b)

**Figure A. 12 Design Choices of $L_n$ & Q (no intersection point cases)**

Obviously there are two possible conditions:

- When purple line above red line, as shown in Fig. A.12 (a);
- When purple line below red line, as shown in Fig. A.12 (b).

For the first case, because the purple line above red line, that means all the design choices along the purple can reach peak current gain larger than one and constant current output capability can always be satisfied. If smaller $L_n$ is chosen, it will lead to narrower switching frequency range but on the other hand requires larger resonant inductor and increase converter size. So in this case, the choice of $L_n$ and Q depends on the trade-off between frequency range under dimming condition and converter size.

For the second case, when purple line below red line, there is no choice along purple line which can achieve peak current gain requirement. In other words, the product of $L_n$ and Q is too large. We need to go back to the second design step and redesign the transformer's magnetizing inductance $L_m$. $L_m$ value needs to be reduced according to (A.5), which will sacrifice the converter's efficiency but ZVS operation can still be achieved. The trade-off needs to be made between peak current requirement and efficiency.

***Loop gain measurement and compensator design of the prototype***

Based on the design procedure and results, a 100kHz, 200W, 4-string $MC^3$ LLC LED driver has been built. The circuit diagram with real parameters in prototype is shown in Fig. A.13.

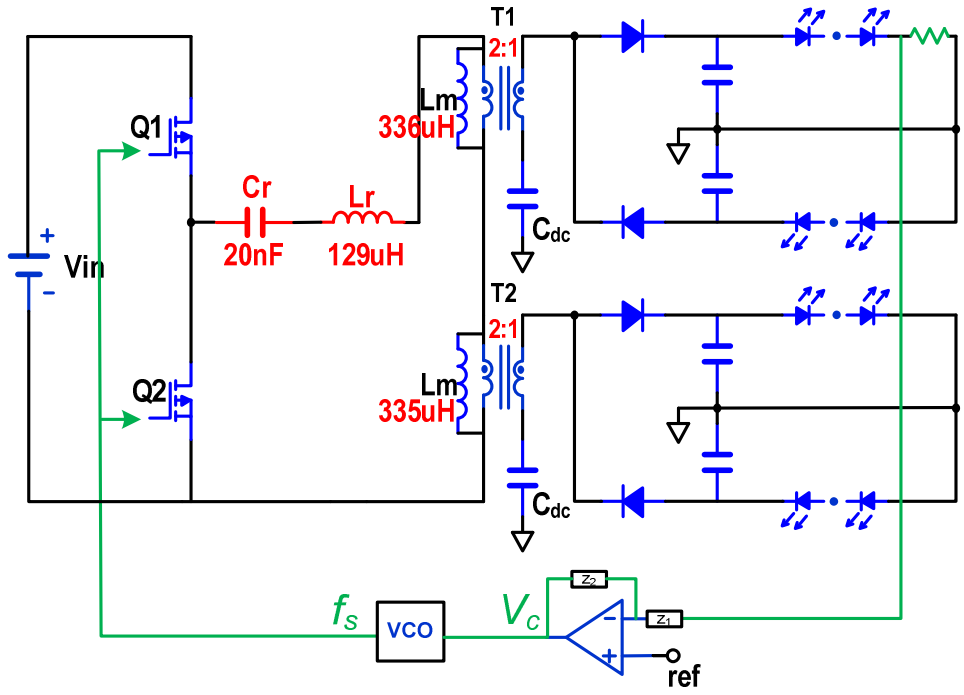


**Figure A. 13 Prototype with Real Circuit Parameters**

In order to design the compensator, the control to output transfer function is simulated under normal condition in Simplis. The bode plot is shown in Fig. A.14.

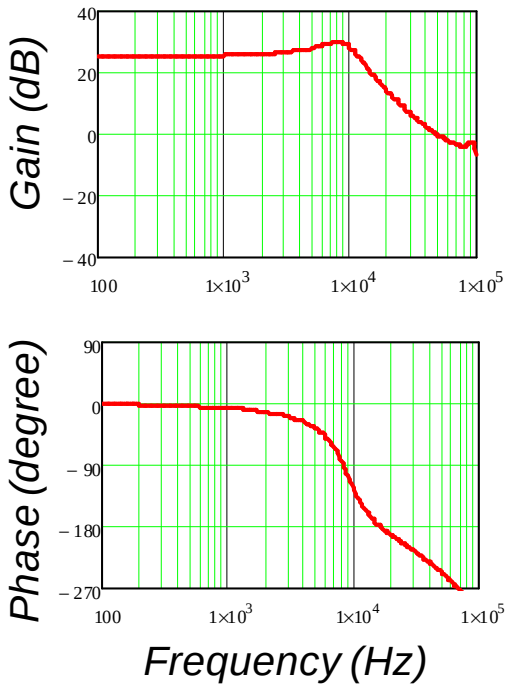


**Figure A. 14 Bode Plot of Control to Output Transfer Function under Normal Condition**

The bandwidth of LLC resonant converter is usually designed to be relatively around several kHz to achieve enough phase margin. In this case, the crossover frequency is also chosen to locate before the double and a simple PI compensator is used, as shown in Fig. A.15.

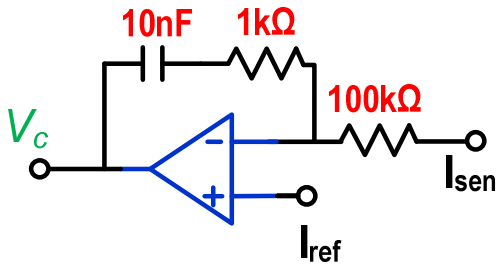


**Figure A. 15 PI Compensator for MC$^3$ LLC LED Driver**

The bode plot of closed loop gain is shown in Fig. A.16. The crossover frequency is about 2.5kHz and phase margin is 82 degree. During the closed-loop experiment, the circuit has been verified to be stable and the LED load current can be maintained as desired value within either line or load changes.

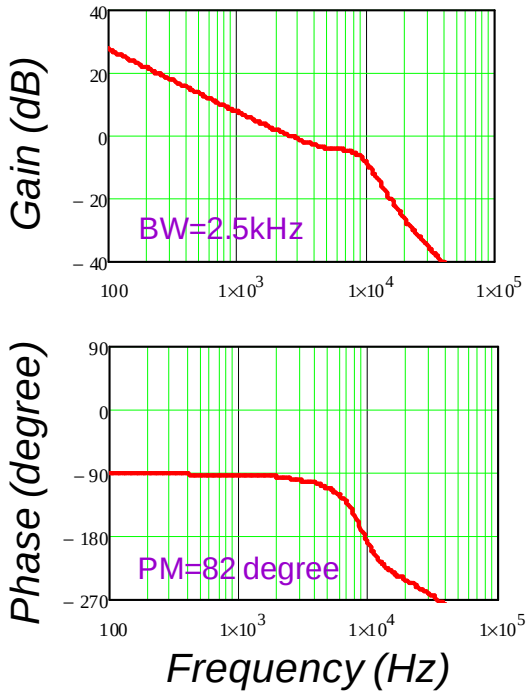


**Figure A. 16 Bode Plot of Loop Gain**

# REFERENCES

[1] J. Y. Tsao, “Solid-state lighting: Lamps, chips and materials for tomorrow,” IEEE Circuits and Devices Magazine, vol. 20, no. 3, pp. 28–37, May 2004.

[2] M. G. Craford, “LEDs Challenge the Incandescents,” IEEE Circuits and Devices Magazine, vol. 8, no. 1, pp. 24–29, Aug. 1992.

[3] M. S. Shur and A. Zukauskas, “Solid-state lighting: Toward superior illumination,” Proceedings of the IEEE, vol. 93, no. 10, pp. 1691–1703, Nov. 2005.

[4] Y. K. Cheng and K. W. E. Cheng, “General study for using LED to replace traditional lighting devices,” in Proc. ICPESA 2006, pp. 173–177, Nov. 2006.

[5] Mark Harris, “Let there be light”, IET Engineering & Technology (E&T) Magazine, vol.4, no. 20, pp.18-21, Nov. 2009.

[6] X. Tao, and S.Y.R. Hui, "A general photo-electro-thermo-temporal theory for light-emitting diode (LED) systems", in Proc. IEEE ECCE 2010, pp. 184-191, Sept. 2010.

[7] Solid-State Lighting Research and Development, U.S. Department of Energy, Mar. 2009.

[8] Cree, "Cree 231 Lumen Per Watt LED Shatters LED Efficacy Records", May 2011. Available: http://www.cree.com/press/press_detail.asp?i=1304945651119

[9] Samsung, "LED Backlight", July 2006.

Available:

http://www.samsung.com/uk/business/b2b/pdf/case_studies/LED_BLU_White_Paper.pdf

[10] Sungjin Choi, "Symmetric current balancing circuit for multiple DC loads", in Proc. IEEE APEC 2010, pp. 512-518, Feb. 2010.

[11] Solid State Lighting Status and Future, U.S. Department of Energy, Aug. 2004.

[12] H. van der Broeck, G. Sauerlander, and M. Wendt, “Power driver topologies and control schemes for LEDs,” in Proc. IEEE APEC 2007, pp. 1319-132, Feb. 2007.

[13] Y. Hu and M. M. Jovanovic, “LED driver with self-adaptative drive voltage,” IEEE Trans. Power Electron., vol. 23, no. 6, pp. 3116–3125, Nov. 2008.

[14] C.-C. Chen, C.-Y. Wu, Y.-M. Chen, and T.-F. Wu, “Sequential color LED backlight driving system for LCD panels” IEEE Trans. Power Electron., vol. 22, no. 3, pp. 919–925, May 2007.

[15] C. Y. Wu, T. F. Wu, J. R. Tsai, Y. M. Chen, and C. C. Chen, “Multi-string LED backlight driving system for LCD panels with color sequential display and area control,” IEEE Trans. Industrial Electron., vol. 55, no. 10, pp. 3791–3800, Oct. 2008.

[16] M. Doshi and R. Zane, “Reconfigurable and fault tolerant digital phase shifted modulator for luminance control of LED light sources”, in Proc. IEEE PESC 2008, 4185--4191, June 2008.

[17] Huang-Jen Chiu, Yu-Kang Lo, Jun-Ting Chen, Shih-Jen Cheng, Chung-Yi Lin, and Shann-Chyi Mou “A High-Efficiency Dimmable LED Driver for Low-Power Lighting

Applications” IEEE Trans. Industrial Electron., vol. 57, no. 2, 2010, pp. 735-743, Feb. 2010.

[18] TLC5690 datashteet, Texas Instruments.

[19] LM3464 datasheet, National Semiconductor.

[20] MAX16823 datasheet, Maxim Integrated Products.

[21] TPS54160 datashteet, Texas Instruments.

[22] LM3402 datasheet, National Semiconductor.

[23] MAX16832 datasheet, Maxim Integrated Products.

[24] MP4688 datasheet, Monolithic Power Systems.

[25] Shu Ji, Haoran Wu and Fred C. Lee, "Multi-channel constant current ($MC^3$) LED driver", in Proc. IEEE APEC 2011, pp. 718-722, Mar. 2011.

[26] Garcia, O.; Barrado, A.; Cezon, J.; Cobos, J.A.; Olias, E., “PCB based transformers for multiple output DC/DC converters”, in Proc. IEEE International Power Electronics Congress, pp. 51-55, Oct. 1995.

[27] Schultz, C.P, “A contribution to the theory of multiple winding transformers”, in Proc. IEEE Southeastcon 2009, pp. 175-177, Mar. 2009.

[28] B. Yang, “Topology investigation of front end DC/DC converter for distributed power system,” Ph.D. dissertation, Dept. Elect. Eng., Virginia Tech., Blacksburg, VA, 2003.

[29] D. Fu, “Topology investigation and system optimization of resonant converters,” Ph.D. dissertation, Dept. Elect. Eng., Virginia Tech., Blacksburg, VA, 2010.

[30] Texas Instruments User’s Guide, “UCC28810EVM-003 110-W Multiple String LED Driver with Universal Line Input and PFC,” November 2009.

[31] Xinke Wu, Junming Zhang, Zhaoming Qian, “A simple two-channel LED driver with automatic precise current sharing, ” IEEE Trans. Industrial Electron., vol. 58, no. 10, pp. 4783-4788, Oct. 2011.

[32] B. Yang and F. C. Lee, “LLC Resonant Converter for Front End DC/DC Conversion,” in Proc. IEEE APEC 2002, pp. 1108–1112, Aug. 2002.

[33] B. Lu, W. Liu, Y. Liang, F. C. Lee and J. D. van Wyk, “Optimal Design Methodology for LLC Resonant Converter,” in Proc. IEEE APEC 2006, pp. 533–538, Mar. 2002.

[34] S. Hong, H. Kim, J. Park, Y. Pu, K. Lee, J. Cheon and D. Han, “Secondary Side LLC Resonant Controller IC with Dynamic PWM Dimming and Dual-slope Clock Generator for LED Backlight Units,” IEEE Trans. Power Electron., Apr. 2011.

[35] On Semiconductor Application Note, “HB-LLC LED Driver Board,” Jan. 2009.

[36] W. Feng, F. C. Lee, P. Mattavelli, D. Huang and C. Prasantanakorn, “LLC resonant converter burst mode control with constant burst time and optimal switching pattern,” in Proc. IEEE APEC 2011, pp. 6–12, Mar. 2011.